The Role of Large Artery Stiffness in Cerebrovascular Dysfunction and Neurodegeneration: Mechanisms and Therapeutic Strategies

by

Emily Hope Reeve

A dissertation accepted and approved in partial fulfillment of the

requirements for the degree of

Doctor of Philosophy

in Human Physiology

Dissertation Committee:

Ashley E. Walker, Ph.D, Chair

John R. Halliwill, Ph.D, Core Member

Christopher Minson, Ph.D, Core Member

Emily Sylwestrak, Ph.D, Institutional Representative

University of Oregon

Summer 2025

© 2025 Emily Hope Reeve

DISSERTATION ABSTRACT

Emily Hope Reeve

Doctor of Philosophy in Human Physiology

Title: The Role Of Large Artery Stiffness In Cerebrovascular Dysfunction And Neurodegeneration: Mechanisms And Therapeutic Strategies

Increased large artery stiffness is strongly associated with age-related diseases. Some mixed dementias, such as Alzheimer's disease (AD) and vascular dementia, are modulated by the effects of increased large artery stiffness. Increased pulse pressure from stiff arteries damages the cerebral endothelial cells, contributing to cerebrovascular dysfunction and cognitive impairment. But it is unclear the exact mechanisms by which large artery stiffness contributes to neurodegeneration and AD. Thus, understanding the mechanisms of how increased large artery stiffness impacts cerebrovascular dysfunction and neurodegeneration could lead to new therapeutic strategies to target age-related diseases like AD.

Currently, there are no treatments to prevent or delay the onset of AD. Age-related increases in large artery stiffness and cerebrovascular dysfunction are promising therapeutic targets for ameliorating neurodegenerative diseases. Reductions in collagen crosslinking decrease large artery stiffness, but it is unknown what effects it will have on the cerebrovasculature and neurodegeneration. A treatment targeting mitochondrial function reduced large artery stiffness and improved vascular endothelial function, but effects on the cerebrovasculature and neurodegeneration are unknown. I hypothesized that large artery stiffness

mediates neurodegeneration by inducing cerebrovascular dysfunction, and that treatments targeting large artery stiffness would preserve cerebral artery function and mitigate signs of neurodegeneration. To test these hypotheses, I completed the following aims:

Aim 1: Identify the effect of long-term exposure to elastin haploinsufficiency in cerebrovascular dysfunction and cognitive decline. We found that long-term exposure to elastin haploinsufficiency causes aortic wall remodeling, impairs spatial memory, and may contribute to higher levels of neuroinflammation. Also, there are differences in how this long-term exposure to elastin haploinsufficiency affects males compared with females.

Aim 2: Determine the effect of a collagen cross-link breaker on mitigating age-related large artery stiffness, cerebrovascular dysfunction, and cognitive impairment. We found that long-term treatment with ALT-711 in old mice did not reduce large artery stiffness, preserve endothelial function, or lower collagen crosslinking. We found that cerebral artery stiffness is related to endothelial dysfunction and cognitive dysfunction in old mice.

Aim 3: Identify the effect of mitochondrial antioxidant treatment on attenuating age-related large artery stiffness, cerebrovascular dysfunction, and Alzheimer's disease (AD)-like pathology. The main takeaways from this study are that treatment with the mitochondrial targeted antioxidant (MitoQ) in an AD mouse model showed therapeutic potential for mitigating cognitive impairment. MitoQ treated mice also showed modest beneficial effects on vascular function.

Overall, these studies demonstrate that therapeutic intervention to prevent age-related cerebral artery dysfunction could be a promising target for reducing cognitive impairment and

signs of neurodegenerative disease. Reducing cerebral artery stiffness and promoting mitochondrial health have positive effects on cerebrovascular and cognitive function.

CURRICULUM VITAE

NAME OF AUTHOR: Emily Hope Reeve

GRADUATE AND UNDERGRADUATE SCHOOLS ATTENDED:

University of Oregon, Eugene, OR
Ursinus College, Collegeville, PA

DEGREES AWARDED:

Doctor of Philosophy, Human Physiology, 2025, University of Oregon
Master of Science, Human Physiology, 2021, University of Oregon
Bachelor of Science, Health & Exercise Physiology, 2019, Ursinus College

AREAS OF SPECIAL INTEREST:

Vascular function
Aging
Large artery stiffness
Neurodegenerative disease

PROFESSIONAL EXPERIENCE:

Graduate Employee, Department of Human Physiology, University of Oregon, 2021 – Present.

Graduate Teaching Fellow, Department of Human Physiology, University of Oregon, 2019 -2021

Teaching Assistant, Department of Health & Exercise Physiology, Ursinus College, 2018-2019

Undergraduate Research Student, The HEART Lab, Ursinus College, 2017 - 2019

GRANTS, AWARDS, AND HONORS:

OSLER TL1 (TL1TR002371) Fellowship, University of Oregon / Oregon Health & Sciences University 2023 - 2025

General University Scholarship, University of Oregon, 2022
Promising Scholar, University of Oregon, 2020

First year merit award, University of Oregon, 2019-2020

PUBLICATIONS:

1. **Reeve EH**, Barnes JN, Moir ME, Walker AE. Impact of arterial stiffness on cerebrovascular function: a review of evidence from humans and preclinical models. Am J Physiol Heart Circ Physiol. 2024 Mar 1;326(3):H689-H704. doi: 10.1152/ajpheart.00592.2023. Epub 2024 Jan 12. PMID: 38214904; PMCID: PMC11221809.
2. Feairheller DL, Smith M, Carty M, **Reeve EH**. Blood pressure surge with alarm is reduced after exercise and diet intervention in firefighters. Blood Press Monit. 2023 Jun 1;28(3):134-143. doi: 10.1097/MBP.0000000000000649. Epub 2023 Apr 12. PMID: 37070561; PMCID: PMC10132461.
3. Winder NR, **Reeve EH**, Kronquist EK, Khurana A, Lee B, Nguyen T, Henson GD, Walker AE. High pulse pressure impairs cerebral artery endothelial function in young, but not old, mice. Exp Gerontol. 2023 Mar;173:112101. doi: 10.1016/j.exger.2023.112101. Epub 2023 Jan 20. PMID: 36690049; PMCID: PMC9974894.
4. **Reeve EH**, Kronquist EK, Wolf JR, Lee B, Khurana A, Pham H, Cullen AE, Peterson JA, Meza A, Colton Bramwell R, Villasana L, Machin DR, Henson GD, Walker AE.

Pyridoxamine treatment ameliorates large artery stiffening and cerebral artery endothelial dysfunction in old mice. J Cereb Blood Flow Metab. 2023 Feb;43(2):281-295. doi: 10.1177/0271678X221130124. Epub 2022 Oct 2. PMID: 36189840; PMCID: PMC9903220.

5. Almeida, Andrew A. BS; **Reeve, Emily H. MS**; Dickinson, Rachel L. BS; Carty, Megan BS; Gilpin, Julia BS; Feairheller, Deborah L. PhD. Civilians Have Higher Adherence and More Improvements in Health With a Mediterranean Diet and Circuit Training Program Compared With Firefighters. Journal of Occupational and Environmental Medicine 64(6):p 488-494, June 2022. | DOI: 10.1097/JOM.0000000000002478.
6. **Reeve EH**, Picicci F, Feairheller DL (2021) Validation of a Mediterranean Diet Scoring System for Intervention Based Research. J Nutri Med Diet Care 7:053. doi.org/10.23937/2572-3278/1510053.
7. Winder NR*, **Reeve EH***, Walker AE. Large artery stiffness and brain health: Insights from Animal Models. *Am J Physiol Heart Circ Physiol,* 320:H424-H431, 2021 *Contributed equally

ACKNOWLEDGMENTS

I give my sincere gratitude to everyone who has supported me throughout completion of my dissertation. I give my deepest gratitude to my doctoral advisor, Dr. Ashley Walker, for helping me grow as a student and scientist. Dr. Walker has guided me through my Master's thesis, and now my doctoral dissertation. Thank you for believing in me and my abilities to grow as a researcher and person. Thank you for pushing me to think critically about science and the way I view the world. The scientist I am today is because of your care and mentorship, which has been invaluable to me. To my committee members, Dr. John Hallwill, Dr. Christopher Minson, and Dr. Emily Sylwestrak, thank you for providing me with feedback on my dissertation project. Thank you for being flexible with my timeline and supporting my ideas with this work. Your time and guidance have helped make this dissertation great.

Thank you to the research animals who have sacrificed themselves not just for this project, but all noble research endeavors that make scientific discoveries possible. I wish to acknowledge the incredible animal care staff at University of Oregon who have cared for all of the research animals used in this study. Thank you to the OSLER TL1 training fellowship at Oregon Health and Sciences University for the opportunity to pursue my research questions and University of Oregon for providing me with the resources and funding to be successful.

Lastly, thank you to all of my colleagues and undergraduate students who have made data collection and analysis possible for this project. Science is a collaborative affair, and I wouldn't have been able to make this possible without you all.

DEDICATION

I would like to dedicate this dissertation to my five-year-old self. This degree has taught me things I never knew and shown me aspects of myself unseen. I have grown into a scientist that my former self would admire. This dissertation taught me that I can achieve way more than I dare to even dream, and I hope the five-year-old version of myself never stops dreaming.

Table of Contents

DISSERTATION ABSTRACT 3
CURRICULUM VITAE 6
PUBLICATIONS 7
ACKNOWLEDGMENTS 9
LIST OF FIGURES 13
2. Figure 2.2 42 13
LIST OF TABLES 15
1. Table 2.1 40 15
2. Table 3.1 77 15
I. INTRODUCTION 16
1.1 Specific Aims 16
Aim #1: Identify the effect of long-term exposure to elastin haploinsufficiency in cerebrovascular dysfunction and cognitive decline 17
Aim #2: Determine the effect of a collagen cross-link breaker on mitigating age-related large artery stiffness, cerebrovascular dysfunction, and cognitive impairment 17
Aim #3: Identify the effect of mitochondrial antioxidant treatment on attenuating age-related large artery stiffness, cerebrovascular dysfunction, and AD-like pathology 18
1.2 Literature Review 19
1.2.1 Aging 19
1.2.2 Neurodegenerative Diseases 20
1.2.3 Large Artery Stiffness 21
1.2.6 Large artery stiffness and cerebrovascular dysfunction 23
1.2.7 Endothelial Dysfunction 24
1.2.8 Vascular Mitochondrial Dysfunction 25
1.2.9 AGEs and vascular dysfunction 26
1.2.10 Therapeutic Strategies to Combat Vascular Dysfunction 27
1.2.11 Gap in Knowledge 28
1.3 Purpose of this Dissertation 29
II. SEX MEDIATES THE EFFECTS OF LONG-TERM ELASTIN HAPLOINSUFFICIENCY ON LARGE ARTERY, CEREBRAL ARTERY, AND COGNITIVE FUNCTION 31
2.1 Introduction 31

2.2 Methods 32
2.3 Results 38
2.4 Discussion 62
2.5 Limitations 68
2.6 Conclusion 68
III. LARGE ARTERY STIFFNESS AND CEREBROVASCULAR FUNCTION ARE UNALTERED WITH LONG-TERM TREATMENT OF COLLAGEN CROSSLINK-BREAKER, ALAGEBRIUM CHLORIDE (ALT-711) 70
3.1 Introduction 70
3.2 Methods 71
3.4 Discussion 82
3.5 Limitations 85
3.6 Conclusion 85
IV. PROTECTIVE EFFECTS OF MITOQUINOL MESYLATE (MITOQ) ON VASCULATURE AND COGNITION IN AN ALZHEIMER'S DISEASE MOUSE MODEL. 86
4.1 Introduction 86
4.2 Methods 89
4.3 Results 96
4.4 Discussion 117
4.5 Limitations 121
4.6 Conclusion 121
V. DISCUSSION 122
5.1 Summary and Conclusions of Chapter I 122
5.2 Summary and Conclusions of Chapter II 122
5.3 Summary and Conclusions of Chapter III 122
5.4 Summary and Conclusions of Chapter IV 123
5.5 Future Directions 123
5.6 This Dissertation in a Paragraph 124
VI. REFERENCES 125

LIST OF FIGURES

Figure Page

1. Figure 2.1 38
2. Figure 2.2 41
3. Figure 2.3 42
4. Figure 2.4 44
5. Figure 2.5 45
6. Figure 2.6 47
7. Figure 2.7 49
8. Figure 2.8 51
9. Figure 2.9 53
10. Figure 2.10 55
11. Figure 2.11 57
12. Figure 2.12 58
13. Figure 2.13 59
14. Figure 2.14 60
15. Figure 3.1 73
16. Figure 3.2 75
17. Figure 3.3 77
18. Figure 3.4 78
19. Figure 4.1 86
20. Figure 4.2 98

21. Figure 4.3 99
22. Figure 4.4 99
23. Figure 4.5 101
24. Figure 4.6 102
25. Figure 4.7 103
26. Figure 4.8 104
27. Figure 4.9 105
28. Figure 4.10 106
29. Figure 4.11 107
30. Figure 4.12 108
31. Figure 4.13 110
32. Figure 4.14 111
33. Figure 4.15 112
34. Figure 4.16 113

LIST OF TABLES

Table Page

1. Table 2.1 39

2. Table 3.1 74

3. Table 4.1 94

4. Table 4.2 96

I. INTRODUCTION

1.1 **Specific Aims**

The prevalence of age-related disease has multiplied in recent years, with dementia predicted to increase substantially by 2050. While previous research has focused on neuronal signaling, recent research suggests a strong link between age-related cardiovascular dysfunction and Alzheimer's disease (AD), a major neurodegenerative disease. The aging process causes increased stiffness in large elastic arteries, that elevates pulse pressure and risks damage to vulnerable target organs like the brain. Elevated pulse pressure damages the cerebrovasculature, ultimately limiting blood flow and contributing to neuroinflammation. An age-related increase in large artery stiffness is predictive of cognitive impairment as well as AD prevalence and progression. Large artery stiffness is also strongly correlated with amyloid-β burden, an important biomarker implicated in AD. However, the causative effect of large artery stiffness and potential therapeutic effect of large artery stiffness attenuation on cerebrovascular function, cognitive function, and AD progression has yet to be understood. Without a clear understanding of the mechanisms by which age-related vascular dysfunction influences cognitive impairment or AD, the promise of effective therapeutic targets to mitigate neurodegenerative diseases is restricted.

The primary objective of this project is to better characterize the role that age-related large artery stiffness plays in influencing cerebrovascular dysfunction and cognitive impairment. A secondary objective is to investigate potential therapeutic mechanisms by which attenuating age-related large artery stiffness can delay neurodegenerative onset or progression. Preliminary data using a mouse model of large artery stiffness reveal that the physiological processes of aging and large artery stiffness synergistically lead to cerebrovascular dysfunction and increased biomarkers of neuroinflammation. Furthermore, attenuation of age-related large artery stiffness via

antioxidant activity mitigated cerebrovascular dysfunction in aged wildtype mice. Therefore, our working hypothesis is that long-term exposure to large artery stiffness increases the severity of cerebrovascular dysfunction and cognitive impairment, but attenuation of these processes during aging could delay neurodegenerative onset, progression, or extremity.

Aim #1: Identify the effect of long-term exposure to elastin haploinsufficiency in cerebrovascular dysfunction and cognitive decline. I hypothesize that long-term exposure to large artery stiffness will stimulate the greatest amounts of cerebrovascular dysfunction and cognitive impairment compared to short-term or controlled exposure to large artery stiffness. To test this hypothesis, I will use a mouse model of congenital large artery stiffness (Elastin heterozygote knockout, $Eln^{+/-}$) and wildtype genotype ($Eln^{+/+}$) in an old (24 months) group and young (6 months) group. I will compare the effects of age, genotype, and their interaction, on a) large artery stiffness, b) cerebrovascular function, and c) cognitive function.

Aim #2: Determine the effect of a collagen cross-link breaker on mitigating age-related large artery stiffness, cerebrovascular dysfunction, and cognitive impairment. I hypothesize that long-term treatment with the collagen cross-link breaker, Alagebrium Chloride (ALT-711), will prevent age-related, large artery stiffness, cerebrovascular dysfunction, and cognitive impairment. To test this hypothesis, I will use aged (20-24 months old) C56BL/6 mice and measure the following in mouse either treated or untreated daily with ALT-711, a) aorta and carotid artery stiffness, b) assessment of endothelial function, structure, and markers of oxidative stress and inflammation in cerebral arteries and c) cognitive function testing and neuroinflammatory measurements.

Aim #3: Identify the effect of mitochondrial antioxidant treatment on attenuating age-related large artery stiffness, cerebrovascular dysfunction, and AD-like pathology. I hypothesized that long-term treatment with a mitochondrial antioxidant (MitoQ), will mitigate age-related large artery stiffness, cerebrovascular dysfunction, and AD-like pathology. To test this hypothesis, a mouse model of late-onset AD received either mitochondrial antioxidant treatment (4 months) or vehicle in drinking water. Among treated and untreated groups, I compared the extent of A) age-related large artery stiffness, B) cerebrovascular dysfunction, and C) cognition impairment and biomarkers of AD-like pathology.

The aims studied in this project elucidate the role of large artery stiffness and its associated mechanisms as a causal component of age-related cerebrovascular and cognitive dysfunction. Additionally, results from these studies will inform future research on potential therapeutics and/or their targets to combat vascular aging and neurodegenerative diseases.

1.2 Literature Review

1.2.1 Aging

Societal advancements in sanitation, medical technology, and healthcare knowledge have greatly increased the global lifespan (1). With the increasing lifespan, the phenomenon of aging has emerged, along with an increase in age-related chronic disease. Aging is characterized by progressive physiological changes to cells, tissues, and organ systems over time that ultimately impair their ability to carry out proper functions. Prominent biological hallmarks of aging include time-dependent and environmental modifications resulting in DNA damage, cellular senescence, mitochondrial dysfunction and impaired intercellular communication among others (2–4). Oxidative stress and chronic inflammation have emerged as mechanisms that underlie these adverse biological changes with age (5, 6). Superoxide levels increase with age and are known to be linked to aging-related diseases, notably cardiovascular disease and neurodegenerative diseases (7). These physiological changes over time lead to greater dysfunction at the tissue and organ level in multiple body systems, contributing to the development of chronic disease. Understanding the biological processes involved in aging is critical to understanding pathological etiology since aging is one of the strongest risk factors for complex diseases such as cancers, cardiovascular disease, and neurodegenerative disease.

While the field of aging research is growing, diseases are multifaceted, and the mechanisms by which aging contributes to the development of chronic disease are still poorly understood. The economic burden of disease continues to grow with the aging population. However, discovering therapeutic targets to combat the aging process is a promising area of research that will influence treatment and prevention strategies for age-related disease

development and benefit human well-being (8). Thus, further research on the mechanisms of aging and age-related disease manifestation is essential for improving the health span of people worldwide.

1.2.2 Neurodegenerative Diseases

A major category of age-related diseases expected to grow in prevalence is neurodegenerative diseases. Neurodegenerative diseases are chronic diseases that are characterized by the progressive loss of neuronal tissue and function. Dementia is an umbrella term describing a disease with many different etiologies. Examples of dementia are AD, vascular dementia, mixed dementia, Lewy Body dementia, etc. These diseases ultimately impair memory and functional abilities of the brain, negatively impacting activities of daily living. Currently, there are no known effective treatments or interventions to help prevent the onset or delay the progression of dementia and its main symptom, cognitive impairment.

While decades of research have been focused on mechanisms of AD pathology in neuronal tissue, recent evidence suggests that vascular dysfunction strongly contributes to dementia onset. Over 50% of individuals with AD have a co-morbidity diagnosis of Vascular Dementia. To continue, age-related changes to vascular function can be identified as soon as a decade prior to symptoms of AD. This finding highlights the importance of understanding age-related changes to vascular function, with the possibility of identifying therapeutic targets of disease.

1.2.3 Large Artery Stiffness

One prominent change to the vascular system with age is increases in large artery stiffness (9, 10). Large arteries, namely the aorta and carotid arteries, remodel with age. Young, healthy large arteries contain a high ratio of elastin content compared to collagen (11). This unique structural feature of large arteries serves to protect the systemic circulation from damage. While important for all arteries, elastin is especially crucial in large arteries to attenuate pulse pressure (12). The higher elastin content in healthy large arteries allows them to expand during systole and recoil during diastole. This function protects target organs by damping pulse pressure. Importantly for this dissertation, the brain is a low pressure, high flow environment where undamped high pulse pressures can cause impairment.

When evaluating arterial stiffness, it is important to account for both active components and passive components of stiffness. Active components of large artery stiffness are determined largely by contributions made by the vascular smooth muscle cells (VSMC) vasoconstriction. Passive components are determined by the content that makes up the extracellular matrix of the arterial wall. The content of elastin, collagen, and other proteins contribute to the absolute stiffness of the artery and can be assessed when smooth muscle activity, blood pressure, and heart rate are controlled experimentally.

Understanding the multiple contributors of arterial stiffness helps inform research to understanding its role in development of disease. The accepted gold standard for measuring large artery stiffness is a technique known as pulse wave velocity (PWV) (13). PWV assesses arterial stiffness of large arteries, mainly the aorta, by determining the time it takes for a pulse wave to traverse a set distance. In animal models it is traditional to measure the transit time between the aortic arch to the abdominal aorta. In human studies, PWV has been strongly correlated with

cognitive impairment and potential cognitive decline (13, 14). Therefore, it is hypothesized that finding ways to prevent age- related large artery stiffening will also prevent cognitive decline or impairment associated with aging.

Mechanisms of Large Artery Stiffness

A combination of changes to both the active and passive factors lead to the stiffening of large arteries with aging and disease. Changes in vascular tone, leading to increased VSMC constriction, is an important factor that influences the stiffness of arteries (15). With aging, VSCM can become hyperactive to vasoconstrictor stimuli, such as endothelin-1 (ET-1), leading to an increase in vascular tone (16, 17).

Structural changes to the arterial wall also cause stiffening of large arteries. Increased collagen: elastin ratio, increased elastin fragmentation, and collagen cross-link formation are all contributing factors to the stiffening of the large arteries (11, 12). Elastin proteins become fragmented with aging, which decreases the ability of these proteins to absorb pressure exerted on the arterial walls. Elastases such as matrix metalloproteinase (MMP) 9, are upregulated with age, causing the degradation of elastin (18). Structural changes to collagen content also contribute to large artery stiffness. Excess pressure on the arterial wall stimulates production of reactive oxygen species (ROS), propagating a cell signaling cascade that upregulates collagen production. While collagen is important for maintaining the structural integrity of the arterial wall, an imbalance in the ratio of elastin and collagen proteins forces collagen to bear the weight of increased pressure on the wall without the benefit of damping pulse pressure. In addition to increased collagen content, collagen proteins become glycated, forming cross-links with one another. These cross-links further increase the structural rigidity of collagen, ultimately

increasing the stiffness of the arterial wall. Advanced glycation end-products (AGEs) are known to contribute to increased large artery stiffness by inducing collagen cross-linking (19–21).

1.2.6 Large artery stiffness and cerebrovascular dysfunction

As large arteries stiffen, compliance decreases, and the ability to attenuate high pulse pressure from the left ventricle weakens (22, 23). As a result, higher than normal pulse pressure (PP) is translated to smaller arteries and microvasculature that are not equipped to handle this extra stress. Higher than average PP leads to increased uniaxial circumferential stress on vessel walls and an increase in mechanical stretch to the endothelium (22, 23). Recent evidence suggests the increase in mechanical stretch on endothelial cells leads to higher levels of inflammation (22, 24–26). Overall, large artery stiffness leads to increased pulse pressure to cerebral arteries and risk of cerebrovascular dysfunction.

Cerebrovascular dysfunction has been found to be associated with cognitive impairment in both aging humans and animal models (8, 23). The brain, although relatively small in body mass compared to the rest of the body, requires approximately 20% of all the body's cardiac output. Brain tissue has virtually no capacity for energy storage and therefore depends on a consistent, continuous, and tightly regulated supply of blood flow to receive appropriate amounts of oxygen, glucose, and other nutrients to function (14). Even slight deviations of this highly regulated system can lead to damage or dysfunction. Specifically, aging-related dysregulation of cerebral blood flow appears to be the main culprit in cognitive decline (14). In addition, cerebrovascular endothelial dysfunction causes impairment of the blood brain barrier (BBB). Increased BBB permeability involves the disruption of tight junctions between endothelial cells, allowing neurotoxic chemical to cross into the brain causing neuroinflammation or damage (27).

Increased bio-markers of inflammation and oxidative stress were strongly correlated with lower cognitive scores in elderly individuals (28). By preventing large artery stiffness, cerebral arteries can be spared from excessive pulse pressure and the risk for cerebrovascular damage can decrease.

1.2.7 Endothelial Dysfunction

Endothelial dysfunction is an age-related change to the vasculature, potentially caused by the increased arterial stiffness, that contributes to AD pathology. Endothelial cells are the single cell inner layer of blood vessel walls that are essential for intercellular communication and blood flow regulation. Endothelial cells secrete both endogenous vasoconstrictors and vasodilators to regulate blood flow (29–32). When activated by shear stress or signaling molecules, the enzyme endothelial nitric oxide synthase (eNOS) produces nitric oxide (NO), a potent vasodilator, causing smooth muscle to relax. This response is known as endothelium-dependent dilation (EDD). This signaling cascade regulates localized blood flow, and this is essential in the brain, which relies on this regulation to rapidly adjust the supply of nutrients to active regions of the brain. Poor EDD ultimately impairs cerebral blood flow to working tissue (33, 34). Previous research shows that NO bioavailability decreases with age in humans, demonstrating further importance of investigating the mechanisms of vascular aging in the context of chronic disease (35). This decrease in NO bioavailability with aging can also influence the response to vasoconstrictors.

Understanding the actions of ET-1 is an important component of understanding the endothelial dysfunction seen with age. ET-1 is an endothelial cell-derived protein that causes vasoconstriction. ET-1 increases with age, contributing to the increases seen in vascular tone (16,

17). NO is a natural inhibitor of ET-1, thus decreases in NO bioavailability may contribute to greater vasoconstriction by decreased inhibition of the constrictor response (36).

ROS, such as superoxide and hydrogen peroxide, also play a role in the decline in EDD with aging. Trott et al. showed that the superoxide scavenger 4-Hydroxy-TEMPO (TEMPOL), and the NADPH oxidase (NOX) inhibitor, apocynin, improved EDD to acetylcholine (ACh) in old mice but blunted dilation in young mice (37). Additional studies have shown that NOX2 up-regulation plays an important role in endothelial dysfunction (38–40). ROS acts to inhibit EDD by sequestering NO, rendering it inactive and unable to communicate with surrounding smooth muscle (41, 42). In sum, endothelial dysfunction can be characterized by impairments in EDD that involve the reduction of NO bioavailability, with contributions from ROS.

1.2.8 Vascular Mitochondrial Dysfunction

One biological theory of aging is mitochondrial dysfunction theory. Mitochondria are important for cellular metabolism and energy production, but they also are a major contributor to the state of oxidative stress. For this reason, the health of vascular cell mitochondria is crucial for maintaining proper vascular function. Damage to vascular mitochondria can have severe ramifications on the cardiovascular system, often leading to diseased states (43). Dysfunctional mitochondria can impair vascular endothelial cell function by increasing circulating ROS and reducing NO bioavailability. Additionally, increases in mitochondrial ROS production contribute to an inflammatory cellular environment, creating a vicious cycle with further damage (44). However, more research is needed to understand how controlling mitochondrial derived ROS may preserve vascular and endothelial cell health. For now, a mitochondrial specific antioxidant such as Mitoquinone Mesylate (MitoQ) shows promising therapeutic potential.

1.2.9 AGEs and vascular dysfunction

AGEs are known to contribute to increased large artery stiffness by inducing collagen cross-linking (19–21). AGEs form via non-enzymatic glycation reactions of proteins and fats with circulating blood glucose (19, 45, 46). AGEs can form as protein cross-links in the extracellular matrix, or as free molecules that interact with their receptor (RAGE), to stimulate pro-inflammatory intracellular signaling cascades (19, 20). Collagen cross-linking, formed by the joining of two collagen proteins with a di-carbonyl compound, is a significant contributor to arterial stiffening with age (21, 47).

Multiple types of AGEs have been identified. Among them, the most studied have been the AGEs precursors, carboxymethyl lysine (CML) and carboxyethyl lysine (CEL). In fact, plasma levels of CML increase with age (48). Research shows increased AGEs accumulation in the large arteries of aged mice (49). AGEs are further implicated in vascular function as treatment with a RAGE inhibitor increased EDD in aged rat aortas (50). High levels of AGEs in arterial walls quench NO, reducing bioavailability and ultimately decreasing EDD (51). Thus, a reduction in collagen cross- links or the production of AGEs is a hopeful target for mitigating vascular aging (52–54).

1.2.10 Therapeutic Strategies to Combat Vascular Dysfunction

One therapeutic strategy to target vascular aging is the prevention or attenuation of increased large artery stiffness. Since large artery stiffness is implicated in many age-related diseases, particularly neurodegenerative disease, it's hypothesized that reducing large arteries stiffness is a promising approach to mitigating neurodegenerative disease. In a previous study, I used pyridoxamine, a form of vitamin B6, to prevent age-related increases in arterial stiffness.

Pyridoxamine was previously shown to inhibit the formation of AGEs. In my MS degree project, I found that long-term pyridoxamine treatment prevented increases in large artery stiffness, lowered blood pressure, and preserved cerebral artery endothelial function (52). However, in that study, I did not find a reduction in AGEs with pyridoxamine treatment, leading me to believe that these effects were mainly attributed to pyridoxamine's antioxidant actions (55, 56). Thus, other therapeutic strategies to prevent age-related increases in arterial stiffness are needed.

ALT-711 is a collagen cross-link breaker that breaks carbon-carbon bonds between AGEs and collagen, thereby reducing arterial stiffness both in animal models and some human trials (47, 57–61). ALT-711 is both a safe and effective drug that has previously been approved for clinical trials, thus making the outcomes of this project more translatable to the human population than other AGE formation inhibitors (59). Currently, no published studies have identified the effects of ALT-711 on cerebrovascular function and cognitive function. After successful completion of this research, my contributions will have great potential to introduce ALT-711 as a novel therapeutic for aging, cerebrovascular dysfunction, and neurodegenerative disease.

A mitochondrial specific antioxidant such as Mitoquinone Mesylate (MitoQ) shows promising therapeutic potential for mitigating cerebrovascular dysfunction and neurodegenerative disease (62). MitoQ is a mitochondrial targeted antioxidant that is a modified coenzyme Q10 molecule with a lipophilic cation attached. This ensures MitoQ can enter the mitochondrial membrane. MitoQ is reduced to mitoquinol which can then scavenge ROS and prevent lipid peroxidation. MitoQ has shown beneficial effects on the aging vasculature in both mice and humans by reducing large artery stiffness and improving endothelial function (63–66).

The potential beneficial effects of MitoQ on the cerebrovasculature have not previously been investigated.

1.2.11 Gap in Knowledge

There are still no drugs or therapeutics available to prevent or delay the onset of AD. Targeting vascular dysfunction, particularly the increases in arterial stiffness and cerebrovascular dysfunction with age, are potential therapeutic strategies to mitigate the onset and/or severity of AD. However, a gap in knowledge exists as to the impacts of elastin haploinsufficiency, and cerebrovascular dysfunction on the brain, particularly when considering age and sex differences. Furthermore, there remains a need to identify therapeutic strategies to reduce age-related vascular dysfunction and thereby mitigate AD.

1.3 Purpose of this Dissertation

The overarching purpose of this dissertation is to identify mechanisms by which age-related large artery stiffness and cerebrovascular dysfunction leads to cognitive impairment. This dissertation also explores potential therapeutics to target vascular aging. By investigating mechanisms of vascular dysfunction with age in the context of AD, potential therapeutic targets could be discovered that will influence future treatments or interventions.

Aim 1 of my dissertation used a genetically modified mouse model to better understand how both the short-term and long-term exposure to elastin haploinsufficiency impairs cerebrovascular and cognitive function. Additionally, this aim seeks to understand sex differences implicated in elastin haploinsufficiency and the related consequences to cognitive

impairment. Additionally, isolating the effects of both short- and long-term elastin haploinsufficiency on cerebrovascular function is a novel

The second study of my dissertation used an aged rodent model to determine if reductions in large artery stiffness with age can preserve cerebrovascular function and cognitive function. ALT-711 is an FDA approved drug that breaks the collagen crosslinked AGEs found in arteries. The purpose of Aim 2 was two-fold, 1) Determine if breaking collagen crosslinking can result in reduced large artery stiffness, 2) Determine the therapeutic potential of ALT-711 in preventing or delaying cognitive decline and cerebrovascular impairment with aging.

The final aim of my dissertation is to investigate a different therapeutic treatment targeting mitochondrial oxidative stress. For this aim, I used a rodent model displaying time-dependent, AD-like pathology. I supplemented the mice with MitoQ to prevent mitochondrial ROS production, and measured the effects of the mitochondrial antioxidant on arterial stiffness, cerebrovascular function, and AD pathology.

II. SEX MEDIATES THE EFFECTS OF LONG-TERM ELASTIN HAPLOINSUFFICIENCY ON LARGE ARTERY, CEREBRAL ARTERY, AND COGNITIVE FUNCTION.

2.1 Introduction

In humans, elastin insufficiency can lead to adverse cardiovascular effects like supravalvular aortic stenosis and aortic aneurysm (11, 67). Elastin is an extracellular matrix protein that is prone to degradation with age. Elastin degradation and fragmentation are contributing factors to the age-related increase in large artery stiffness (12, 22). Increased large artery stiffness is strongly associated with target organ damage and disease, notably in the brain (14, 68). But, understanding the role that elastin plays in vascular dysfunction and cognitive impairment could be crucial in determining the root cause of age-related neurodegenerative disease. Therefore, further research into the implications of elastin haploinsufficiency on brain health is the focus of this study.

Elastin is a critical extracellular matrix protein located throughout the body. In the wall of large arteries, elastin helps damp pulse pressure. A transgenic mouse model displaying elastin haploinsufficiency ($Eln^{+/-}$) exhibits reduced elastin production, increased aortic stiffness, and systolic blood pressure (69–71). Additionally, in this model, elastin haploinsufficiency causes cerebral artery endothelial dysfunction (72). This endothelial dysfunction contributes to neuroinflammation and development of neurodegenerative disease. Thus, it is important to further study the mechanisms of haploinsufficiency on cerebrovascular and cognitive function.

The effects of chronic exposure of elastin haploinsufficiency on cerebrovascular function have not been investigated. Additionally, there may be sex differences in the response to short-term and long-term elastin haploinsufficiency on cerebrovascular and cognitive function outcomes. Vascular dysfunction and neurodegenerative disease progression in females is more

rapid than males, presumably due to the loss of the protective actions of estrogen on the vasculature (73, 74). It is unknown how males and females may adapt differently to this elastin deficiency.

The primary objective of this study was to characterize the interactive effect of age and elastin haploinsufficiency on large artery stiffness, and cerebrovascular and cognitive function. A secondary objective of this study was to investigate sex differences in these outcomes. We hypothesized that $Eln^{+/-}$ mice would have greater large artery stiffness, cerebrovascular dysfunction, and cognitive impairment compared to $Eln^{+/+}$ mice. We also hypothesized that old $Eln^{+/-}$ mice would have the greatest impairment in function. Second, we hypothesized females would have greater impairments at old ages but similar or better function at young ages compared with males.

2.2 Methods

Mouse Model

We used a transgenic mouse model, with a heterozygote deletion of exon 1 of the elastin gene, $Eln^{+/-}$, displaying reduced elastin haploinsufficiency. In previous studies with this mouse model, $Eln^{+/-}$ mice had less total elastin protein (~50%) compared to their wildtype counterparts (70, 75). In this study we had 4 primary groups 1) young (6 months) $Eln^{+/+}$, 2) young $Eln^{+/-}$, 3) old (24 months) $Eln^{+/+}$, and 4) old $Eln^{+/-}$. All mice were fed a normal chow diet (Lab Diet, PicoLab Rodent Diet 20, 5053), with *ad libitum* access to food and water. Animals were housed in an animal care facility on a 12/12-hour light-dark cycle at 24°C. Investigators were blinded to age, genotype, and sex of the mouse when analyzing data. All animal procedures conform to the *Guide to the Care and Use of Laboratory Animals* (8th edition, revised 2011) and were

approved by the Institutional Animal Care and Use Committees at the University of Oregon.

Tissue Collection

At the time of study, mice were anesthetized via isoflurane and euthanized via cardiac puncture in accordance with IACUC guidelines. After euthanasia, the heart, liver, spleen, soleus, gastrocnemius (gastroc), and white adipose tissue (WAT) were collected, and their wet weights were recorded. Additionally, the carotid artery, aorta, cerebral cortex, and hippocampus were excised and frozen in −80°C for preservation. The right hemisphere was fixed in 4% paraformaldehyde solution in phosphate buffered saline (PBS) for 48 hours, then transferred to PBS and stored at 4°C until future use.

Pulse Wave Velocity (PWV)

To assess large artery stiffness, we measured *in vivo* PWV on all mice within 1 month prior to study (76, 77). Mice were anesthetized by 2% inhaled isoflurane in 100% oxygen and situated on a temperature-controlled heating pad (37°C) to maintain body temperature. The distal part of the fore and hind limbs were placed on electrodes to record ECG information, while 20 MHz Doppler transducers were placed on the aortic arch and abdominal aorta. Indus Doppler Flow Velocity System (Webster, Texas) was used to record and analyze data. The time for each beat to travel from aortic arch to abdominal aorta was measured and was divided by the distance between the two locations to determine the PWV value. Two researchers analyzed the same PWV files and data were averaged. Inter-research variability for all averages were <10% difference.

Passive Stiffness

Following a 60-minute incubation in calcium free solution to eliminate effects of myogenic tone, passive arterial stiffness was measured *ex vivo* in carotid arteries and posterior cerebral arteries (PCAs). Lumen diameter and medial wall thickness were measured following increasing intralumenal pressure (72, 78). Arteries were isolated and cannulated between glass pipette tips on a myograph as previously described (72). Measurements for each artery were recorded from 5 to 100 cmH_2O (3.7–73.5 mmHg) in 5 cmH_2O increments. Stress was calculated as:

$$\sigma = PD/2WT$$

where P is pressure in dyne cm^{-2}, D is lumen diameter and WT is wall thickness.

Strain was calculated as:

$$\varepsilon = (D - Di)/Di$$

where D_i is the initial starting diameter.

Data for each artery were fit to the curve:

$$\sigma = \sigma i e^{\beta \varepsilon}$$

where σ_i is the initial starting stress (5 cmH_2O) and β is the slope of tangential elastic modulus versus stress. A higher β represents a stiffer artery (79–81).

Aorta Histology

Sections of thoracic aorta and carotid arteries were frozen in optimal cutting temperature (OCT) compound and then sliced into 8 μm sections using a cryostat (Nikon, Minato, Tokyo,

Japan) and adhered to a charged slide (72). A Masson's Trichrome stain was used to quantify media and media + adventitial (M+A) layers of the arterial wall. Arterial wall thickness was analyzed using FIJI by ImageJ software. Collagen was assessed by immunofluorescence using a collagen 1 primary antibody (Abcam, AB270993, 1:250) for 2 hours followed by secondary antibody (Goat anti-Mouse IgG, Alexafluor 647, 1:1,000) for 1 hour. Aortas were imaged on a Deltavision widefield fluorescent microscope. Mean gray intensity was quantified for both collagen 1 and elastin (autofluorescent) in aortas using FIJI by ImageJ software.

Endothelial Function

Endothelium-dependent dilation (EDD) was assessed *ex vivo* in isolated, pressurized PCAs as previously described in detail (72). Briefly, PCAs were excised and placed in myograph chambers (DMT Inc.) with physiological salt solution containing 145 mM NaCl, 4.7 mM $CaCl_2$, 1.17 mM $MgSO_4$, 1.2 mM NaH_2PO_4, 5.0 mM glucose, 2.0 mM pyruvate, 0.02 mM EDTA, 3.0 mM MOPS buffer, and 1 g/100 mL BSA, pH 7.4 at 37°C, cannulated onto glass micropipettes and secured with nylon (11-0) sutures. Once cannulated, arteries were warmed to 37°C, pressurized to 50 mmHg, and allowed to equilibrate for approximately 1 hour. All arteries were submaximally preconstricted with phenylephrine (1-6 μM to obtain ~15-40% pre-constriction). Next, increases in luminal diameter in response to increasing concentrations of the endothelium-dependent dilator, acetylcholine (ACh, $1x10^{-9}$ to $1x10^{-4}$ M) and endothelium-independent dilator, sodium nitroprusside (SNP, $1x10^{-10}$ to $1x10^{-4}$ M) were determined. As a secondary outcome, tissues were then incubated in N omega-Nitro-L-arginine methyl ester hydrochloride (L-NAME, 0.1 mM for 30 minutes), to examine EDD after nitric oxide synthase

(NOS) had been inhibited. After L-NAME incubation, the same ACh dose-response protocol was used.

Cognitive Tests

We used a 2-day rotarod protocol to measurement motor coordination (47650 Rota-Rod NG, Ugo Basile, Gemonio, Italy). During the first day, mice were made to acclimate to the rotarod for 90 seconds at a rate of 4 rpm. On day two, mice were place on the rotarod increasing in speed from 4 – 40 rpms. Time was recorded when mice fell off or spun on the rod for 2 rotations. The average of 3 trials were recorded.

A nest building test was used to assess instinctual cognitive behavior (82). Mice were singly housed overnight in a cage with food, water, and a condensed cotton nestlet. In the morning, a researcher placed mice back in communal housing and scored each nest on a scale of 0–5 based on the quality of the nest.

The Morris Water Maze (MWM) cognitive test was used to assess learning and spatial memory. Mice underwent a 3-day training period, including 2 sessions per day, of 3 trials per session. On the fourth day, a probe trial was performed, followed by a beacon trial. All sessions were recorded and analyzed with EthoVision XT12 software (Noldus, Wageningen, the Netherlands) (83).

Gene expression

RNA from cerebral arteries and hippocampus was isolated by a standard protocol using Qiazol and RNAeasy Micro/Mini Kits (Qiagen, Hilden, Germany) and then quantified using a

NanoDrop 2000 (Thermo Fisher). Reverse transcription was performed to produce cDNA with a Qiagen Quantitect Reverse Transcription Kit. The cDNA samples underwent real-time qPCR using ThermoFisher PowerUp Sybr Green. RNA expression was calculated using the $2^{-\Delta\Delta CT}$ method. *18s* rRNA is a highly conserved gene encoding a ribosomal subunit, that was used as a housekeeping gene transcript to control for tissue concentration, and values were normalized to the young $Eln^{+/+}$ group. Specific genes measured include: NADPH oxidase (*Nox2*), superoxide dismutase (*Sod*)*1*, *Sod2*, *Sod3*, receptor for AGEs (*Ager*), interleukin 1β, (*Il1β*), and tumor necrosis factor (*Tnfα*).

Brain Histology

The right hemisphere was fixed in 4% paraformaldehyde/PBS solution for 48 hours. Samples were transferred to a 100% PBS solution and stored at 4°C until further use. Immunohistochemical stains were applied to paraffin sections after deparaffinization and antigen retrieval (5 min treatment at room temperature with 95% formic acid, followed by 30 min incubation in citrate buffer [pH 6.0] at 90°C). Tissue sections were blocked with 5% nonfat dry milk in phosphate-buffered saline and labeled with primary antibodies Glial fibrillary acidic protein (GFAP, 1:500, Proteintech, Cat: 16825-1-AP). Results were visualized after application of appropriate secondary antibodies using diaminobenzidine (DAB). Regions of the entorhinal cortex, hippocampus, and thalamus from these sections were imaged at 20x using a Leica Microscope (Leica, Wetzlar, Germany) and Leica LAS software. Cell count, size, and percent area were analyzed by the same researcher. For cell count, the particle count range was between 10 – 3000. Threshold. The cell size was determined by the size of the particle. For percent area, cells were quantified as ‘area fraction’ per region. One image per region of interest was acquired

for each animal. Images were analyzed using FIJI by ImageJ. On ImageJ, the brown image using the H-DAB deconvolution channel was used for analysis.

Statistical Analysis

Statistical analyses were performed using SPSS 26 (Armonk, NY), and Graphpad Prism 10. All data was assessed for normality. If data was not normal, the equivalent non-parametric test was used. For all gene expression data, the 2^{-ddct} value was transformed to $\ln(2^{-ddct}$ value) to normalize the data set. For EDD dose response curves and MWM train trials, a repeated measure analysis of variance (RM-ANOVA) was used and manually adjusted for multiple comparisons. For whole group, male, and female data. A 2-way ANOVA was used to compare the main effects for age, genotype, and interaction between the two variables. A Fisher's LSD was used for post-hoc comparisons on all 2-way ANOVA comparisons. All data is reported as mean±standard deviation (SD). On graphs, each dot represents a data point from one mouse.

2.3 Results

A conceptual display of the animal groups used in this study is represented in Figure 1. The were 4 main groups in this study using *Eln*$^{+/-}$ mice and their wildtype (*Eln*$^{+/+}$) littermates. Data from males and females in each group were separated and used for secondary analysis of

sex differences in relation to our primary question.

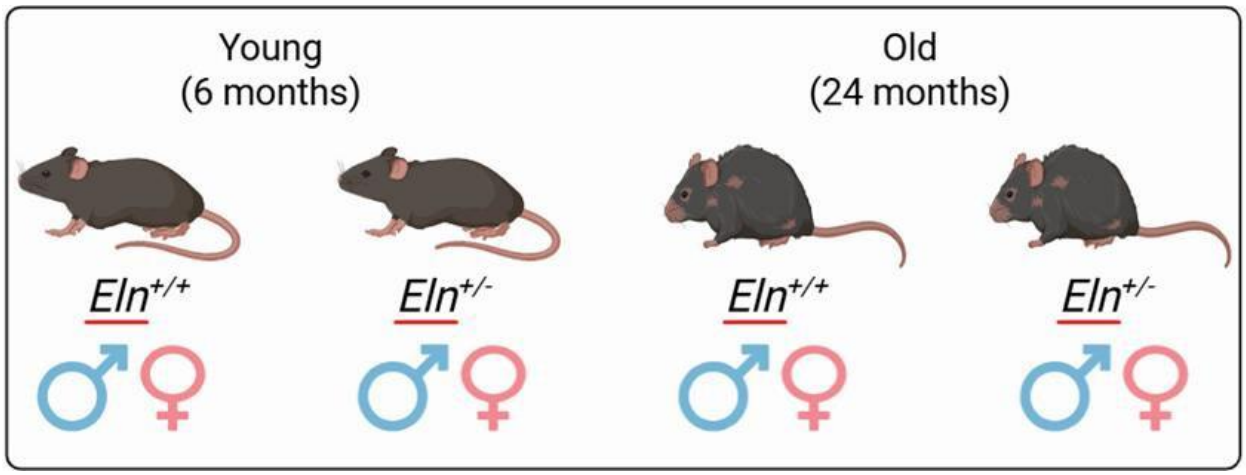

Figure 2.1 Study design for Chapter 2. This study investigated the effects of either, short-term exposure, or long-term exposure to elastin haploinsufficiency, on cerebrovascular function and cognitive impairment. This study uses *Eln* haploinsufficient ($Eln^{+/-}$) mice with $Eln^{+/+}$ mice serving as control.

Animal Characteristics

A detailed display of animal age, tissue weights, and frailty index (old animals only) can be found in Table 2.1.

Table 2.1 Animal Characteristics

Variable	Young				Old			
	Eln$^{+/+}$		*Eln*$^{+/-}$		*Eln*$^{+/+}$		*Eln*$^{+/-}$	
	Male	Female	Male	Female	Male	Female	Male	Female
n	18	12	12	14	17	17	11	12
Age (months)	6.3±0.3	6.4±0.4	6.5±0.7	5.62±1.2	23.9±0.2	24.1±0.6	24.0±0.2	24.0±0.5
Body mass (g)	30.4±2.1	23.3±1.4	30.4±2.0	24.0±1.6	36.2±3.9	33.3±6.2	34.4±4.3	29.7±4.6
Heart mass, mg	144±25	113±11	154±18	123±18	171±15	138±32	166±15	159±17
Percent heart :body mass	0.47±0.07	0.48±0.04	0.50±0.06	0.50±0.07	0.50±0.07	0.43±0.07	0.44±0.05	0.52±0.12
Liver mass, mg	1466±166	1008±214	1519±230	1202±202	2005±343	1637±525	1816±380	1476±251
Percent liver: body mass	4.78±0.56	4.33±0.90	5.00±0.64	4.86±0.67	5.64±0.91	4.85±1.0	4.89±0.66	4.75±0.94
Spleen mass, mg	80±11	89±11	90±14	93±13	126±66	171±130	101±33	126±29
Percent splee n:body mass	026±0.03	0.38±0.04	0.29±0.05	0.38±0.05	0.36±0.21	0.54±0.40	0.28±0.09	0.41±0.06
WAT mass, mg	762±276	586±165	691±292	532±190	1276±817	1552±805	1388±775	1392±793
Percent WAT: body mass	2.47±0.77	2.50±0.60	2.36±0.76	2.27±0.73	3.42±1.99	4.17±1.57	4.17±1.98	4.63±2.43
Gastroc mass , mg	170±22	133±24	156±39	128±24	154±27	128±17	161±21	129±14
Percent gastr oc:body mass	0.56±0.06	0.57±0.12	0.52±0.10	0.52±0.09	0.44±0.09	0.42±0.09	0.46±0.12	0.46±0.08
Soleus mass, mg	12±1.8	9±1.8	13±1.6	11±2.2	11±0.0	11±1.1	14.2±6.1	11.3±1.4
Percent soleu s: body mass	0.04±0.01	0.04±0.01	0.04±0.01	0.05±0.00	0.03±0.01	0.04±0.01	0.04±0.02	0.04±0.01
n	----	----	----	----	9	9	4	6
Frailty Index	----	----	----	----	0.29±0.05	0.28±0.09	0.27±0.08	0.31±0.06

Table 2.1 Animal Characteristics. Data are mean±SD. White adipose tissue (WAT), gastrocnemius (gastroc).

Large artery stiffness.

For aortic PWV, there was a main effect of age ($p=0.002$) and a main effect of genotype ($p<0.0001$, Fig. 2A). As expected, PWV was higher in old $Eln^{+/-}$ mice compared to young $Eln^{+/-}$ mice ($p=0.013$), with a strong trend for $Eln^{+/+}$ mice ($p=0.059$). Surprisingly, PWV was higher in young $Eln^{+/+}$ mice compared to young $Eln^{+/-}$ ($p=0.0001$), and old $Eln^{+/+}$ mice compared to old $Eln^{+/-}$ ($p=0.010$).

Amongst males, there was no main effect for age ($p=0.091$), but a main effect for genotype ($p<0.0001$) and interaction effect between two ($p=0.034$, Fig. 2B). In post-hoc analyses, this effect was present in young male $Eln^{+/+}$ mice compared to young male $Eln^{+/-}$ mice ($p<0.0001$) and young male $Eln^{+/-}$ mice compared to old male $Eln^{+/-}$ mice ($p=0.016$). In females, main effects of age ($p=0.01$) and genotype ($p=0.028$) were present (Fig. 2C). In post-hoc analysis, only old female $Eln^{+/+}$ mice had greater PWV compared with young female $Eln^{+/+}$ ($p=0.015$). All other comparisons were not significant ($p>0.05$). Overall, these data suggest that aortic stiffness was higher in old age and was higher in $Eln^{+/+}$ mice compared with $Eln^{+/-}$ mice, and these genotype effects were strongest in males.

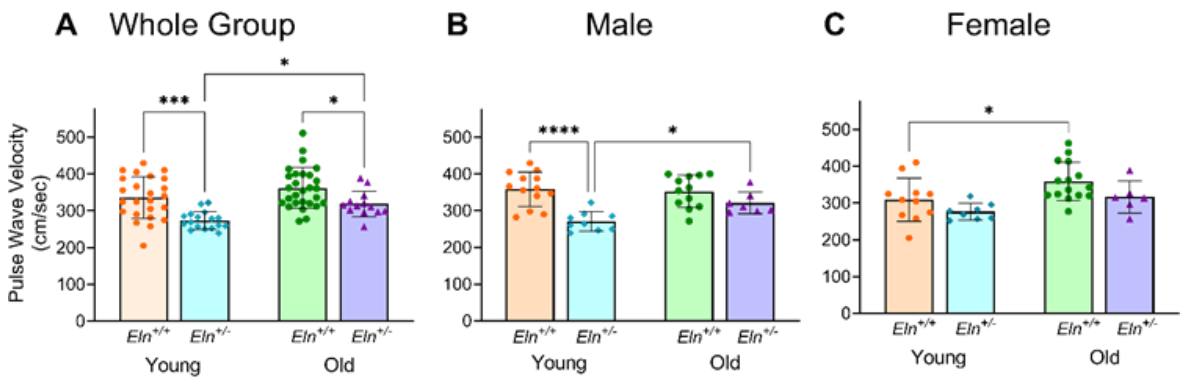

Figure 2.2 PWV increases with age but genotypic effects on PWV are sex specific. Comparison of pulse wave velocity in A) whole group, B) males, and C) females. Statistics include a 2-way ANOVA and Fisher's LSD test. Data are mean±SD. *p<0.05, ***p<0.001, ****p<0.0001.

We also investigated the passive properties of large artery stiffness by creating stress-strain curves for the carotid artery (Fig. 3A-C). There was no difference in carotid β-stiffness among any of the groups (p>0.05). In elastic modulus at low pressures, there was a main effect for genotype in the whole group (p=0.01). In the post-hoc analysis, old $Eln^{+/+}$ mice had greater EM than young $Eln^{+/+}$ mice (p=0.04). However, old $Eln^{+/-}$ mice had lower EM than old $Eln^{+/+}$ mice (p=0.01). In males, there was a genotype effect (p=0.04 in the elastic modulus at low pressures, showing old male $Eln^{+/-}$ mice have lower elastic modulus than old male $Eln^{+/+}$ mice (p=0.013). We found no other differences in β-stiffness, elastic modulus at low pressures or elastic modulus at high pressures in the whole group, males, or females (p>0.05 for all, Fig. 3A-C). These data suggest that passive properties of large artery stiffness are not impacted by elastin haploinsufficiency in this study.

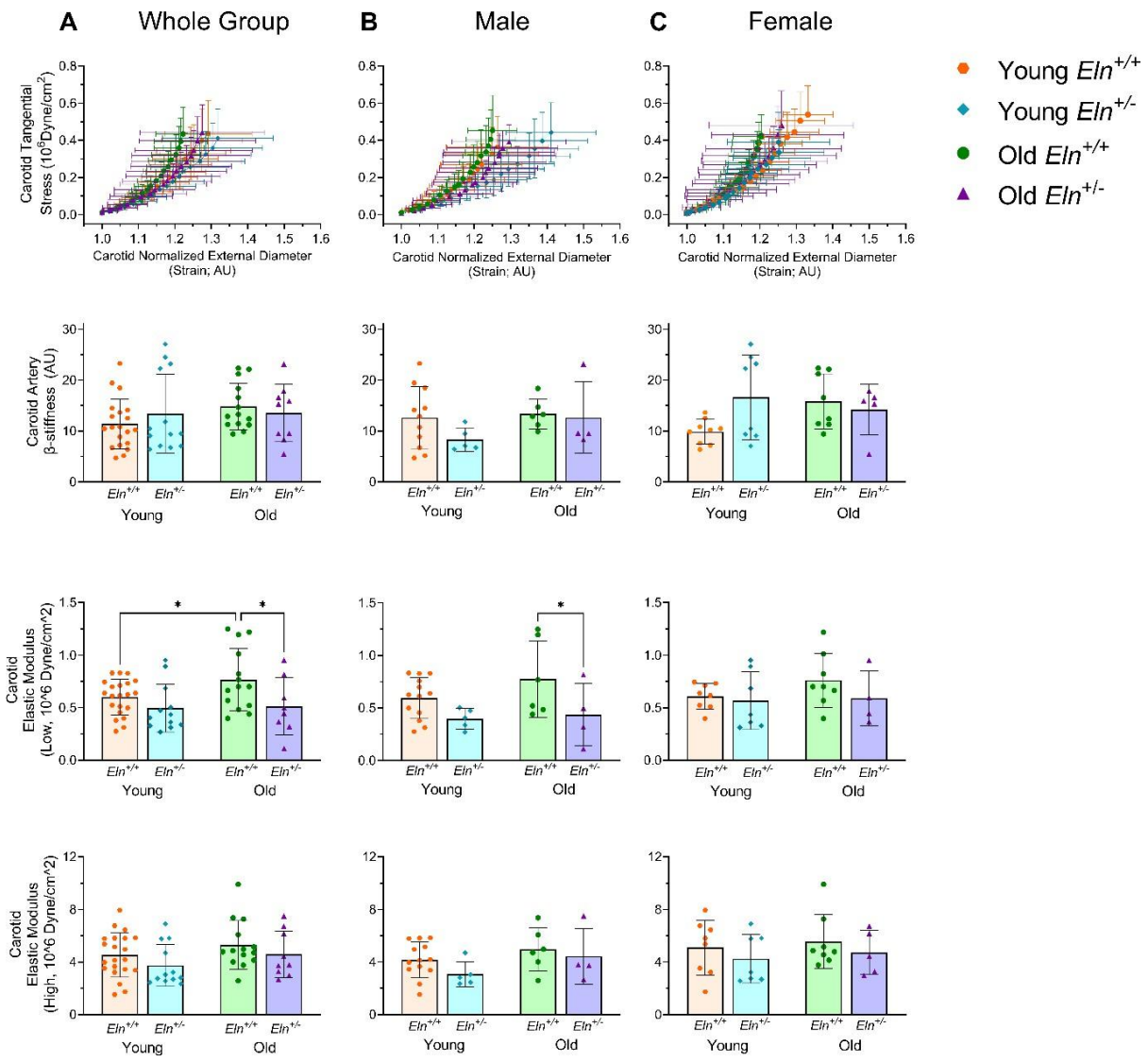

Figure 2.3 Carotid EM at low pressures is lower in old *Eln*$^{+/-}$ mice. Row 1: Carotid artery stress/strain curves; Row 2: β-stiffness; Row 3: elastic modulus at low pressure; and Row 4: elastic modulus at high pressure displayed in A) whole group, B) males, and C) females. Statistics include a 2-way ANOVA and Fisher's LSD test. Data are mean±SD. *p<0.05.

Large Artery Histology

Wall Thickness

Aortic wall thickness trends were similar for both the media and media + adventitia (M+A) layers in all groups (Fig 4A-C). In the whole group there was an interaction effect (media: p=0.005, M+A: p=0.012) between age and genotype. There was a main effect for genotype (media: 0.004, M+A: p<0.0001), and age (media: p=0.0001, M+A: p=0.001). In post-hoc analysis, wall thickness was greater in old $Eln^{+/-}$ mice compared to old $Eln^{+/+}$ mice (media: p=0.0002, M+A: p<0.0001. Wall thickness was also greater in old $Eln^{+/-}$ mice compared to young $Eln^{+/-}$ mice (media p<0.0001, M+A: p=0.0001).

The patterns for wall thickness were similar in males and females as they were for the whole group (Fig. 4B-C). In males, there was an interaction effect between age and genotype for media thickness (p=0.019), but not M+A thickness (p=0.12). There was a main effect for increased wall thickness with age (media: p=0.003, M+A: p=0.031) and genotype (media: p=0.02, M+A: p=0.007). In post-hoc analysis, wall thickness was greater in old male $Eln^{+/-}$ mice compared to old male $Eln^{+/+}$ mice (media: p=0.002, M+A: p<0.005). Wall thickness was also greater in old male $Eln^{+/-}$ mice compared to young male $Eln^{+/-}$ mice (media p=0.0004, M+A: p=0.014).

In females, there was a main effect for increased wall thickness with age (media: p=0.024, M+A: p=0.035). There was a main effect of genotype in the M+A (p=0.004), but not for media only (p=0.12). There was no interaction effect between age and genotype in the females (p>0.05 for both). In post-hoc analysis, wall thickness was greater in old female $Eln^{+/-}$ mice compared to old female $Eln^{+/+}$ mice (media: p=0.057, M+A: p=0.005). Wall thickness was

also greater in old female *Eln*$^{+/-}$ mice compared to young female *Eln*$^{+/-}$ mice (media p=0.01, M+A: p=0.006).

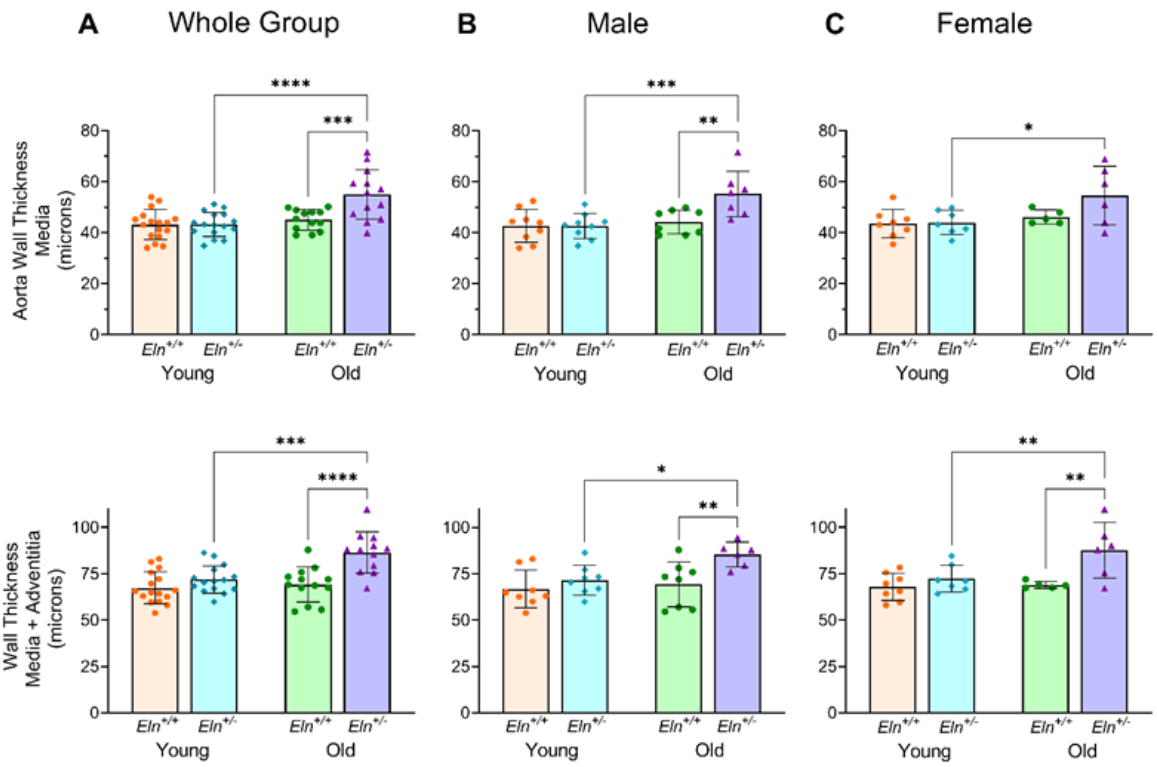

Figure 2.4 Aortic wall thickness is greater with age and *Eln*$^{+/-}$ genotype. Aortic wall thickness in the media (top), and media + adventitia (bottom) for A) whole group, B) males, and C) females. Statistics include a 2-way ANOVA and a Fisher's LSD test . Data are mean±SD. *p<0.05, **p<0.01, ***p<0.001, ****p<0.0001.

Elastin and collagen properties

There were no main effects for aortic elastin content in the whole group but there was a trend for a main effect of genotype (p=0.07, Fig 5A). This was primarily driven by males, as

there was a main effect for genotype amongst males (p=0.038), but not females (p=0.27, Fig 5B-C). There were no interaction effects for any of the groups (p>0.05 for all).

For collagen, there was a decrease in collagen with age (p=0.001) in the whole group. Post-hoc analysis shows a decrease in collagen content with age in both old $Eln^{+/+}$ mice compared to young $Eln^{+/+}$ mice (p=0.03), and old $Eln^{+/-}$ mice compared to young $Eln^{+/-}$ mice (p=0.005). There were no main effects for age or genotype in the males (p>0.05 for all), however there was a main effect for age in the females (p=0.03) but not significant post-hoc comparisons.

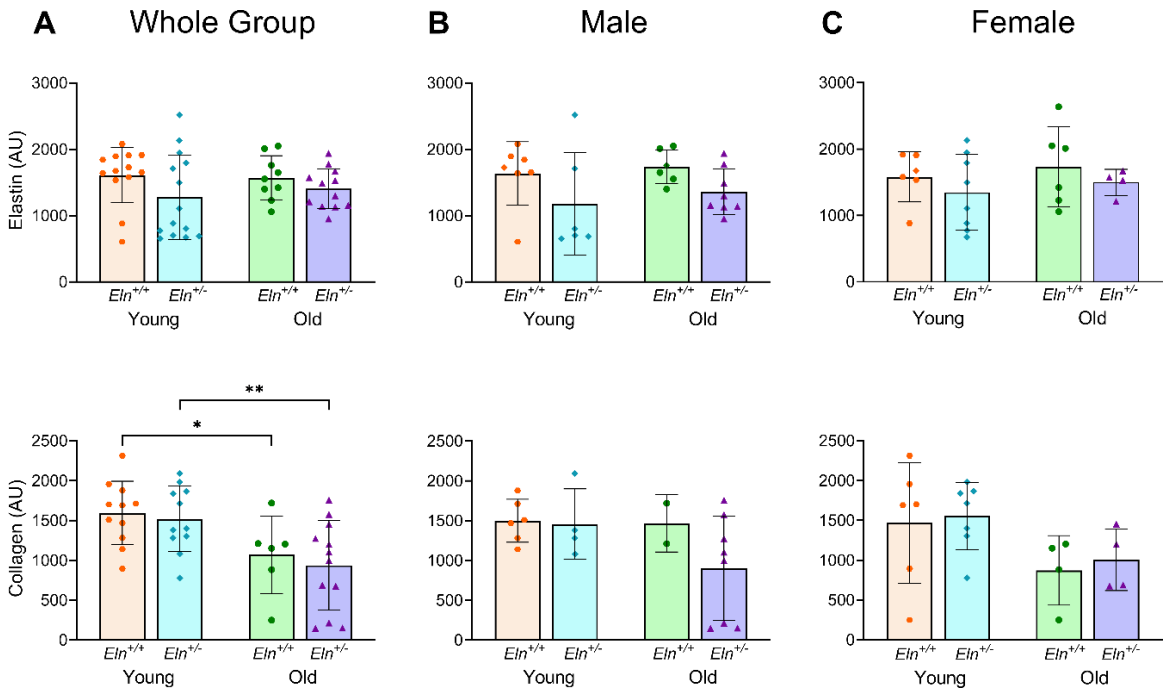

Figure 2.5 Collagen content decreases in large arteries with age. Mean gray values for elastin (top) and collagen 1 (bottom) content in aortas measured by immunofluorescence in for A) whole group, B) males, and C) females. Statistics include a 2-way ANOVA and a Fisher's LSD test. Data are Mean±SD. *p<0.05, **p<0.01.

Cerebral artery endothelial function

In the whole group analysis, the PCA dose response to ACh was impaired in old $Eln^{+/+}$ mice compared to young $Eln^{+/+}$ mice (p=0.0003), as well as percent maximal dilation to ACh (p<0.0001, fig. 6A). This was also true in the old $Eln^{+/-}$ PCA ACh dose response (p=0.02) and percent maximal dilation to ACh (p=0.002) compared to young $Eln^{+/-}$ mice. However, there was no difference in dose response among genotypes in both young (p=0.635) and old (p=0.645) mice. We also observed no genotypic differences in max dilation values for the whole group (p>0.05). As expected, L-NAME incubation reduced PCA dilation to ACh in all groups compared to the original ACh response (p<0.001), but there were no differences among groups in the L-NAME dose responses (p>0.05 for all).

In males, the same trend exists as the whole group analysis, with a lower dose-response (p=0.002) and maximal vasodilation (p=0.0005) to ACh in old vs. young for only $Eln^{+/+}$ mice (Fig. 6B). The pattern for PCA response to ACh was slightly different for females (fig. 7C). For females, there was an impaired ACh response in both old $Eln^{+/+}$ mice compare to young $Eln^{+/+}$ mice (dose-response: p=0.029, maximal: p=0.037) and old $Eln^{+/-}$ mice compared to young $Eln^{+/-}$ mice (dose-response: p=0.013, maximal: p=0.004).

There were no differences in response on maximum dilation to SNP in all groups, indicating that differences in dilation to ACh were due to the impaired endothelium, and not smooth muscle cells (p>0.05 for all, fig. 6A-C). Overall, we found that age reduced EDD in the PCA of mice regardless of genotype.

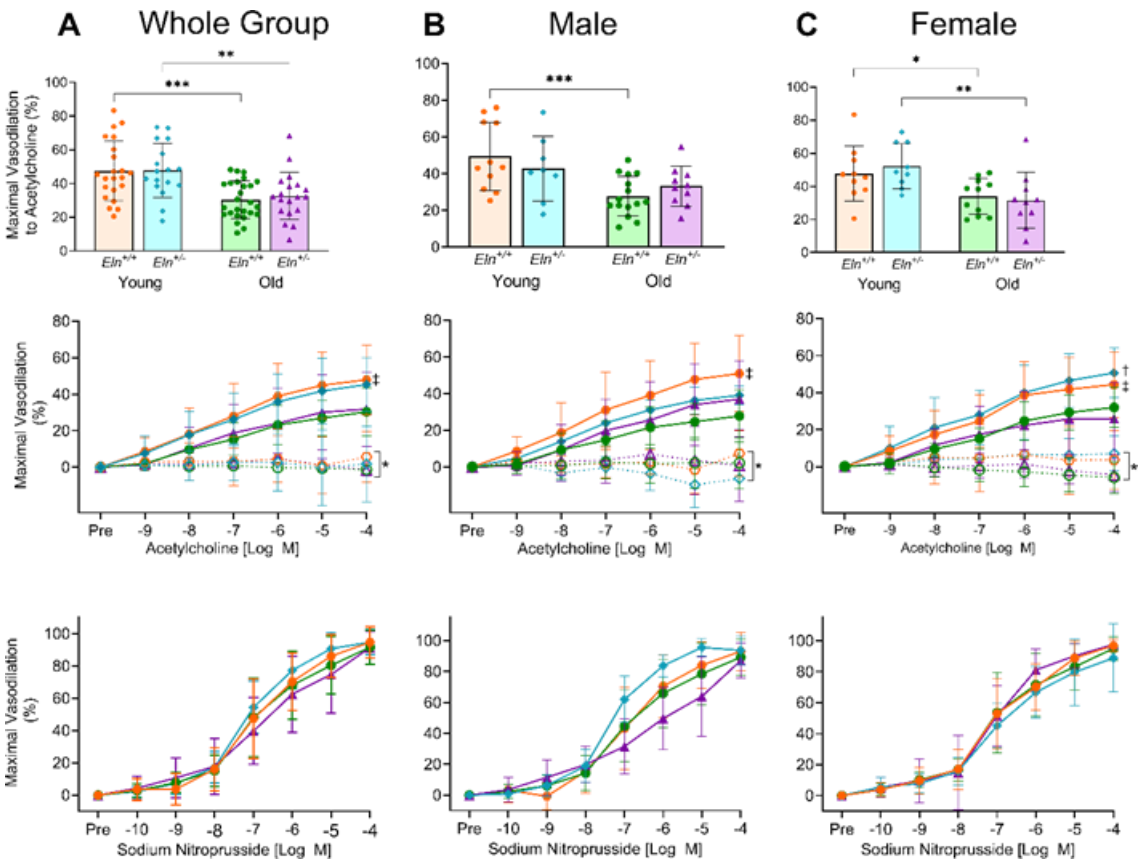

Figure 2.6 Endothelium-dependent dilation is impaired in old *Eln*$^{+/+}$ and *Eln*$^{+/-}$ mice. PCA maximum dilation to ACh (top), and dose response curves ACh (middle), and SNP (bottom) for columns A) whole group, B) males, and C) females. Statistics include a 2-way ANOV, a Fisher's LSD test, and corrected RM-ANOVAs. Data are mean±SD. *p<0.05, **p<0.01, ***p<0.001. †p<0.05 vs. old *Eln*$^{+/+}$, ‡p<0.05 vs. old *Eln*$^{+/-}$. For middle row: *p<0.05 within-group ACh vs ACh+L-NAME.

Cerebral Artery Stiffness

In the whole group analysis, PCAs had greater β-stiffness with age (p=0.0004, Fig. 7A). This comparison was true for both old $Eln^{+/+}$ mice compared to young $Eln^{+/+}$ mice (p=0.039), and old $Eln^{+/-}$ mice compared to young $Eln^{+/-}$ mice (p=0.003). PCA EM at low pressures was significantly greater with age (p=0.001), and genotype (p=0.037), with a trend towards an interaction effect (p=0.07). EM at low pressures were greater in old $Eln^{+/+}$ mice compared to old $Eln^{+/-}$ mice (p=0.013) and old $Eln^{+/-}$ mice compared to young $Eln^{+/-}$ mice (p=0.002). EM at high pressure was greater with age in the whole group (p=0.021), but no other multiple comparisons were significantly difference (p>0.05 for all).

The males and females both displayed similar trends to whole group data. PCAs had greater β-stiffness with age (males: p=0.005, females: p=0.035, Fig. 7B-C). For post-hoc analysis, old male $Eln^{+/-}$ mice had greater β-stiffness than young male $Eln^{+/-}$ mice (p=0.013). For EM at low pressures, there was an age (p=0.002), genotype (p=0.003), and interaction effect (p=0.004) in male mice. Old male $Eln^{+/-}$ mice had greater EM compared to both old $Eln^{+/+}$ mice (p=0.0004) and young $Eln^{+/-}$ mice (p=0.0004). Only a main effect of age was significant in females (p=0.048) with no other post-hoc significance. No statistically significant differences were observed for EM at high pressures in neither males nor females (p>0.05 for all).

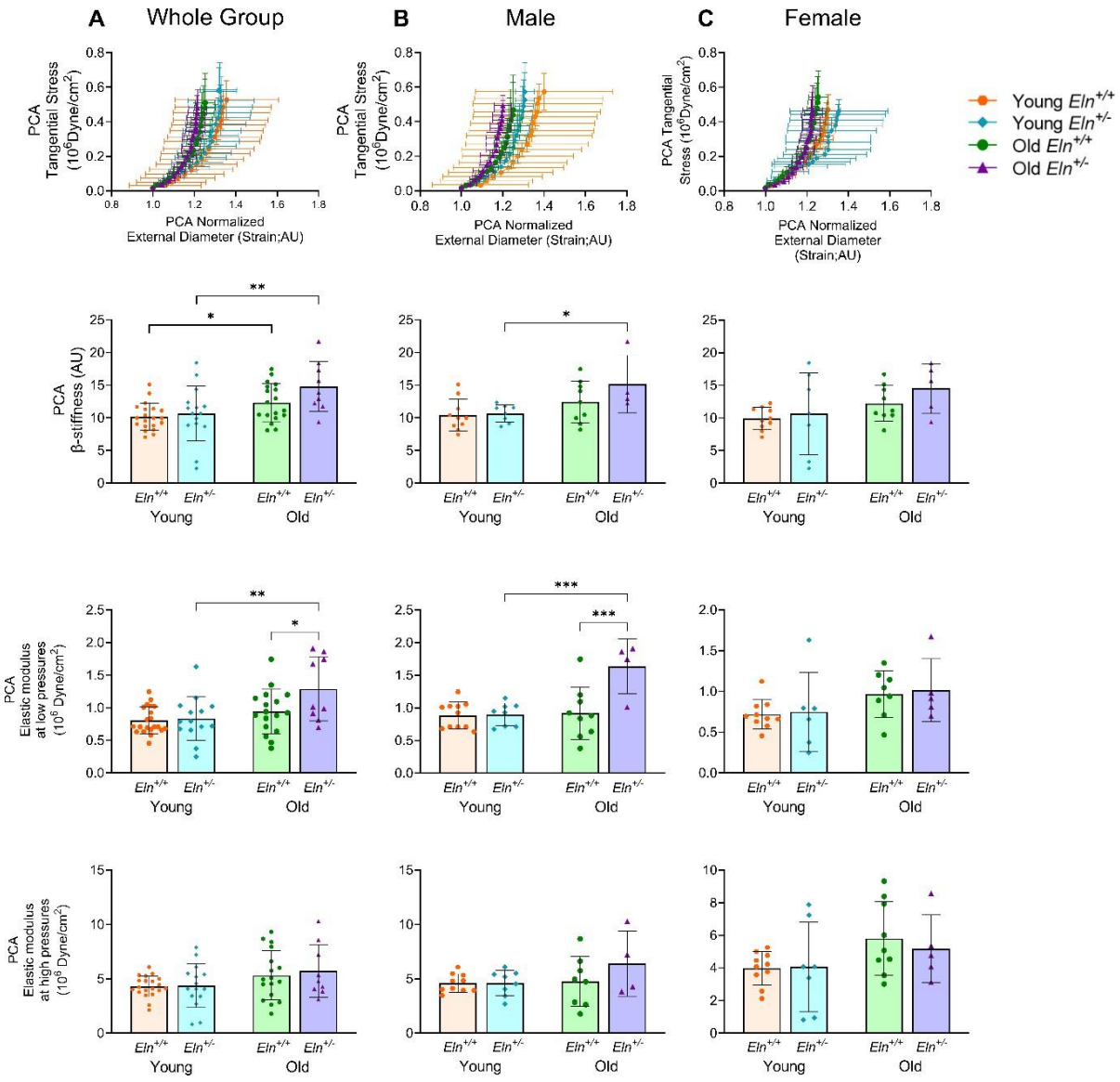

Figure 2.7 PCA stiffness is higher with age, and EM is higher in *Eln*$^{+/-}$ mice.
Row 1: PCA artery stress/strain curves; Row 2: β-stiffness; Row 3: elastic modulus at low pressures; and Row 4: elastic modulus at high pressures displayed in A) whole group, B) males, and C) females. Statistics include a 2-way ANOVA and a Fisher's LSD test. Data are mean±SD. *p<0.05, **p<0.01, ***p<0.001

Rotarod

Time spent on the rotarod was markedly lower in old mice compared to young mice (fig. 8A-C). This finding was true for the whole group, males, and females ($p<0.0001$ for all). Whole group post-hoc analysis showed that lower time on the rotarod with age is true for both $Eln^{+/+}$ and $Eln^{+/-}$ mice in the whole group ($p<0.0001$ for both $Eln^{+/+}$ and $Eln^{+/-}$). Data on males and females display identical findings at the whole group.

In males, the post-hoc analysis showed that rotarod time was lower in both old $Eln^{+/+}$ mice compared to young $Eln^{+/+}$ mice ($p=0.003$), and old $Eln^{+/-}$ mice compared to young $Eln^{+/-}$ mice ($p=0.001$). In females, the post-hoc analysis showed that rotarod time was lower in both old $Eln^{+/+}$ mice compared to young $Eln^{+/+}$ mice ($p=0.001$), and old $Eln^{+/-}$ mice compared to young $Eln^{+/-}$ mice ($p=0.001$).

Nest Building

Nest building score was lower with age in the whole group comparison ($p=0.006$, Fig. 8A-C). However, this age effect was only seen in $Eln^{+/+}$ ($p=0.001$), not $Eln^{+/-}$ mice ($p=0.367$). An interesting finding occurred among the males and females. Females displayed the same findings as demonstrated in whole group, with a decline in scores in $Eln^{+/+}$ mice with age ($p=0.01$), but not $Eln^{+/-}$ mice ($p=0.069$). Surprisingly, in males, there was no impairment in nest building scores with age ($p=0.330$).

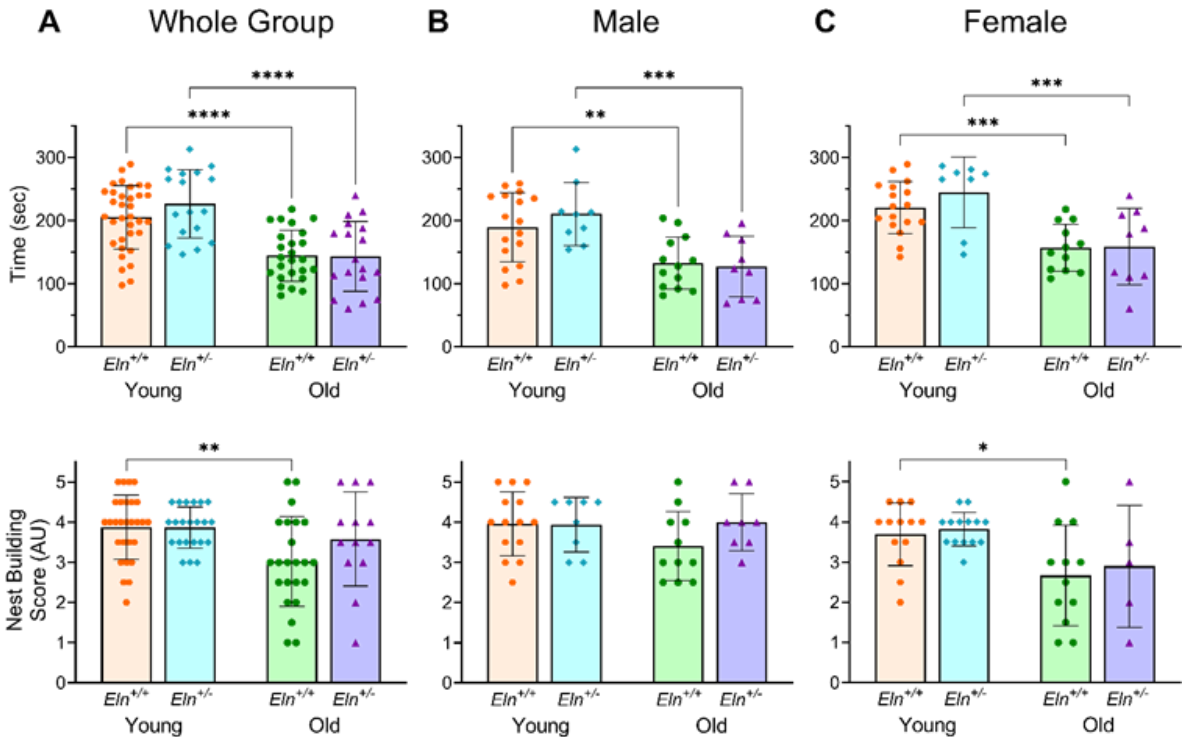

Figure 2.8 Rotarod and nest building scores are lower with age but not *Eln*$^{+/-}$ genotype. Duration on the rotarod (top), and nest building scores (bottom) for columns A) whole group, B) males, and C) females. Statistics include a 2-way ANOVA and a Fisher's LSD test. Data are mean±SD. **p<0.01, ***p<0.001, ****p<0.0001.

MWM

The MWM test measured spatial learning and memory to assess cognitive impairment. Due to a limited sample size, analysis was performed for the whole group only. During the training

trials, old $Eln^{+/+}$ mice took longer to find the platform compared to young $Eln^{+/+}$ mice, suggesting that age impaired spatial learning capabilities in $Eln^{+/+}$ mice (p=0.026, Fig 9A). During the probe trial with the platform removed, there was an interaction effect between age and genotype (p=0.002). There was a main effect for age where old mice crossed over the platform area less than young mice, indicating impaired special memory (p=0.0004, fig 9B). A post-hoc analysis found young $Eln^{+/-}$ mice crossed the platform more than young $Eln^{+/+}$ (p=0.022), but the trend reversed at old age (p=0.025). Additionally, old $Eln^{+/-}$ mice crossed the platform less than old $Eln^{+/-}$ mice during the probe trial (p<0.0001). $Eln^{+/-}$ mice spent less time in the target quadrant compared to old $Eln^{+/+}$ mice (p=0.013, Fig. 9C). There were no other group differences for the percent of time in the target quadrant were significant (p>0.05 for all). Lastly, we found a main effect for age, where old mice take longer to reach the platform compared to young mice during a beacon trial in which the platform is accessible and visibly marked (p=0.002, Fig. 9D). This was true in both old $Eln^{+/+}$ mice compared to young $Eln^{+/+}$ mice (p=0.010), and old $Eln^{+/-}$ mice compareed to young $Eln^{+/-}$ mice (p=0.047). In sum, the results from the MWM experiment suggest that elastin haploinsufficiency exacerbates cognitive impairment observed in aging.

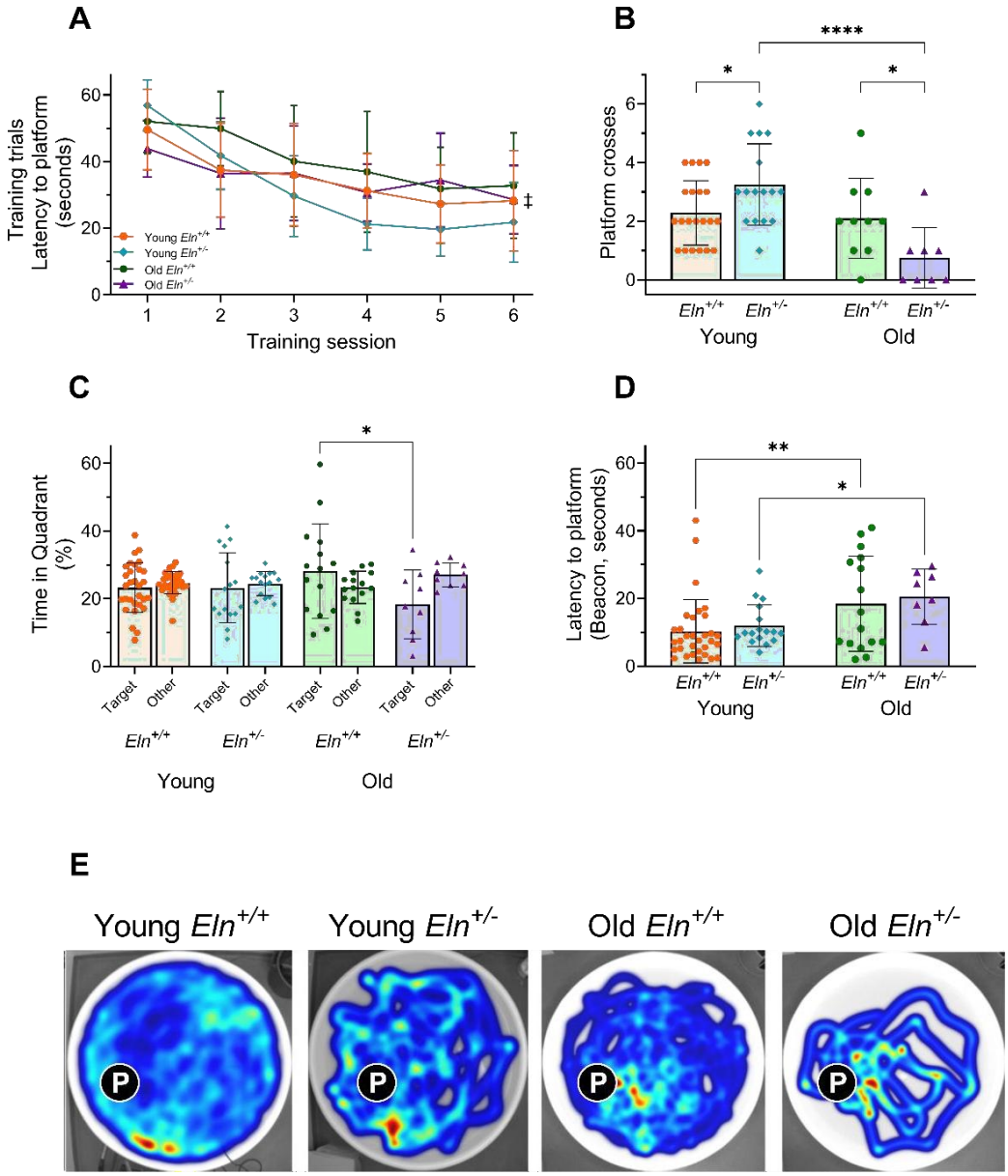

Figure 2.9 Spatial memory is impaired in old *Eln*$^{+/-}$ mice compared to old *Eln*$^{+/+}$ mice. MWM Whole group data only displaying, A) Latency to platform during training trials, B) platform crossing frequency during probe trial, C) Time spent in target quadrant and average of other quadrants during probe trial, D) Latency to platform during beacon trial. Statistics include a 2-way ANOVA, a Fisher's LSD test, and corrected RM-ANOVA. Data are mean±SD. ‡p<0.05 old *Eln*$^{+/+}$ vs. young *Eln*$^{+/+}$, *p<0.05, **p<0.01, ****p<0.0001.

Neuroinflammation

Cortex Gene expression

Due to limited sample size on some measures, gene expression analysis on the cortex tissue was restricted to whole group analysis. First, we investigated expression of pro-oxidant and pro-inflammatory genes. For *Nox2*, there was a main effect for both age (p=0.006) and genotype (p=0.035, fig. 10A). Post-hoc analysis shows the increase in *Nox2* expression with age was driven by $Eln^{+/+}$ mice (p=0.0004), and the genotype effect was driven by old mice (p=0.008). For *Tnfα* gene expression, there was an age effect (p=0.001). But similarly to *Nox2*, this finding was mostly driven by $Eln^{+/+}$ mice, where old mice had greater *Tnfα* expression compared to young mice (p=0.004, fig. 10B). There was both a main effect for age (p<0.0001) and a genotype effect (p=0.006, fig. 10C) for *Il1b*. Post-hoc analysis shows that *Il1*β expression was greater in both $Eln^{+/+}$ and $Eln^{+/-}$ mice (p<0.0001 for both). Contrary to our hypothesis, old $Eln^{+/+}$ mice had greater gene expression of *Il1*β in the cortex than $Eln^{+/-}$ mice (p=0.010). There were no differences among any group for expression of the *Ager* gene (p>0.05 for all).

Next, we investigated gene expression in the cortex for antioxidant genes*:* *Sod1*, *Sod2*, and *Sod3*. While there was no age effect for *Sod1*, there was a strong genotype effect (p=0.001). We found that *Sod1* was notably lower in old $Eln^{+/-}$ mice compared to old $Eln^{+/+}$ mice (p=0.001), but there was no difference among genotype in young mice (p=0.100). Interestingly, the opposite was true for *Sod2*, where the genotype effect (p=0.006) showed decreased gene expression only in young $Eln^{+/-}$ mice compared to young $Eln^{+/+}$ mice (p=0.035). While there was no statistically significant reduction in *Sod2* among old $Eln^{+/-}$, there was a strong trend worth noting (p=0.062) as these results suggest a similar conclusion to *Sod1*. Lastly, there was a main effect for genotype

in gene expression for *Sod3* (p=0.028), but only in old mice as seen with *Sod1* expression (p=0.036).

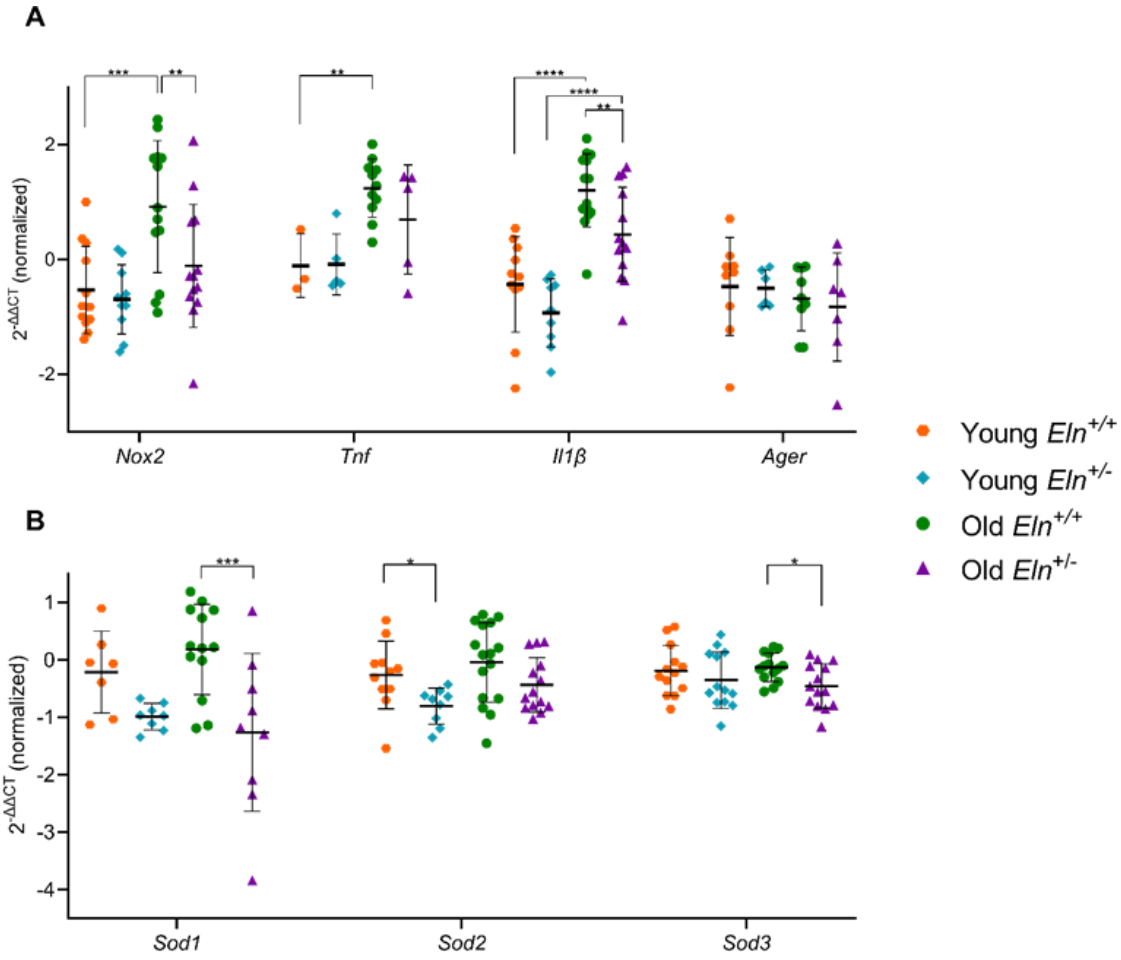

Figure 2.10 Inflammatory genes are expressed more in old mice, and antioxidant genes are expressed less in the cortexes of *Eln*$^{+/-}$ mice. Cortex Gene expression in whole group data for pro-inflammatory (top) and antioxidant (bottom) genes A) *Nox2,Tnf, Il1β, Ager*, and B) *Sod1, Sod2, and* Sod3. Statistics include a 2-way ANOVA and a Fisher's LSD test. Data are mean±SD. *p<0.05, **p<0.01, ***p<0.001, ****p<0.0001.

Brain Histology

We investigated neuroinflammation in the brain by quantifying activated astrocyte number in brain slices stained for GFAP. In the entorhinal cortex, the GFAP cell count and percent area were greater with age in the whole group (cell count: p=0.007, percent area: 0.015, Fig 11A). In the post-hoc analysis, old $Eln^{+/+}$ mice had greater GFAP levels compared to young $Eln^{+/+}$ mice (cell count: p=0.005, percent area: 0.004), but not in $Eln^{+/-}$ mice (cell count: p=0.354, percent area: p=0.645). In males and females, there was a trend towards a main effect for age ($p<0.08$ for both) in the number of GFAP stained cells (Fig. 12A, 13A).

In the hippocampus, GFAP levels were greater in old mice compared to young mice (cell count and percent area: $p<0.0001$, Fig 11B). This was true in $Eln^{+/+}$ mice ($p<0.01$ for both) and $Eln^{+/-}$ ($p<0.05$ for both). In males, greater GFAP levels with age held true (cell count: p=0.003, percent area: p=0.005, Fig. 12B). With multiple comparison tests, GFAP levels were greater in $Eln^{+/+}$ and $Eln^{+/-}$ mice ($p<0.05$ for all). The finding continued in females with greater GFAP levels with age ($p<0.01$ for both, Fig. 13B).

Lastly, the GFAP levels were greater in old mice in the thalamus for the whole group ($p<0.0001$ for both, fig. 11C). In post-hoc analysis, this was true in both $Eln^{+/+}$ mice and $Eln^{+/-}$ mice ($p<0.001$ for all). There was the same age effect in both males and females. In males and females GFAP cell count was greater with age ($p<0.01$ for both). In males and females, GFAP percent area was greater with age ($p<0.05$ for both). Overall, we found that levels of neuroinflammation, measured by levels of GFAP in the entorhinal cortex, hippocampus, and thalamus were all greater with age but were not impacted by genotype.

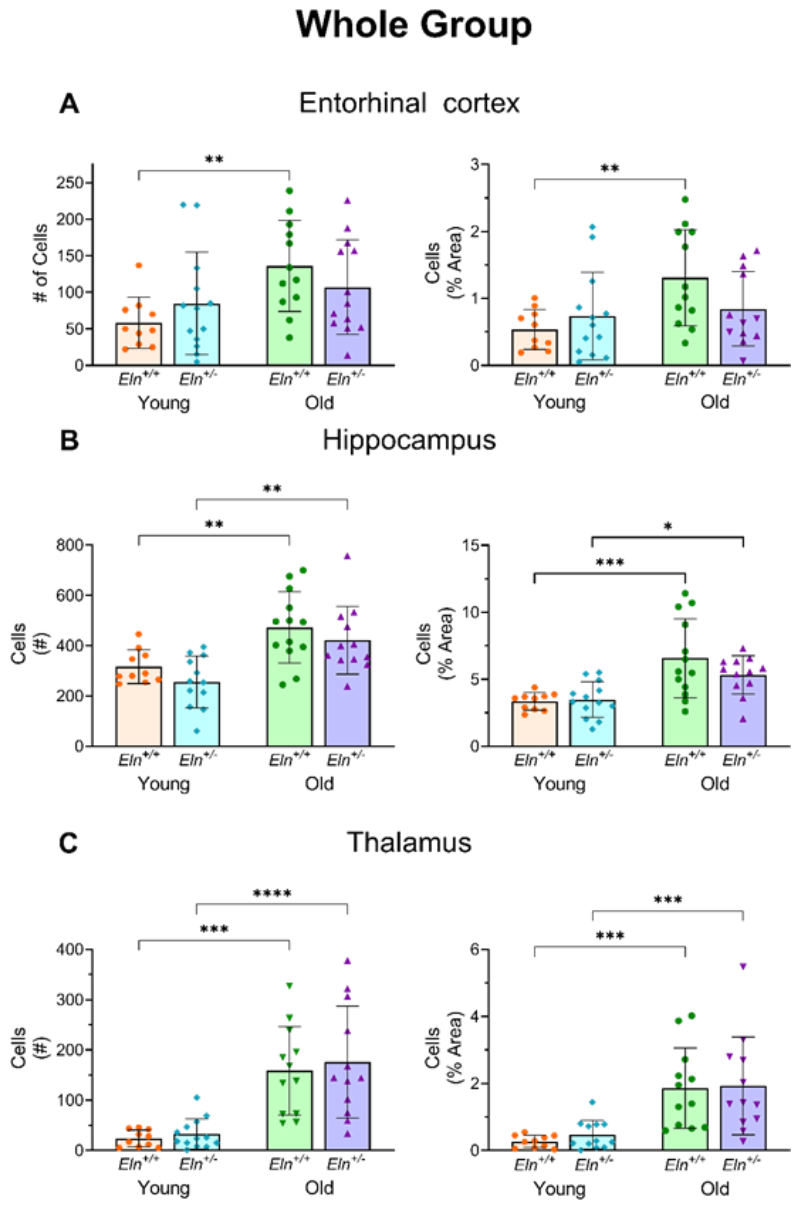

Figure 2.11 Whole group activated astrocyte levels in the brain are greater with age, but not affected by genotype. Whole group glial fibrillary acidic protein (GFAP) in the brain. Data are cell count (left) and cell percent area (right) in the (A) entorhinal cortex, B) hippocampus, and C) thalamus. Statistics include a 2-way ANOVA and a Fisher's LSD test. Data are mean±SD. *p<0.05, **p<0.01, ***p<0.001, ****p<0.0001.

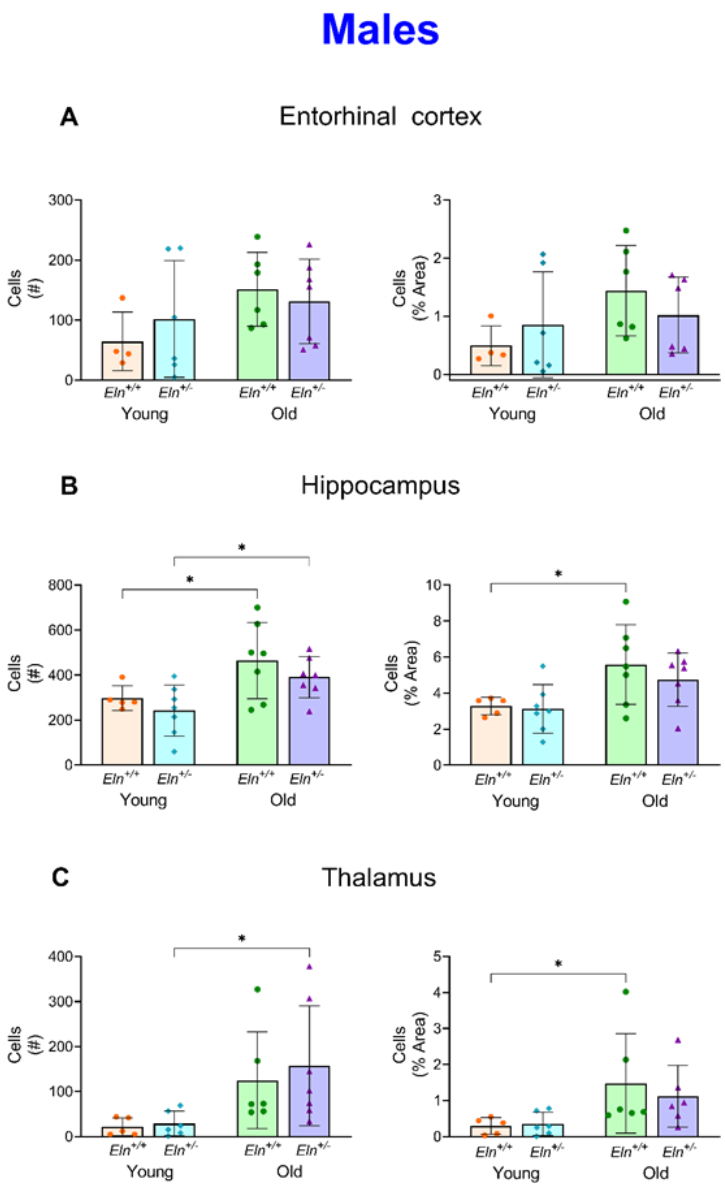

Figure 2.12 Male activated astrocyte levels in the brain are greater with age in hippocampus and thalamus, but not affected by genotype. Male GFAP in the brain displaying cell count (left) and cell percent area (right) in the (A) entorhinal cortex, B) hippocampus, and C) thalamus. Statistics include a 2-way ANOVA and a Fisher's LSD test. Data are mean±SD. *p<0.05.

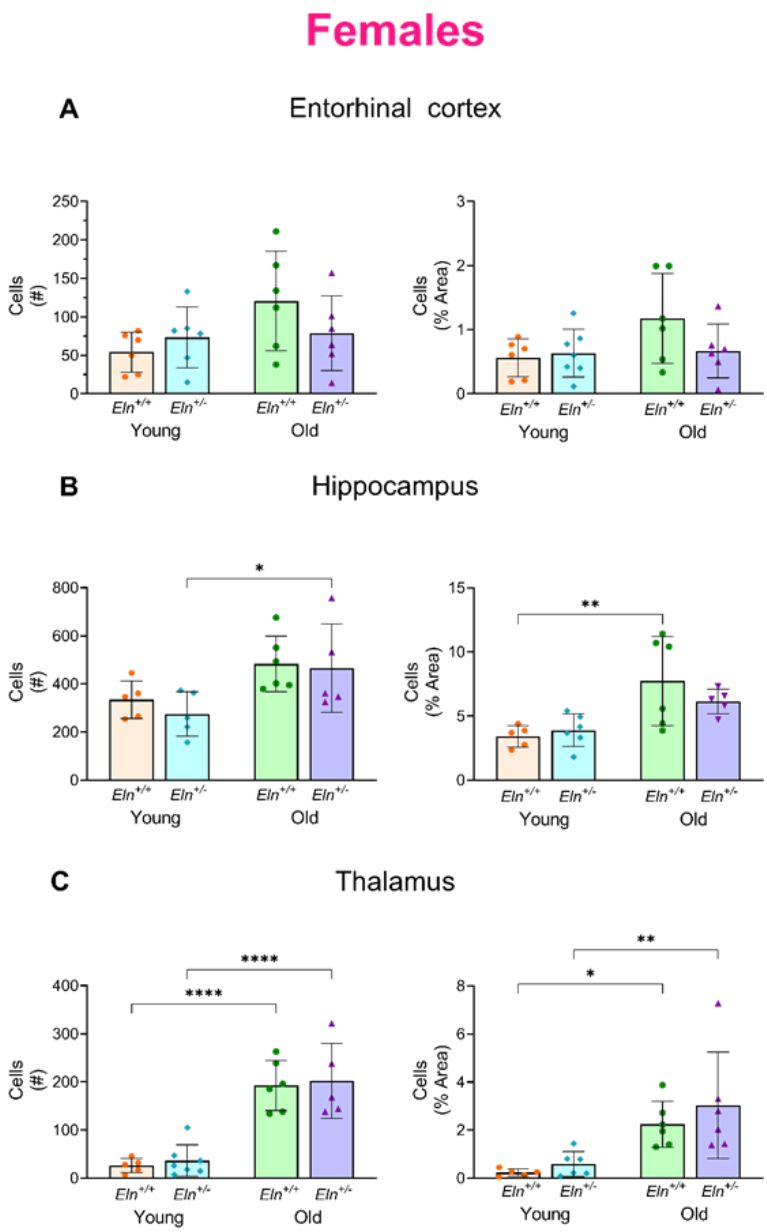

Figure 2.13 Female activated astrocyte levels in the brain are greater with age in hippocampus and thalamus, but not affected by genotype. Female GFAP in the brain displaying cell count (left) and cell percent area (right) in the (A) entorhinal cortex, B) hippocampus, and C) thalamus. Statistics include a 2-way ANOVA and a Fisher's LSD test. Data are mean±SD. *p<0.05, **p<0.01, ****p<0.0001.

Cerebral artery gene expression

Due to small sample size, only whole group comparisons were done for this outcome. There was an interaction effect for age and genotype in *Sod3* expression (p=0.033, Fig 14). Post-hoc analysis showed that old $Eln^{+/+}$ mice had a higher level of *Sod3* expression compared to old $Eln^{+/-}$ mice (p=0.034).

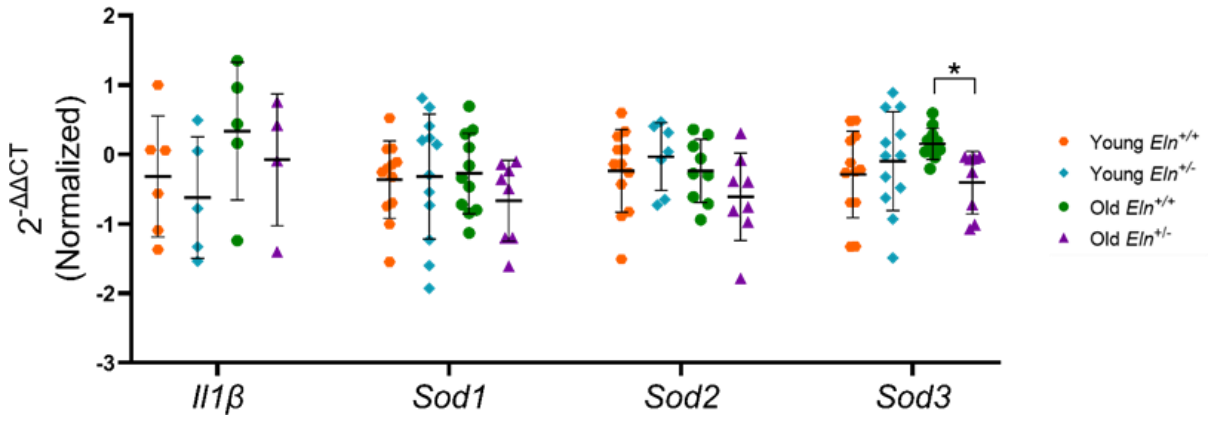

Figure 2.14 Cerebral artery *Sod3* gene expression is lower in old $Eln^{+/-}$ vs old $Eln^{+/+}$ mice. Whole group cerebral artery gene expression levels of *Il1*β, *Sod1, Sod2, and Sod3*. Statistics include a 2-way ANOVA and a Fisher's LSD test. Data are mean±SD. *p<0.05.

2.4 Discussion

The purpose of this study was to investigate the effects of short-term and long-term elastin haploinsufficiency on cerebrovascular dysfunction and cognitive impairment. Secondly, we investigated sex differences in the response to these conditions. We hypothesized that old $Eln^{+/-}$ mice would have greater impairments in vascular function and cognitive function compared to young and $Eln^{+/+}$ mice. We also hypothesized that these impairments would be

exacerbated in $Eln^{+/-}$ female mice since vascular function declines more rapidly with in females after menopause. In our study, we found that long-term elastin haploinsufficiency lead to greater levels of cerebral artery stiffness, cognitive impairment, and weaken antioxidant defense in the brain. These results point to elastin playing a role in maintaining cerebral artery structure and cognitive function.

Large artery stiffness

Large artery stiffness is strongly associated with cerebrovascular dysfunction and neurodegenerative disease (84–87). We assessed large artery stiffness by measuring in vivo PWV and ex vivo passive stiffness on the carotid artery. For PWV, we found that young $Eln^{+/+}$ mice had higher PWV than young $Eln^{+/-}$ mice, indicating greater aortic stiffness. This was contrary to our hypothesis. Upon further analyses, we found that this was true only for the whole group and males, but not females. We also found that differences in PWV among the old $Eln^{+/-}$ mice, and these were not observed when the groups were divided by sex. We found no differences in β-stiffness or elastic modulus among any comparisons. This was again contrary to our hypothesis as we expected $Eln^{+/-}$ mice to display higher levels of β-stiffness compared to $Eln^{+/+}$ mice.

Previous research has shown $Eln^{+/-}$ mice display greater PWV than $Eln^{+/+}$ mice at younger ages (70, 75, 88–90). An explanation as to why we did not observe these findings could be due to the unnaturally high PWV occurring in the young $Eln^{+/+}$ mice, particularly in the young male mice. While intended to be a control group, the $Eln^{+/+}$ mice could have developed higher PWV than seen previously.

An important note is that we rederived our colony with a C57Bl/6J background due to the health status of imported mice. Thus, the genetic background and health status for our mice varies from studies performed at other institutions. Some rederived lines may have contained a phenotype different from each other, or different from what have previously been studied. Additionally, the $Eln^{+/-}$ mouse model exhibits high levels of renin, which regulate blood pressure (88). A recent study by Brengle et al. used a new $Eln^{+/-}$ mouse model that does not have high renin. They found that the $Eln^{+/-}$ mice maintained their hypertension and arterial stiffness phenotypes without increases in renin levels (71). We did not measure renin or hemodynamic changes in this study; thus we do not know the effect that long-term elastin haploinsufficiency plays on these variables in this study. Mice were housed free of pathogens and fed a diet high in phytoestrogens which effect vasodilation (91). This could have contributed to adaptions that combat the elastin haploinsufficient phenotype previously shown these mice.

Large artery histology

When comparing aortic wall thickness, we found a similar trend in the data for both the media layer alone, and the M+A layers. We found that wall thickness increased with age in $Eln^{+/-}$ mice, but not $Eln^{+/+}$ mice. This trend was seen in the whole group as well as both males and females. These results suggest that long-term exposure to elastin haploinsufficiency causes remodeling in the aorta leading to greater wall thickness.

Previous studies using the $Eln^{+/-}$ mouse model show a lower elastin content in the large arteries (69, 70). In our study, we observed no differences in elastin content in the aorta from $Eln^{+/-}$ mice compared to $Eln^{+/+}$ mice, despite confirmed genotypic differences between the two. This is contrary to previous findings, but may explain why we observed no differences in large

artery stiffness measured between the two genotypes. Future studies should investigate mechanisms of adaptation that resisted the decreased elastin phenotype seen in this study.

Cerebrovascular function

Previous research using the $Eln^{+/-}$ model and carotid calcification model demonstrated that large artery stiffness causes cerebral artery endothelial dysfunction, reduced cerebral blood flow, and increased oxidative stress (72, 92–94). Thus, we expected at least a reduction in cerebral artery EDD in $Eln^{+/-}$ mice. In our study, in the whole group comparisons, we observed only an impairment in EDD in old mice *(*$Eln^{+/+}$ and $Eln^{+/-}$). But we noticed a unique finding when comparing male and female data alone. Males had age-dependent declines in only $Eln^{+/+}$ mice, while females displayed age-dependent declines in both $Eln^{+/+}$ and $Eln^{+/-}$ mice. This could indicate the females are more susceptible to the negative impacts of long-term exposure to elastin haploinsufficiency compared to males. Past research has shown $Eln^{+/-}$ mice display impaired cerebral artery EDD mainly due to contributions of large artery stiffness, and do not have reduced elastin content in the cerebral artery wall (72, 92). Mice in our study did not display greater large artery stiffness, which could explain the similarities in EDD function between $Eln^{+/+}$ and $Eln^{+/-}$ mice that we observed in our results. Previous studies have used male only mice cohorts, while this study used both males and females. This means that any sex differences in response to elastin haploinsufficiency would impact the overall group mean.

Changes in cerebral artery stiffness with age are not well documented. A previous study from our lab found that cerebral artery stiffness increases with age, potentially protecting against the effects of increased pulse pressure (95). Data on cerebral artery stiffness in old $Eln^{+/-}$ has not been published, making this study the first to report these findings. In this study we found the

PCA elastic modulus at low pressures increased with age, and this effect was exacerbated in *Eln*$^{+/-}$ mice. While elastin haploinsufficiency had no effect on large arteries, it is possible that altered hemodynamic changes in *Eln*$^{+/-}$ could contribute to protective remodeling. Other studies have shown increased systolic blood pressure in this mouse model, but we did not confirmed blood pressure hemodynamics in this study (71).

Cognitive impairment

Cognitive function declines with age in humans and is a sign of neurodegenerative diseases (96–98). In our study, we observed reduced rotarod time in both *Eln*$^{+/+}$ and *Eln*$^{+/-}$ mice with age. In the nest building assessments, we found that only *Eln*$^{+/+}$ mice displayed reduced nest building behavior with age. This finding suggests that the *Eln*$^{+/-}$ genotype does not lead to an exacerbated decline in motor coordination or nest building behaviors.

However, we found that spatial memory, assessed during MWM, was severely impacted by both age and *Eln* genotype. At young ages, *Eln*$^{+/-}$ mice surprisingly performed better. But when exposed to elastin haploinsufficiency long term, old *Eln*$^{+/-}$ mice performed worse than their age matched counter parts by crossing the platform less and spending less time in the target quadrant compared to old *Eln*$^{+/+}$ mice. Another important thing to note is that the young *Eln*$^{+/+}$ cohort performed more poorly on cognitive tests than expected. This could also be a potential explanation as to why that long-term exposure to elastin haploinsufficiency can lead to greater declines in spatial memory. In the carotid calcification mouse model, modeling carotid artery stiffness and increased pulse pressure, arterial stiffness directly impaired cognitive function and performance (93). Our findings corroborate with previous research, further solidifying the relationship seen between age, cerebrovascular dysfunction, and neurodegeneration.

Neuroinflammation

Neuroinflammation contributes to cognitive impairment and could explain the link between cerebral artery dysfunction and neurodegenerative diseases (99). Because of this relationship, we expected levels of pro-oxidant and pro-inflammatory genes to be elevated with age. We found that age-related increases in gene expression for pro-oxidant and pro-inflammatory genes in the cortex were mostly observed in $Eln^{+/+}$ mice. $Eln^{+/-}$ mice only had an age-related increase in gene expression in *Il-1β*, and had less expression of these genes compared to $Eln^{+/+}$ at old ages. While this is contrary to our initial hypothesis, we found interesting results among antioxidant genes that help complete the picture. Expression of *Sod1* and *Sod3* were significantly lower in old $Eln^{+/-}$ mice compared to old $Eln^{+/+}$ mice. This indicates that the antioxidant defense system in old $Eln^{+/-}$ mice is compromised. Without proper antioxidant defenses, ROS accumulates in cells causing oxidative and damage and cellular dysfunction. Thus, it is logical that decreased *Sod* levels in the cortex of $Eln^{+/-}$ mice might increase the neuroinflammatory environment contributing to cognitive impairments observed in these mice. vidence for changes in the expression of antioxidant defense with age has been conflicting in both humans and animals (100). Overall, long-term exposure to elastin haploinsufficiency leads to lower antioxidant gene expression in the cortex, which could contribute to a heightened state of inflammatory proteins in the issue.

2.5 Limitations

There are some limitations to this study that should be noted. The transgenic manipulation to model elastin haploinsufficiency is helpful to answer our questions but may not represent a completely translatable model to human aging, as humans with elastin

haploinsufficiency display other co-morbidities that limit lifespan and make it difficult to study. Additionally, the elastin haploinsufficiency in this model is not specific to the vasculature. Elastin protein is present multiple tissue types which may cause off target effects. We have not assessed elastin content in the cerebral arteries so we cannot confirm the effect of elastin haploinsufficiency or content in the cerebral arteries. However, previous using this mouse model has shown that this elastin haploinsufficiency effects elastin production primarily in large arteries, not systemic arteries (72). Lastly, as previously mentioned, we did not assess renin or hemodynamic measures in these mice. While previous studies show that $Eln^{+/-}$ mice display increased systolic blood pressure, we cannot confirm this phenotype in our study. Additionally, this makes it difficult to interpret the contributions of blood pressure on the outcomes in our study.

2.6 Conclusion

Overall, the results of this study suggest that long-term exposure to elastin haploinsufficiency causes aortic wall remodeling, impairs spatial memory, and may contribute to higher levels of neuroinflammation. Also, there are differences in how this long-term exposure to elastin haploinsufficiency affects males and females where females tend to be more susceptible to these effects compared to males. In summary, long-term exposure to elastin haploinsufficiency can cause detrimental effects on cerebrovascular function and cognitive function. Most importantly, finding a treatment or therapeutic intervention to prevent the detrimental effects of elastin haploinsufficiency could be a promising target for preserving cerebral artery function and reducing cognitive impairment seen in neurodegenerative disease.

III. LARGE ARTERY STIFFNESS AND CEREBROVASCULAR FUNCTION ARE UNALTERED WITH LONG-TERM TREATMENT OF COLLAGEN CROSSLINK-BREAKER, ALAGEBRIUM CHLORIDE (ALT-711).

3.1 Introduction

Stiffening of the large arteries is an age-related change to the vascular system that increases the risk of neurodegeneration (14, 87). Stiff arteries lose the ability to damp pulse pressure. This causes an increase in pulse pressure transmitted to smaller, resistance vessels (101). Increased mechanical and circumferential stress from high pulse pressure damages the fragile layer of endothelium that is crucial for vascular function (29, 102). There are strong correlations between cerebrovascular dysfunction, neuroinflammation, and cognitive impairment (103–105). Cerebrovascular dysfunction reduces cerebral blood flow, one of the highest predictors of Alzheimer's disease development (106, 107). Increased pulse pressure due to large artery stiffness leads to cerebrovascular dysfunction (108)

Previous work by our lab indicates that elevated large artery stiffness impairs cerebral artery endothelium-dependent dilation (EDD) by reducing nitric oxide (NO)-mediated vasodilation (72). Previously, we showed that pyridoxamine, a vitamin B6 isomer known to reduce the formation of AGEs, attenuates large artery stiffness, and preserves cerebrovascular EDD with modest effects on cognition. However, pyridoxamine could work through non-AGE-related mechanisms as it acts as an antioxidant affecting multiple target organs (52). Alagebrium Chloride (ALT-711), is a collagen-crosslink breaker shown to decrease arterial stiffness and improve large artery vascular function and left ventricle function in rodents, primates, and humans (59, 109–111). However, the effects of ALT-711 on cognitive and cerebrovascular function have yet to be investigated despite robust associations between the three.

Thus, the purpose of this study was to investigate the effects of the collagen-crosslink breaker ALT-711 on preserving cerebrovascular and cognitive function by reducing large artery stiffness. We hypothesized that old mice treated with ALT-711 would show reduced large artery stiffness and preserved cerebrovascular and cognitive function compared to control mice. To test these hypotheses, we treated old C57BL/6 mice with ALT-711 for 16 weeks and measured aortic stiffness monthly. At the end of the intervention, we assessed cognitive function and cerebrovascular function by measuring endothelium-dependent dilation and passive stiffness.

3.2 Methods

Intervention

Aged C57BL/6 male and female mice were obtained from the National Institute on Aging colony at Charles River (20 months, n = 19). All mice were fed a normal chow diet with *ad libitum* food and water and were housed in an animal care facility on a 12/12-hour light-dark cycle at 24°C. Animals were matched for baseline aortic stiffness values and assigned either treatment or control group by block randomization (n = 8 / group, 4 males, 4 females). Mice received daily oral gavage of either Alagebrium Chloride (ALT-711, 1mg/kg/day) or distilled water for 3 weeks, followed by one recovery week, for a total of 16 weeks. A young C57BL/6 control group was used for comparison for the hydroxyproline assay (6 months, n = 7, all males). Mice were euthanized by exsanguination under isoflurane immediately prior to ex vivo vascular studies. After euthanasia, the heart, liver, spleen, soleus, gastrocnemius (gastroc), and white adipose tissue (WAT) were collected, and their wet weights were recorded. In addition, cerebral arteries, carotid artery, aorta, cerebral cortex, and hippocampus were excised and frozen at −80°C for preservation. All animal procedures conform to the *Guide to the Care and Use of Laboratory Animals* (8th edition, revised 2011) and were approved by the Institutional Animal

Care and Use Committees at the University of Oregon. Following the intervention, mice were sacrificed ethically according to the Animal Care and Use Committee guidelines.

Pulse wave velocity (PWV)

We measured pulse wave velocity (PWV) using the Indus Doppler Flow Velocity System (Webster, Texas) from the descending aorta to the abdominal aorta (76, 77). Three consecutive measurements were analyzed by researchers for each time point, with an inter-researcher variability <10%. PWV measurements were made at baseline and the completion of months 1, 2, 3, and 4 of the intervention.

Passive stiffness

Carotid arteries and posterior cerebral arteries (PCAs) from each mouse were isolated and mounted on a pressure myograph (DMT Inc., Denmark) as previously described (72). Arteries were pressurized and incubated with a physiological salt solution free of calcium to eliminate the effects of myogenic tone. We recorded changes in lumen diameter and medial wall thickness following increasing intralumenal pressure from 5 to 100 cmH_2O (3.7–73.5 mmHg) in 5 cmH_2O increments (72). Stress was calculated as:

$\sigma = PD/2WT$

where P is pressure in dyne cm^{-2}, D_i is lumen diameter and WT is wall thickness.

Strain was calculated as:

$\varepsilon = (D - D_i)/D_i$

where D_i is the initial starting diameter.

Data for each artery were fit to the curve:

$\sigma = \sigma_i e^{\beta\varepsilon}$

where σ_i is the initial starting stress (5 cmH_2O) and β is the slope of tangential elastic modulus versus stress. A higher β represents a stiffer artery. From this slope we also calculated Young's modulus (low and high) (79–81).

Cerebral Artery Endothelial Function

PCAs from each mouse were excised and placed in a myograph chamber (DMT Inc., Aarhus, Denmark) with physiological salt solution that contained 145.0 mm NaCl, 4.7 mm KCl, 2.0 mm $CaCl_2$, 1.17 mm $MgSO_4$, 1.2 mm NaH_2PO_4, 5.0 mm glucose, 2.0 mm pyruvate, 0.02 mm EDTA, 3.0 mm MOPS buffer and 1 g/100 ml BSA, pH 7.4 at 37°C, cannulated onto glass micropipettes and secured with nylon (11-0) suture. All arteries were pre-constricted with phenylephrine (1–6 μM to obtain 20%–40% pre-constriction) and we measured changes in luminal diameter in response to increasing concentrations of endothelium-dependent dilator acetylcholine (ACh, 1×10^{-9} to 1×10^{-4} M). ACh dose responses were repeated after incubation with the nitric oxide synthase (NOS) if inhibitor, N_ω-Nitro-L-arginine methyl ester hydrochloride (L-NAME, 0.1 mM, 30-minute incubation). We also measured the changes in diameter to increasing doses of the endothelium-independent dilator, sodium nitroprusside (SNP, 1×10^{-10} to 1×10^{-4} M).

Nest building

We assessed cognitive function by measuring instinctual nest-building behavior (82). Mice were individually housed with food and water overnight in a cage containing a condensed cotton nestlet. In the morning, the nests were scored on a scale of 1 – 5 based on the quality of their nest.

Collagen Crosslinking

To determine collagen concentration present in the tissue, we used the hydroxyproline assay with modifications for aortic tissue (112–114). Aortas were thawed and digested in a pepsin solution to separate the soluble and insoluble collagen protein. tissue and standard hydroxyproline was hydrolyzed by incubation for 24 h at 110 °C in 6 M HCl. The sample was mixed with 150 µL isopropanol and 75 µL of chloramine-T (Millipore Sigma, St. Louis, MO, USA) in citrate buffer and oxidized for 10 min at room temperature. The oxidized samples were then mixed with 1 mL of a 3:13 solution of Ehrlich reagent (3 g of *p*-dimethylaminobenzaldehyde (Sigma-Aldrich, St. Louis, MO, USA), 100% ethanol, and 675 µL sulfuric acid) to isopropanol and incubated for 30 min at 58 °C . The reaction was stopped on ice for 10 min and quantified by measuring absorbance at 558 nm on a 96-well plate reader in triplicate. Hydroxyproline concentration (µg/mg tissue) was then determined using a standard curve of trans- 4-hydroxy-l-proline (Sigma-Aldrich, St. Louis, MO, USA) .

Statistical analysis

All data was tested for normality using a Shapiro-Wilk test. For pulse wave velocity measurements, we used a two-way analysis of variance (A.NOVA) comparing time by treatment, and a repeated measures ANOVA to compare PWV over the course of the intervention. For β-stiffness measurements in the carotid and PCA arteries, an unpaired t-test was used to compare ALT-711 and control groups. For dose-response data, we used a t-test with Bonferroni correction to compare group max ACh. For all other responses including, within group ACh and ACh+L-NAME responses, between-group ACh+L-NAME responses, and between group SNP responses, we used a non-parametric Mann-Whitney. Additionally, we compared dose responses using a repeated-measures ANOVA (RM-ANOVA) and corrected for comparison. For hydroxyproline

measurements, a one-way ANOVA was used to compare values between a young control, old ALT-711, and old control groups. Pearson correlations were performed using all old mice (control and ALT-711 combined) to determine relationships between vascular stiffness, endothelial function, and collagen cross-linking. Pearson correlation was calculated using SPSS 26. All other comparisons were run in GraphPad Prism 10. A p-value <0.05 was considered statistically significant. For Bonferroni corrections, a p-value < 0.025 was considered statistically significant. Data are displayed at mean±standard deviation (SD).

3.3 Results

Large artery stiffness

Aortic PWV in both control mice and mice treated with ALT-711 did not significantly change over the course of the intervention ($p>0.05$ for all, Fig. 1A). Additionally, there were no differences in PWV between treatment, time , and the interaction ($p > 0.05$ for all).

We calculated β-stiffness for the carotid artery using a stress-strain curve (fig. 1B-C). There were no significant differences in carotid artery β-stiffness between the ALT-711 and control groups ($P > 0.05$). Carotid elastic modulus at high pressures was significantly higher in ALT-711 treated mice compare to control mice ($p=0.03$, Table 1). There were no other differences in stiffness outcomes in the Overall, the PWV and passive stiffness data suggest that ALT-711 treatment did not prevent or reverse large artery stiffness in these mice.

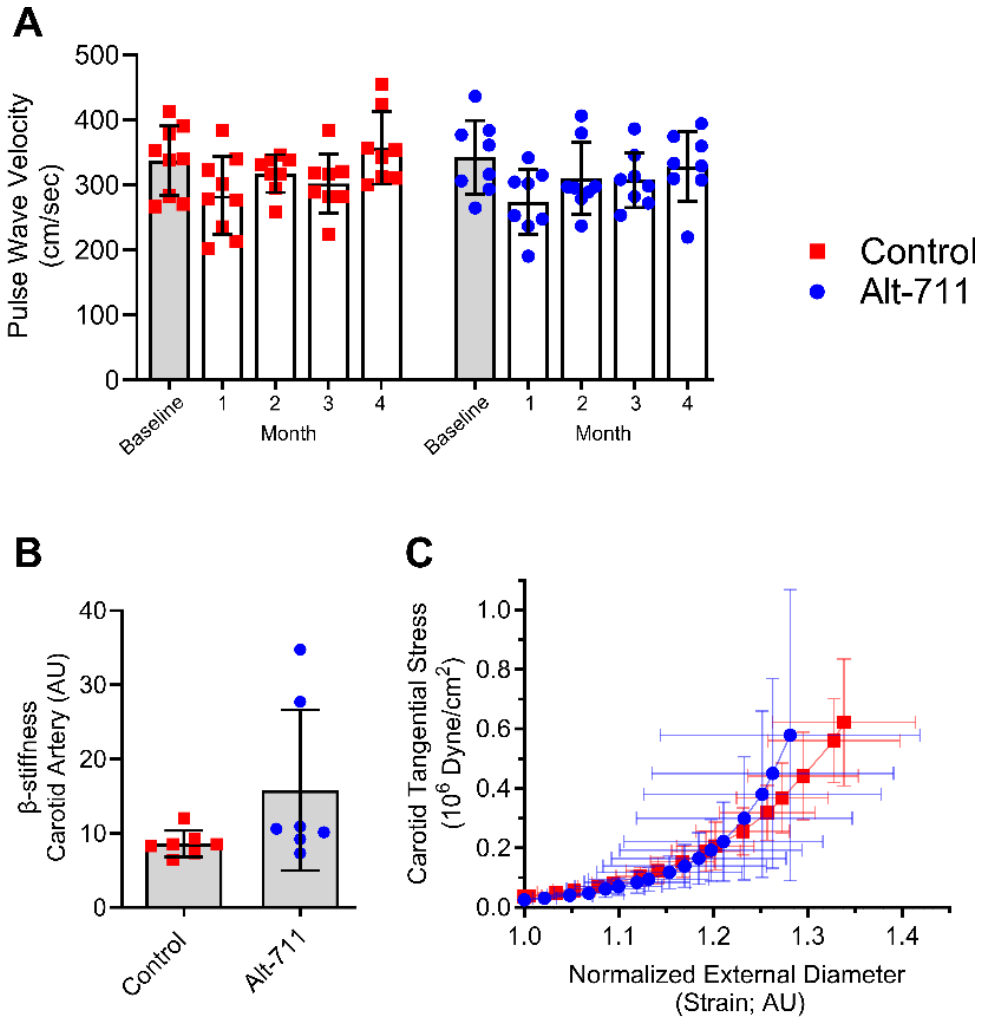

Figure 3.1 No effects of ALT-711 treatment on large artery stiffness in mice. A) Pulse Wave Velocity (PWV) in ALT-711 treated mice and control mice from baseline to month 4 of intervention. B) Carotid artery β-stiffness in ALT-711 treated mice and control mice. C) Stress-strain curve from passive stiffness measurements in ALT-711 treated mice and control mice. Data are mean±SD. Statistics include a 2-way ANOVA, a RM-ANOVA, and an unpaired t-test.

Table 3.1 Carotid artery passive stiffness.

Variable	Group		P-value
	Control	ALT-711	
N	8	7	
Carotid EM_{low}	0.63±0.2	0.92±0.5	0.10
Carotid EM_{high}	4.9±1.7*	8.0±3.6	0.03
N	7	7	
PCA EM_{low}	0.98±0.4	1.14±0.4	0.23
PCA Em_{high}	4.39±2.8	3.10±2.9	0.19

Table 3.1 ALT-711 treatment does not affect passive stiffness of the carotid artery or posterior cerebral artery. Average for elastic modulus (EM) at low and high pressures calculated from stress/strain curves. Data are mean±SD. Statistics include a Student's t-test. PCA – posterior cerebral artery. *p<0.05 Control vs. ALT-711.

Cerebrovascular endothelial function

We found no difference in the PCA vasodilation response to ACh between control and treatment groups for either the dose-response ($p = 0.46$, Fig 2A) or the maximal vasodilation ($p=0.30$). Both the control group and ALT-711 groups had a significant reduction in ACh response in the presence of L-NAME for the dose-response ($p < 0.001$ for both) and the maximal vasodilation ($p < 0.001$). There were also no differences in the ACh+L-NAME responses between the two groups ($p= 0.43$). This indicates the endothelial NO signaling pathway contributed to the vasodilation of ACh. Lastly, the response to SNP did not differ between

groups, indicating that smooth muscle cell response to NO was not different between groups (p = 0.26, Fig 2B).

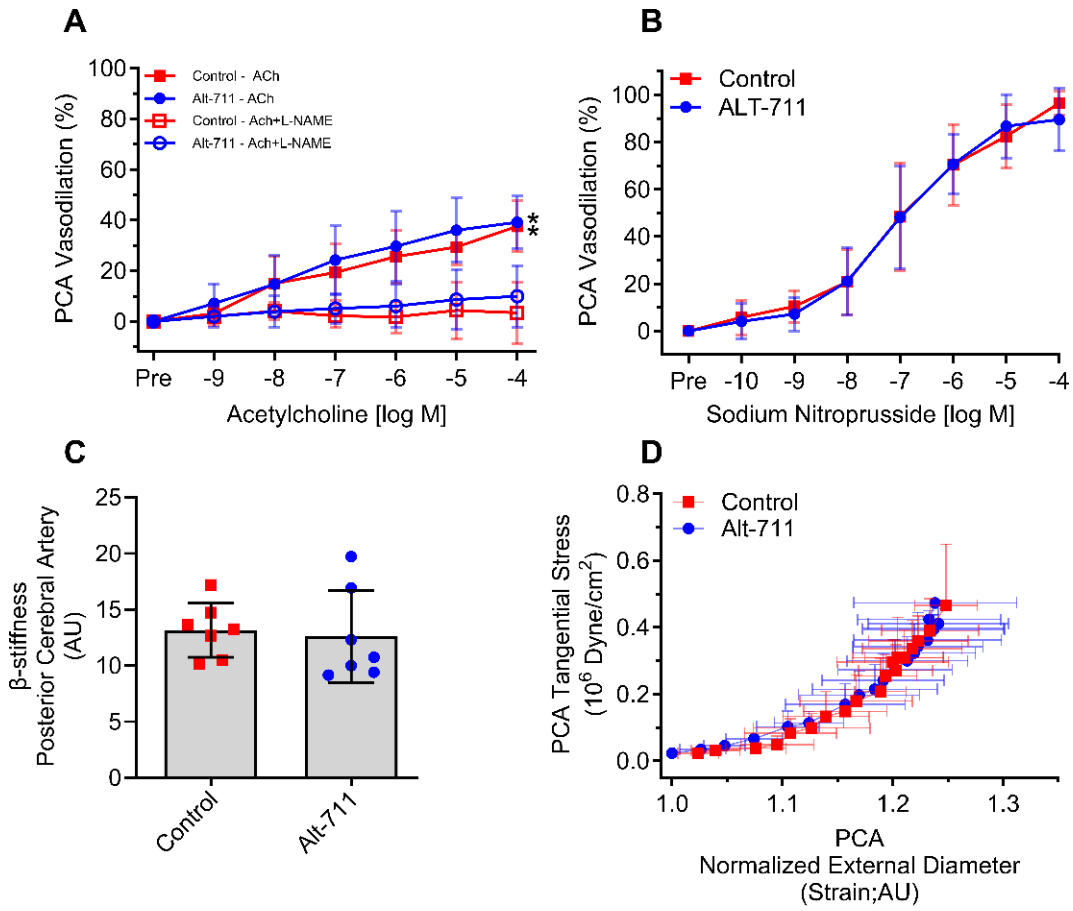

Figure 3.2 No effects of ALT-711 on cerebrovascular function and stiffness. A) Dose response curves to ACh and ACh+L-NAME for ALT-711 treated mice and control mice. B) Dose response curves to SNP for ALT-711 treated mice and control mice. C) PCA β-stiffness in ALT-711 treated mice and control mice. D) Stress-strain curves from passive stiffness measurements in ALT-711 treated and control mice. Data are mean±SD. Statistics include a RM-ANOVA, unpaired t-test with/without Bonferroni correction and Mann-Whitney using Graphpad Prism 10. *p < 0.001 within group ACh vs. ACh+L-NAME.

Cerebral artery stiffness

We calculated PCA β-stiffness using the stress-strain curve (Fig 2C-D). In the PCA, there was no difference in β-stiffness between ALT-711 treated mice and control mice (Fig 2C-D). There were no differences in elastic modulus at low or high pressures between treatment groups ($p > 0.05$ for all, Table 1). These results suggest that ALT-711 does not alter cerebral artery stiffness.

Collagen Crosslinking

Both ALT-711 treated mice ($p < 0.001$) and control mice ($p < 0.01$) had a greater PIF:PSF ratio, a measure of collagen crosslinking, compared to young mice (Fig 3A-B). However, there were no differences in the PIF:PSF ratio between ALT-711 treated mice and control mice ($p = 0.43$). These results indicate that there is greater collagen crosslinking with age, but ALT-711 treatment did not reduce collagen crosslinking. As expected, all groups showed a significantly higher level of PIF (insoluble, crosslinked collagen) compared to PSF (soluble, not crosslinked collagen; $p<0.0001$ for all, Fig. 3B). Both the control group ($p = 0.04$) and ALT-711 group ($p = 0.01$) had less PSF on average compared to the young group. This same finding was true for PIF, where the young group displayed more PIF compared to control mice ($p = 0.008$) and ALT-711 mice ($p < 0.001$). This indicated that young mice have overall higher levels of collagen compared to old mice, but old mice have a greater ratio of crosslinked collagen compared to young mice.

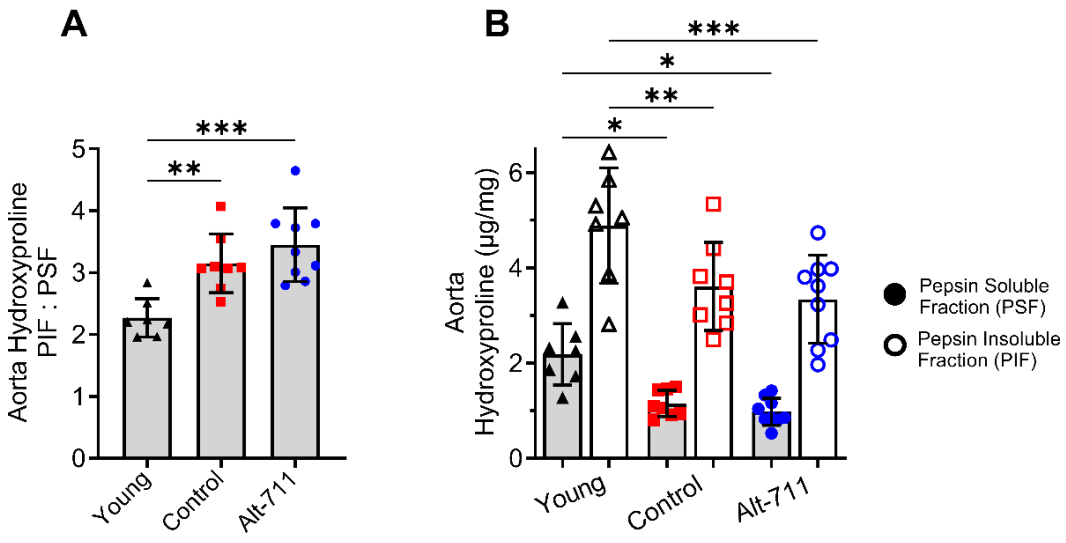

Figure 3.3 No effect of ALT-711 treatment on aortic collagen crosslinking. A) Aorta hydroxyproline PIF:PSF ratios, a measure of collagen crosslinking, in young, ALT-711 treated, and control mice. B) PSF and PIF values from hydroxyproline assay in aortas of young, ALT-711 treated, and control mice. Pepsin soluble fraction: PSF. Pepsin insoluble fraction: PIF. Statistics include a 2-way ANOVA, a one-way ANOVA, and Tukey test for multiple comparison. *p<0.05, **p<0.01, ***p<0.001.

Correlations

Among old mice, we found that aortic PSF negatively correlated with carotid EM at high pressures (r = -0.7, p = 0.004, Fig 4A). PCA maximal dilation to ACh was negatively correlated with both PCA β-stiffness (r = -0.72, p = 0.01, Fig. 4B), and PCA EM at high pressures (r = -0.81, p = 0.001, Fig. 4C). Lastly, PCA (r = 0.72, p = 0.002). Lastly, PCA β-stiffness was negatively correlated with nest building scores (r = -0.756, p = 0.001, Fig. 4D). Overall, these correlations demonstrate that increased collagen PSF, cerebral artery stiffness, cerebral artery function, and cognitive function and all associated with one another. The main findings from these correlations are the increased cerebral artery stiffness is correlated with decreased cerebral

artery function and cognition.

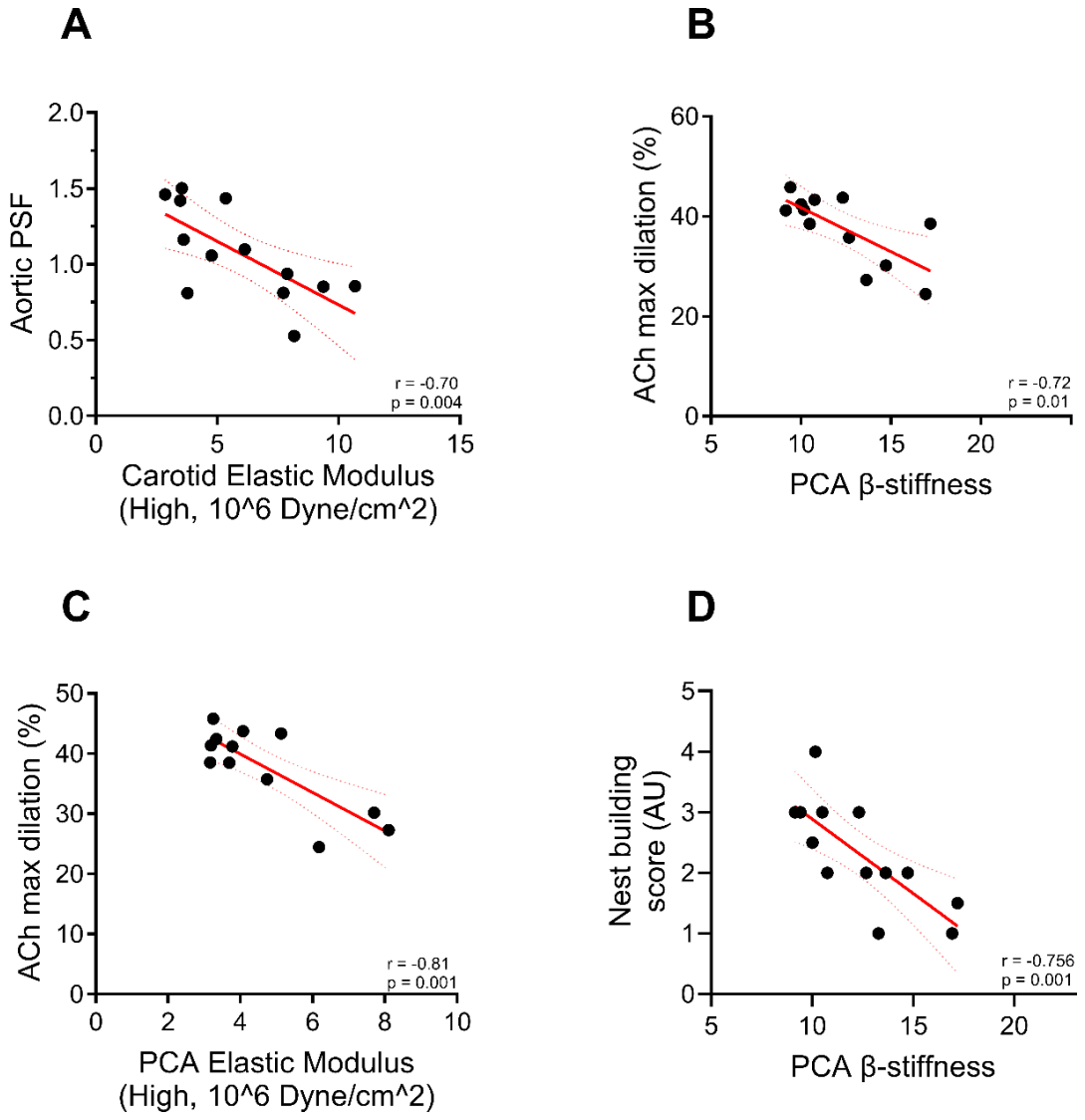

Figure 3.4 Cerebral artery stiffness is negatively correlated with cerebral artery endothelial function and cognition. Pearson's Correlations between, large artery stiffness, collagen crosslinking, cerebral artery stiffness, cerebrovascular function, and cognition. **A)** Carotid elastic modulus at high pressures and aortic PSF. **B)** PCA β-stiffness and percent maximal dilation to ACh. **C)** PCA elastic modulus at high pressures and percent maximal dilation to ACh. **D)** PCA β-stiffness and nest building score. Solid red line indicates mean trend and 95% confidence interval in red dotted line.

3.4 Discussion

The results of this study suggest that long-term ALT-711 treatment in mice did not affect large artery stiffness, cerebral artery function, or cognitive impairment. However, we did find a few notable correlations of interest among the old mice. We found that large artery stiffness related to collagen-crosslinking as expected (47, 115). We also show the novel finding that cerebral artery stiffness is related to cerebral artery endothelial function and cognitive function.

Large Artery stiffness and collagen crosslinking

Despite prior evidence indicating the beneficial effects of ALT-711 on cardiovascular function, we saw no changes in cardiovascular outcomes of aged rodents treated long-term with the compound (61, 110, 111, 116). Previous studies in rodents have demonstrated that ALT-711 reduces large artery stiffness and improves vascular health in type 2 diabetes models (57, 109, 117). Further work by Kass et al. (2001) with ALT-711 treatment in humans suggested that ALT-711 was effective in improving arterial compliance and reducing pulse pressure in older adults with vascular stiffening (59). In contrast, in our study, we found no effects of ALT-711 treatment on either aortic PWV or carotid artery passive stiffness. We used old C57Bl/6 mice for this study as they display age-dependent increases in large artery stiffness similar to humans (118). Previous studies with ALT-711 treatment in rodents used diseased models like spontaneously hypertensive rats or streptozotocin-induced type 2 diabetes. Thus, there is potential that ALT-711 treatment is primarily effective in the context of disease. Long-term ALT-711 treatment has been investigated previously. We adapted our long-term treatment protocol based on a study by Susic et al. who found that the optimal dose in rats was 1mg/kg/day for 4 months (110).

Prior studies demonstrated that ALT-711 breaks collagen cross-links in vitro (57). After finding no differences in large artery stiffness in these mice, we investigated the efficacy of the ALT-711 compound to break crosslinks in vivo in large arteries. We found that while old mice displayed a notable increase in collagen crosslinking compared to young mice, there was no difference in the amount of crosslinking between the aortas of ALT-711 treated mice and control mice. Increases in collagen crosslinking in the aorta with age have been well documented and align with the current understandings of vascular aging (119). Considering there were no differences in insoluble collagen content, PWV, or carotid β-stiffness, we have concluded that long term treatment of ALT-711 was unsuccessful in breaking collagen crosslinking and reducing large artery stiffness.

Cerebrovascular function

Previous studies demonstrate that increased stiffness of the large arteries leads to impaired cerebrovascular function (72, 84, 120). Thus, we hypothesized that a reduction in large artery stiffness would mitigate arterial stiffness and preserve endothelial function in cerebral arteries. However, we found that long-term treatment with ALT-711 did not affect cerebral artery stiffness or endothelial function, likely due to the lack of effects on large artery stiffness. One study by Hartog et al. that tested ALT-711 treatment in patients with chronic heart failure showed no beneficial effects on cardiac function (121). The results from our study and others suggest that ALT-711 may be beneficial only in certain experimental and clinical conditions.

Since ALT-711 treatment is not specific to large arteries, it is possible that the compound may directly affect the cerebral arteries. Research on the direct effects of ALT-711 treatment on cerebral arteries has not been previously conducted, making this study the first to report these

findings. We were unable to assess the ability of ALT-711 to directly break cross-links in cerebral arteries due to limited tissue. However, our results generally suggest that even if ALT-711 breaks cross-links in cerebral arteries, the function and stiffness of these arteries were unchanged.

Correlations between arterial stiffness and function

Despite the negative findings in this study, we combined data for ALT-711 treated mice and control mice to determine correlations within our dataset. We found that the hydroxyproline aortic PSF, a measure of uncross-linked collagen, was negatively correlated with carotid artery stiffness measurements. This supports that levels of collagen crosslinking contribute to large artery stiffness, corroborating the findings of many previous studies (47, 122, 123).

To continue, cerebral artery stiffness was negatively correlated with both cerebral artery endothelial function and nest building scores. Cerebral artery endothelial cell dysfunction contributes to reduced blood flow and hypoxic environment (124). Reduced blood flow in the cortex can impair cognitive function (125). Therefore, increases in cerebral artery stiffness might contribute to impaired instinctual nest building behavior via the effects on endothelial function. Our findings suggest that stiffness in cerebral arteries has adverse effects on cerebral artery function and cognitive function, to a larger degree than large artery stiffness. Cerebral artery stiffness could be a mediated remodeling from pulse pressure on the vessel wall due to increases in large artery stiffness. In a transgenic mouse model of elastin haploinsufficiency and large artery stiffness, cerebral artery endothelial function was impaired (72). Thus, large artery stiffness indirectly impacts cognitive function by interfering with the cerebral arteries. As it is

technically difficult to measure cerebral artery stiffness in human subjects, it is unknown if these findings translate to older human populations.

3.5 Limitations

While this small pilot study included males and females, the sample sizes were too low to compare sex differences in the effects of ALT-711. Thus, it is possible that the ALT-711 compound affects male and female mice differently. We used the hydroxyproline assay to quantify collagen crosslinking, but a more technical approach to assessing crosslinking using HPLC or cell culture methods might have given stronger conclusions. Mice were treated with ALT-711 at 20 months of age, which may have been too late to observe any treatment effects. It is possible that cerebral artery dysfunction had already occurred prior to treatment making any treatment effects null. Lastly, while we did not find any long-term treatment effects, it is possible an acute supplementation of ALT-711 may yield different results.

3.6 Conclusion

Overall, we found that long-term treatment with ALT-711 in old mice did not reduce large artery stiffness, preserve endothelial function, or lower collagen crosslinking. Among old mice, we found that cerebral artery stiffness is related to endothelial dysfunction and cognitive dysfunction. These results suggest that compounds that reduce cerebral artery stiffness may have beneficial effects on cerebrovascular and cognitive function.

IV. PROTECTIVE EFFECTS OF MITOQUINOL MESYLATE (MITOQ) ON VASCULATURE AND COGNITION IN AN ALZHEIMER'S DISEASE MOUSE MODEL.

4.1 Introduction

As of 2025, approximately 11% of individuals 65 and older have Alzheimer's disease (AD) in the United States (126). However, current treatments for AD are minimally effective, and treatments to prevent or delay the onset of AD are not established. Mitochondrial dysfunction and cerebrovascular dysfunction are highly implicated in AD pathology and could be promising therapeutic targets to pursue (127, 128). Thus, there is a strong need for research investigating therapeutic strategies for disease treatment and prevention.

One major contributor to AD is the increase in oxidative stress associated with age-related mitochondrial dysfunction. Mitochondria are a primary producer of reactive oxygen species (ROS) (129). Excess ROS causes oxidative damage, DNA damage, and cellular dysfunction (130). Mitochondrial dysfunction and ROS are strongly associated with neurodegeneration, with increasing evidence it plays a causative role in age-related disease (131, 132). A study by Trifunovic et al. found that transgenic mice exhibiting dysfunctional mitochondria had a phenotype modeling aging and disease (133). In sum, preserving mitochondrial function and limiting ROS production may be beneficial in preventing or delaying AD onset.

ROS produced by mitochondria may impact AD by causing cerebrovascular dysfunction. Impaired endothelium-dependent dilation (EDD) is a cause of cerebrovascular dysfunction that leads to reduced cerebral blood flow and neuroinflammation. Increased ROS causes a reduction in nitric oxide (NO) bio-availability and uncoupling of endothelial NO synthase (eNOS) (134). NO also acts to inhibit the vasoconstrictor endothelin-1, which contributes to endothelial dysfunction by modulating vascular tone (135, 136). Thus, increased mitochondrial ROS

production could contribute to neurodegeneration and AD pathology by impairing cerebrovascular function.

Previous studies demonstrate that antioxidant supplementation in mice can preserve cerebrovascular and endothelial function (52, 63, 64, 137). Mitoquinone mesylate (MitoQ, MitoQ Ltd, Auckland, New Zealand), is an antioxidant that specifically targets mitochondria to reduce ROS production and has been shown to preserve endothelial function, and reduce aortic stiffness. But the vascular effects of MitoQ have not been tested in the context of AD.

MitoQ has been previously investigated in a 3xTg mouse model of AD (138, 139). These studies demonstrated that MitoQ was beneficial in mitigating brain oxidative stress and amyloid-β (Aβ) accumulation. However, the 3xTg mouse overexpresses AD-related mutations in a constitutive manner and accumulate Aβ plaques early in life, making these findings less translatable to human disease. The APP^{NL-F} mouse strain is a relatively new transgenic strain that models cognitive impairment and significant Aβ deposition at approximately 15 months of age, a timeline similar to that of humans with late-onset AD (140). The APP^{NL-F} mouse has Swedish and Beyreuther/Iberian mutations that are regulated by the mouse *APP* promotor, thus eliminating the constitutive overexpression of *APP,* like the 3xTg model. For this reason, the APP^{NL-F} mouse was ideal for our study.

We chose the age range of 17 – 21 months for this study because during this period, amyloid-β deposition in the brain increases drastically, making it an ideal window for investigating interventions to prevent or mitigate the pathology (140, 141). Additionally, previous studies indicate that these mice display cognitive impairments by 18 months of age, making the 17-

month age ideal for capturing any prevention of cognitive impairment that would be seen with MitoQ treatment.

The purpose of this study was to investigate the potential therapeutic effects of MitoQ on mitigating increases in aortic stiffness, cerebrovascular dysfunction, and AD pathology in a mouse model of AD. Additionally, we characterized cerebrovascular function in the *APP*$^{NL-F}$ mouse which has yet to be described. We hypothesized that *APP*$^{NL-F}$ mice treated with MitoQ would have less large artery stiffness and greater cerebrovascular function.

Secondly, we hypothesized that MitoQ treatment would mitigate Aβ accumulation, neuroinflammation, and cognitive decline. Lastly, we hypothesized that there would be sex differences among these outcomes in male and female *APP*$^{NL-F}$ mice. We hypothesized that females would display greater adverse effects on the vascular with age compared to male mice, due to the loss of vasoprotective estrogen. We also hypothesized that treatment with MitoQ might show greater benefits in female mice for the same reason with MitoQ treatment. In this study, we treated 17-month old male and female *APP*$^{NL-F}$ mice with MitoQ or vehicle in their drinking water for 4 months (Figure 1). To test these hypotheses, we assessed large artery stiffness, aorta histology, cerebral artery endothelial function, neuroinflammation, and cognitive function.

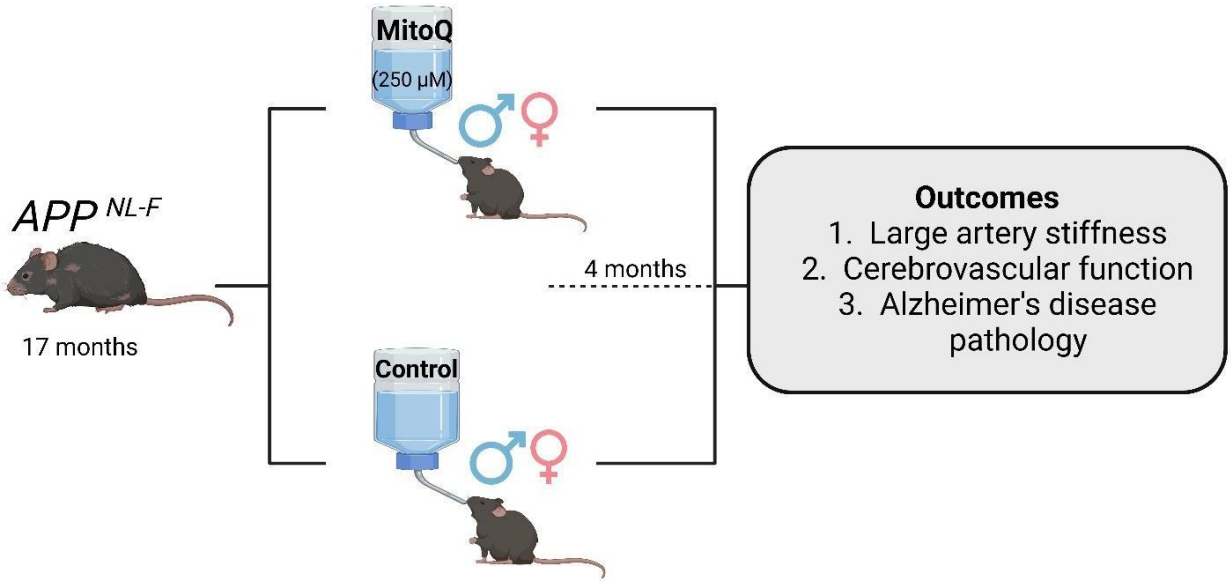

Figure 4.1. Study Design for Chapter 4. 17-month-old *APP*$^{NL-F}$ transgenic mice were randomly assigned to either MitoQ treatment (250 µM) or control (water) for 4 months. Treatment and control groups were matched based on age and sex. After 4 months of treatment, large artery stiffness, cerebrovascular function, and Alzheimer's disease pathology were assessed and compared between groups.

4.2 Methods

Study design

The intervention study design is displayed in Figure 1. To model AD, we used the transgenic *APP*$^{NL-F}$ mouse model. This model contains the human *APP* gene knock-in with Swedish and Iberian mutations on a C57BL/6 background (140). The intervention consisted of treatment with either MitoQ (Mitoquinone mesylate, 250µM) or control (no addition) in their drinking water for 4 months. Solutions were made fresh every 3 days and stored in communal light-protected water dispensers in the cages. At 17 months of age, before starting the treatment, the mice underwent baseline testing. We used block randomization to assign animals to either the treatment or

control group. Groups included sex-matched males and females to assess sex differences in outcomes based on treatment.

An additional cohort (17-month mice, n=4) did not undergo the intervention. These mice were tested for some outcomes at 17 months old to mimic the baseline time point. This group serves as a physiological baseline comparison to determine the influence of age on vascular outcomes in the APP^{NL-F} mouse.

Mice were fed a phytoestrogen-free diet (Envigo, Teklad Global Soy Protein-Free Extruded Rodent Diet, 2920X) with *ad libitum* food and water and were housed in an animal care facility on a 12/12-hour light-dark cycle at 24°C. Investigators were blinded to treatment group when analyzing data. All animal procedures conform to the *Guide to the Care and Use of Laboratory Animals* (8th edition, revised 2011) and were approved by the Institutional Animal Care and Use Committees at the University of Oregon. All reporting of animal data adheres to the ARRIVE guidelines for conducting animal studies.

Frailty

Mouse frailty was assessed using a previously studied 31-item Frailty Index based on established clinical signs of deterioration in C57BL/6J mice (142). Frailty assessment included evaluation of the integumentary, musculoskeletal, vestibulocochlear/auditory, ocular, nasal, digestive, urogenital, and respiratory systems as well as signs of discomfort, body weight, and body surface temperature. The severity of each deficit was assessed and assigned either a 0, 0.5, or 1, with the higher score indicating more severe frailty. Each mouse was examined at approximately the same time of day, following the same order of assessments at both baseline, and within 14 days

of their planned vascular reactivity study. Vision loss was too difficult to assess and therefore not included in the index.

Tissue collection

Mice were euthanized by cardiac perfusion with heparinized saline under isoflurane immediately prior to ex vivo vascular studies. After euthanasia, the heart, liver, spleen, soleus, gastrocnemius (gastroc), and white adipose tissue (WAT) were collected, and their wet weights were recorded. In addition, cerebral arteries, carotid artery, aorta, cerebral cortex, and hippocampus were excised and frozen at −80°C for preservation. A section of descending aorta was taken and frozen in optimal cutting temperature (OCT) for histology sections.

Pulse wave velocity

Aortic stiffness was measured by *in vivo* pulse wave velocity (PWV) as previously described at baseline (17 months) and within 1 week prior sacrifice post-intervention (21 months) (76, 77).Mice were anesthetized by 2% inhaled isoflurane in 100% oxygen and situated on a temperature-controlled heating pad (37°C) to maintain body temperature. Electrodes were placed on the distal parts of limbs to record ECG information, while 20 MHz Doppler transducers were placed on the aortic arch and abdominal aorta. Indus Doppler Flow Velocity System (Webster, Texas) was used to record and analyze data. The time for each beat to travel from aortic arch to abdominal aorta was measured and was divided by the distance between the two locations to determine the PWV value. Two researchers analyzed each Doppler recording. Inter-observer confidence intervals were measured, and PWV measurements with confidence intervals over 15% were excluded.

Artery histology

Sections of thoracic aorta were frozen in optimal cutting temperature (OCT) compound and then sliced into 8 μm sections using a cryostat (Nikon, Minato, Tokyo, Japan) and adhered to a charged slide (72). Sections were stained using an adapted Masson's Trichrome protocol. Slides were imaged using a Leica Microscope (Leica, Wetzlar, Germany) and Leica LAS software. Arterial wall thickness was analyzed using FIJI by ImageJ software.

Cerebral artery endothelial function

After sacrifice, the posterior cerebral arteries (PCA) were excised and placed in a myograph chamber (DMT Inc., Aarhus, Denmark) with a physiological saline solution that contained 145.0 mm NaCl, 4.7 mm KCl, 2.0 mm $CaCl_2$, 1.17 mm $MgSO_4$, 1.2 mm NaH_2PO_4, 5.0 mm glucose, 2.0 mm pyruvate, 0.02 mm EDTA, 3.0 mm MOPS buffer and 1 g/100 ml BSA, pH 7.4 at 37°C, cannulated onto glass micropipettes and secured with nylon (11-0) suture. Once cannulated, arteries were warmed to 37°C, pressurized, and allowed to equilibrate for ~20 minutes.

All arteries were submaximally preconstricted with phenylephrine (2–6 μm to obtain 20–40% preconstriction), and increases in luminal diameter in response to increasing concentrations of the endothelium-dependent dilator, acetylcholine (ACh: 1×10^{-9} to 1×10^{-4} m), and endothelium-independent dilator, sodium nitroprusside (SNP: 1×10^{-10} to 1×10^{-4} m), were determined. Responses to ACh were repeated in the presence of the NO synthase inhibitor N^{ω}-nitro-l-arginine methyl ester (L-NAME: 0.1 mM, 30 min incubation) to determine the contribution of NO to dilatation. Arteries also underwent dose responses (without prior pre-constriction) to increasing doses of the endothelium-dependent constrictor endothelin-1 (ET-1 1×10^{-11} to 1×10^{-7} M) and endothelium-independent constrictor potassium chloride (KCl, 10 to

100 mM.) Additionally, arteries were incubated with either MitoQ (0.5 μM) for 60 minutes or the ET-1 receptor blocker BQ-123 (10 μM) for 30 minutes and then underwent ACh responses. MitoQ incubation assessed the acute effects of the mitochondrial antioxidant on dilation, while BQ-123 assessed the contribution of ET-1 preventing dilation.

Passive Stiffness

Passive arterial stiffness was measured *ex vivo* in carotid arteries and PCAs. Arteries were incubated for 60 minutes in a calcium free solution to eliminate the effects of myogenic tone. Lumen diameter and medial wall thickness were measured following increasing intralumenal pressure (72, 78). Arteries were isolated and cannulated between glass pipette tips on a myograph as previously described (72). Measurements for each artery were recorded from 5 to 100 cmH2O (3.7–73.5 mmHg) in 5 cmH_2O increments. Stress was calculated as:

$\sigma = PD/2WT$

where P is pressure in dyne cm^{-2}, D is lumen diameter and WT is wall thickness.

Strain was calculated as:

$\varepsilon = (D - Di)/Di$

where D_i is the initial starting diameter.

Data for each artery were fit to the curve:

$\sigma = \sigma i e^{\beta \varepsilon}$

where σ_i is the initial starting stress (5 cmH_2O) and β is the slope of tangential elastic modulus versus stress. A higher β represents a stiffer artery (79–81).

Cognitive Testing

Morris Water Maze (MWM)

The MWM cognitive test was used to assess learning and spatial memory. For the test, a 122 cm cylindrical pool of opaque water served as the testing area. The pool was divided digitally into equal quadrants. A 10 cm clear, height-adjustable, circular platform served as an escape pad for the mice. Two days prior to the test, a researcher held the mice for 5 minutes each day to acclimate them to being handled.

Mice underwent a 3-day training period, including 2 sessions per day, of 3 trials per session. During the training sessions, the mouse remained in the pool until they successfully positioned themselves on a hidden platform (1 cm below the surface) for 3 seconds or until 60 seconds elapsed since entering the pool. If 60 seconds elapsed and the mouse did not find the platform, the researcher gently guided the mouse to swim onto the platform.

On the fourth day, a probe trial was performed, followed by a beacon trial. During the probe trial, the platform was inaccessible, and the time spent in target quadrant was tracked. During the beacon trial, the platform was accessible with clear visual markings and the time to reach this platform was tracked as a control test for the time it takes the mouse to swim to a visible platform. All sessions were recorded and analyzed with EthoVision XT18 software (Noldus, Wageningen, the Netherlands) (83).

Rotarod

A 2-day accelerating rotarod protocol was used to assess motor coordination using the Rotarod (47650 Rota-rod NG, Ugo Basile, Gemonio, Italy). During the acclimatization day, mice were required to remain on the wheel for 90 seconds with the rod at 4 rpm. During the test day, mice were paced on the rod accelerating from 4 – 40 rpm. Mice received 3 trials with a 10 minute rest

in between trials. Time was recorded when the mouse fell or had 2 consecutive rotations around the rod. The average time from the 3 trials was used as the final measurement.

Nest Building

A nest building test was used to assess instinctual cognitive behavior ((82). Mice were singly housed overnight in a cage with food, water, and a condensed cotton nestlet. In the morning, a researcher placed mice back in communal housing and scored each nest on a scale of 0–5 based on the following criteria: 0 – untouched nestlet, 1 – nestlet is moved with no tearing, 2 – tearing of nest but no formation of a nest, 3 – tearing and formation of a nest OR nestlet is placed in corner of the cage, 4 – significant tearing and nest formation in corner of cage, 5 – perfect nest with tearing, placement at corner of cage, and high dome-like walls built around corners of the nest.

Brain Slice Histology

The right hemisphere was fixed in 4% paraformaldehyde/phosphate-buffered saline (PBS) solution for 48 hours. Samples were transferred to a 100% PBS solution and stored at 4°C until further use. Brains were paraffin embedded and Immunohistochemical stains were applied to paraffin sections after deparaffinization and antigen retrieval (5 min treatment at room temperature with 95% formic acid, followed by 30 min incubation in citrate buffer [pH 6.0] at 90°C) Tissue sections were blocked with 5% nonfat dry milk in phosphate-buffered saline and labeled with primary antibodies Glial fibrillary acidic protein (GFAP, 1:500, Proteintech, Cat: 168-25-1-AP), and amyloid-β (4G8, 1:5000, Bio legend, Cat: 800701). Results were visualized after the application of appropriate secondary antibodies using diaminobenzidine (DAB). Regions of the entorhinal cortex, hippocampus, and thalamus from these sections were imaged at

20x using a Leica Microscope (Leica, Wetzlar, Germany) and Leica LAS software. Cell count, size, and percent area were analyzed by the same researcher. For cell count, the particle count range was between 10 – 3000. Threshold. The cell size was determined by the size of the particle. For percent area, cells were quantified as "area fraction" per region. One image per region of interest was acquired for each animal. Images were analyzed using FIJI by ImageJ. On ImageJ, the brown image using the H-DAB deconvolution channel was used for analysis.

Statistical Analysis

All data was tested for normality using a Shapiro-Wilk test. For GFAP staining, a Kruskall Wallis tes was used for the whole group in the entorhinal cortex. A Mann-Whitney test to compared groups based on sex for this outcome. On outcomes where the 17-month group is included, a one-way ANOVA was used to compare means. For PCA stiffness, a Mann-Whitney was used for EM outcomes and a Student's t-test was used for β-stiffness. Repeated measures ANOVA was used to compare dose response data and Morris water maze training data. The repeated measures ANOVAs were manually adjusted for multiple comparisons. A p-value less than 0.05 was considered statistically significant. Data are displayed as mean±standard deviation (SD).

4.3 Results

Animal Characteristics

Animal Characteristics are displayed in Table 1 and Table 2. In the whole group, MitoQ mice drank less water than Control mice (p=0.026, Table 1). When analyzed by sex, MitoQ males drank less than control males (p=0.047), but there was no difference in the females (p=0.23, Table 2).

Table 4.1 Whole group animal characteristics.

Variable	17-month	Control	MitoQ
N	5	19	17
age (months)	-----	20.5±0.2	20.5±0.2
Daily water intake (ml)	-----	4.6±0.7	3.8±0.6*
Daily MitoQ intake (µg/day)	-----	-----	644±102
Body mass (g)	34.8±6.1	37.8±8.8	35.9±5.7
Heart mass, mg	132±17	168±24	163±21
Percent heart:body mass	0.38±0.04	0.45±0.09	0.44±0.08
Liver mass, mg	1513±361	1611±575	1748±410
Percent liver:body mass	4.3±0.57	4.2±0.94	4.9±0.77
Spleen mass, mg	128±35	131±44	122±44
Percent spleen:body mass	0.37±0.10	0.38±0.12	0.35±0.17
WAT mass, mg	1938±766	1593±964	1383±688
Percent WAT:body mass	5.43±1.46	3.93±1.64	3.61±1.37
Gastroc mass, mg	177±16	145±16	149±24
Percent gastroc:body mass	0.52±0.10	0.40±0.10	0.41±0.07
Soleus mass, mg	13±1	14±4	15±6
Percent soleus:body mass	0.04±0.01	0.04±0.01	0.04±0.02

Kidney mass, mg	440±75	538±77	523±63
Percent kidney:body mass	1.28±0.18	0.95±0.78	1.18±0.61
Uterus mass, mg	250±144	237±35	94±40
Percent uterus:body mass	0.71±0.38	0.76±1.1	0.27±0.11
Frailty Index	0.27±0.01	0.28±0.04	0.28±0.04

Table 4.1 Whole group animal characteristics. Data on age, sex, water intake, body mass, tissue weights, and Frailty scores for whole grouped animals included in this study. Data are mean±SD. White adipose tissue (WAT), gastrocnemius (gastroc). *$p<0.05$ vs. within-group control. Uterus weights include female mice only.

Table 4.2 Animal characteristics for groups based on sex.

Variable	Control		MitoQ	
	Male	Female	Male	Female
N	13	6	10	7
age (months)	20.5±0.3	20.5±0.1	20.5±0.3	20.5±0.1
Daily water intake (ml)	4.7±0.6	4.3±1	4.0±0.5*	3.6±0.7
Daily MitoQ intake (µg)	-----	-----	678±85	610±119
Body mass (g)	41.3±8.4	30.2±2.6	37.5±5.3	33.9±5.9
Heart mass, mg	179±21	148±14	166±13	160±30
Percent heart:body mass	0.43±0.11	0.49±0.04	0.43±0.06	0.48±0.14
Liver mass, mg	1804±731	1423±279	2025±484	1520±332
Percent liver:body mass	4.0±0.99	4.7±0.64	5.1±0.70	4.5±0.70
Spleen mass, mg	120±40	152±47	105±32	150±49
Percent spleen:body mass	0.34±0.24	0.51±0.18	0.28±0.11	0.46±0.20
WAT mass, mg	1848±1062	1040±326	1552±709	1443±1095
Percent WAT:body mass	4.16±1.86	3.41±0.93	3.85±1.34	3.87±2.25
Gastroc mass, mg	153±12	130±10	165±13	123±14
Percent gastroc:body mass	0.39±0.10	0.43±0.03	0.43±0.06	0.37±0.08

Soleus mass, mg	15±4	12±2	18±6	10±5
Percent soleus:body mass	0.04±0.01	0.04±0.01	0.05±0.02	0.03±0.02
Kidney mass, mg	571±54	438±26	559±44	458±28
Percent kidney:body mass	1.05±0.78	0.72±0.80	1.31±0.54	1.00±0.71
Uterus mass, mg	----------	237±35	----------	94±40
Percent uterus:body mass	----------	0.76±1.1	----------	0.27±0.11
Frailty Index	0.27±0.05	0.29±0.04	0.29±0.03	0.26±0.05

Table 4.2 Animal characteristics grouped by sex. Data on age, water intake, body mass, tissue weights, and Frailty scores for separate male and female groups included in this study. Data are mean±SD. White adipose tissue (WAT), gastrocnemius (gastroc). *$p<0.05$ vs. within-group control.

Large Artery stiffness

Large artery stiffness was assessed with PWV pre- and post-intervention. In the whole group, there was a significant difference in PWV at baseline between MitoQ mice and control mice (p=0.047, Fig. 2A). There was a trend for baseline differences between groups among the sexes (males: p=0.203, females: p=0.155, Fig. 2B-C). Additionally, there were no differences in PWV seen post treatment in any of the groups (p>0.05 for all).

We used pressure myography to measure passive properties of stiffness in carotid arteries without tone (Ca^{+2} free bath incubation). We found no differences in carotid β-stiffness between any groups (p>0.05 for all, Fig. 3A-C). There were also no significant differences in elastic modulus at low and high pressures in these mice (p>0.05 for all, Fig.4A-C).

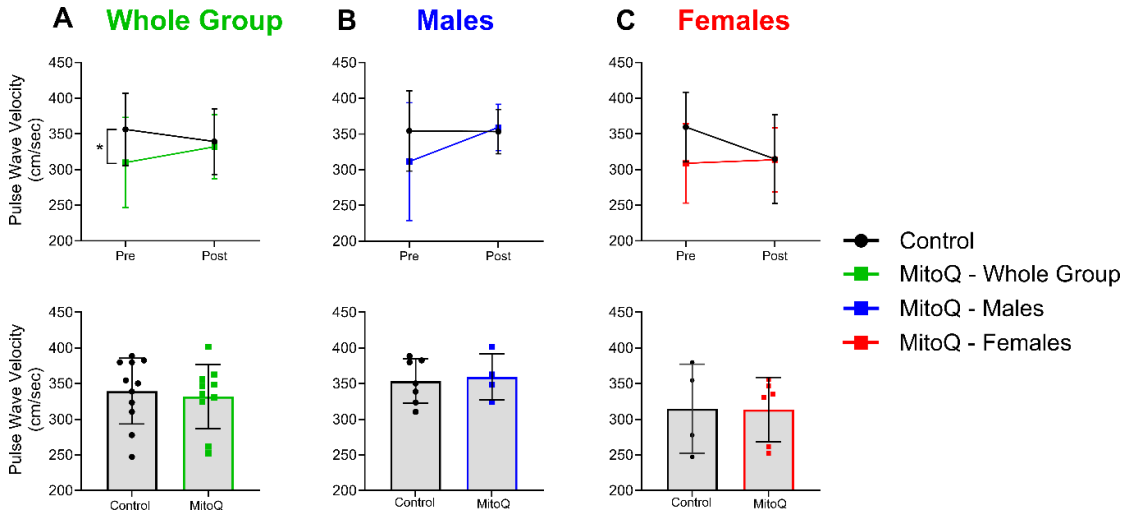

Figure 4.2 Pulse wave velocity did not change or improve with MitoQ treatment. Pulse wave velocity data in control and MitoQ treated mice from pre-to-post intervention (top), and post-intervention (bottom) for **A)** whole group, **B)** males, and **C**) females. Data are mean±SD. Statistics include a RM-ANOVA for pre-to-post data, and a Student's t-test for post intervention data. *p<0.05 control vs. MitoQ.

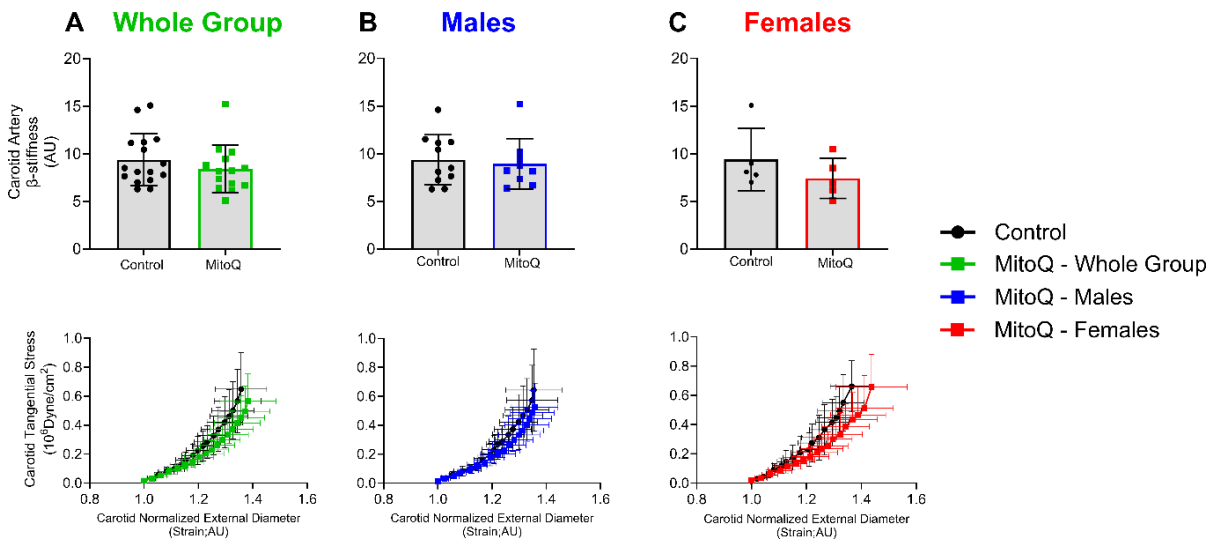

Figure 4.3 Carotid β-stiffness was not different among control and MitoQ treated mice. Control and MitoQ treated Carotid artery β-stiffness (top), and stress/strain curves (bottom) for **A)** whole group, **B)** males, and **C**) females. Data are mean±SD. Statistics include a Student's t-test

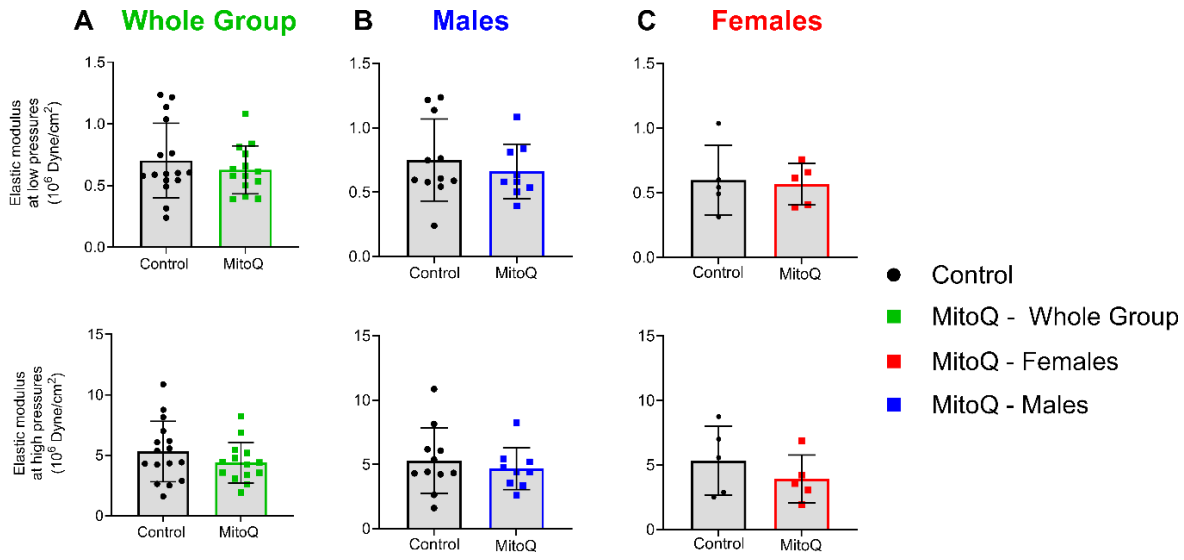

Figure 4.4 Carotid elastic modulus was not different among control and MitoQ treated mice. Control and MitoQ treated carotid artery elastic modulus at low pressures (top), and elastic modulus at high pressures (bottom) for **A)** whole group, **B)** males, and **C**) females. Data are mean±SD. Statistics include a Student's t-test.

Aorta Histology

Aorta sections were stained using an adapted Masson's Trichrome protocol to obtain wall thickness measurements. In the whole group, we found that aortic media wall thickness in MitoQ ($p=0.017$) and Control mice ($p=0.0001$) were greater compared to 17-month mice (Fig. 5A). When grouped by sex, control males had greater wall thickness compared to MitoQ males ($p=0.026$), but this was not the case for females ($p=0.266$, Fig 5B-C). When measuring media and adventitia thickness together, the same finding was true for greater wall thickness in MitoQ mice ($p=0.002$) and control mice ($p=0.001$). However, there was no longer a difference in wall thickness when grouped by sex ($p>0.05$ for both).

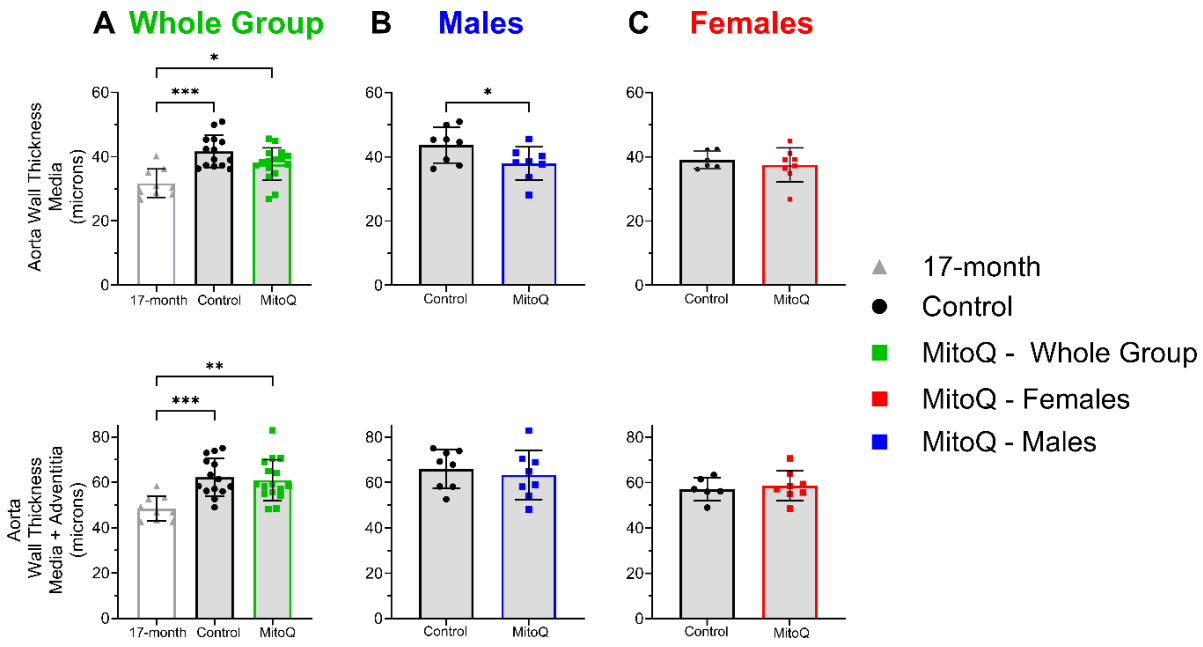

Figure 4.5 Aging leads to greater aortic wall thickness and is mitigated by MitoQ in *APP*$^{NL-F}$ males. 17-month, control, and MitoQ mice aortic media wall thickness (top), and media + adventitia wall thickness (bottom) for **A)** whole group, **B)** males, and **C**) females. Data are mean±SD. Statistics include a student's one-way ANOVA for whole group, and Student's t-test for individual sexes. *p<0.05, **p<0.01, ***p<0.001.

Cerebral artery endothelial function

To determine cerebrovascular function, we measured endothelium-dependent dilation using pressure myography. There were no differences in the response curves to ACh, SNP or percent maximal dilation to ACh, and percent NO-dependent dilation in any of the groups (p>0.05 for all, Fig 6A-D). However, we found that for the whole group, the ACh + L-NAME dose response was significantly higher in MitoQ mice compared to control mice (p=0.032). This response was significant for female MitoQ mice (p=0.015), but not for males (p=0.503). There were no other differences in ACh dose response curves among groups for doses with MitoQ incubation, or BQ-

123 incubation (p>0.05 for all, Fig. 7A-B). Additionally, there were no differences in constriction response in any groups for the ET-1 and KCl (p>0.05 for all, Fig. 7C-D).

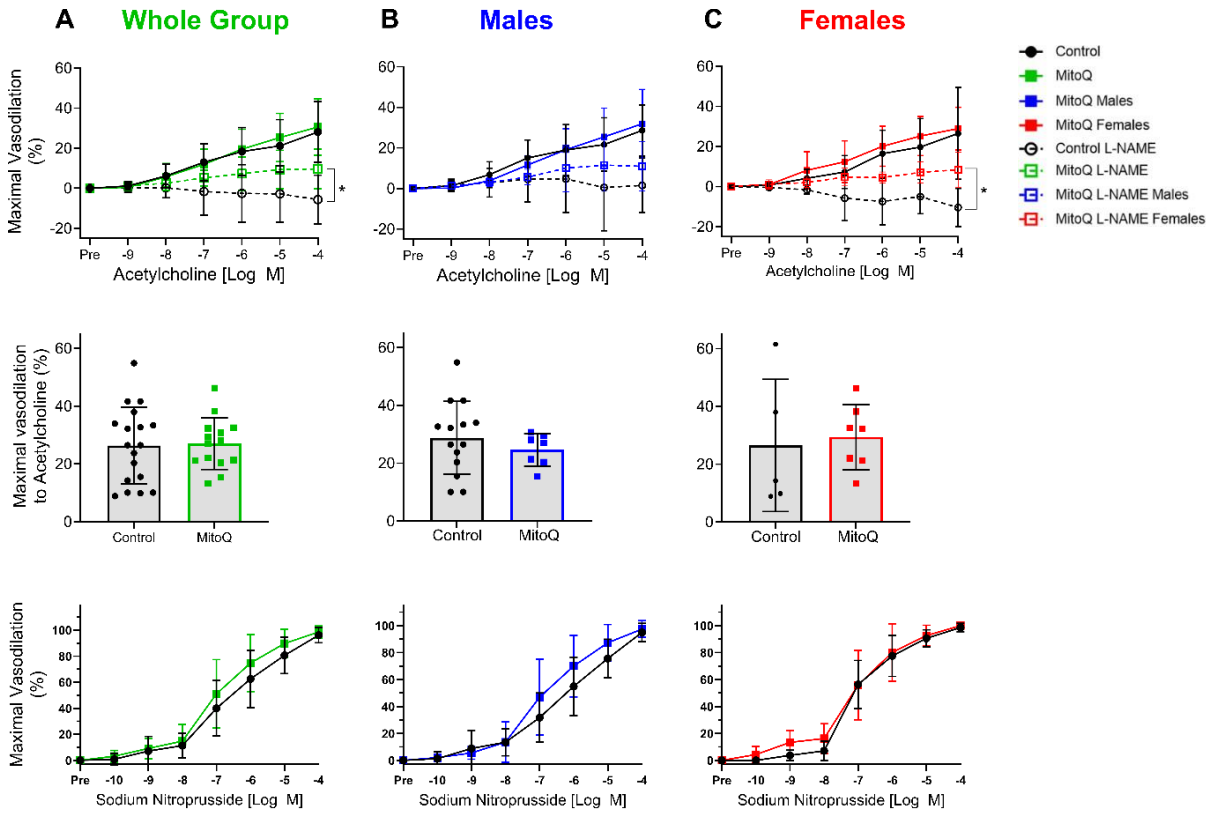

Figure 4.6 MitoQ treated mice are resistant to ACh-mediated vasoconstriction. Dose response curves for ACh with and without L-NAME (top), percent maximal dilation to ACh (middle), and dose response curves to SNP (bottom) in **A)** whole group, **B)** males, and **C)** females in control and MitoQ treated mice. Arteries were incubated with L-NAME [0.1mM] for 30 minutes. Data are mean±SD. Statistics include a RM-ANOVA, and Student's t-test for all groups.

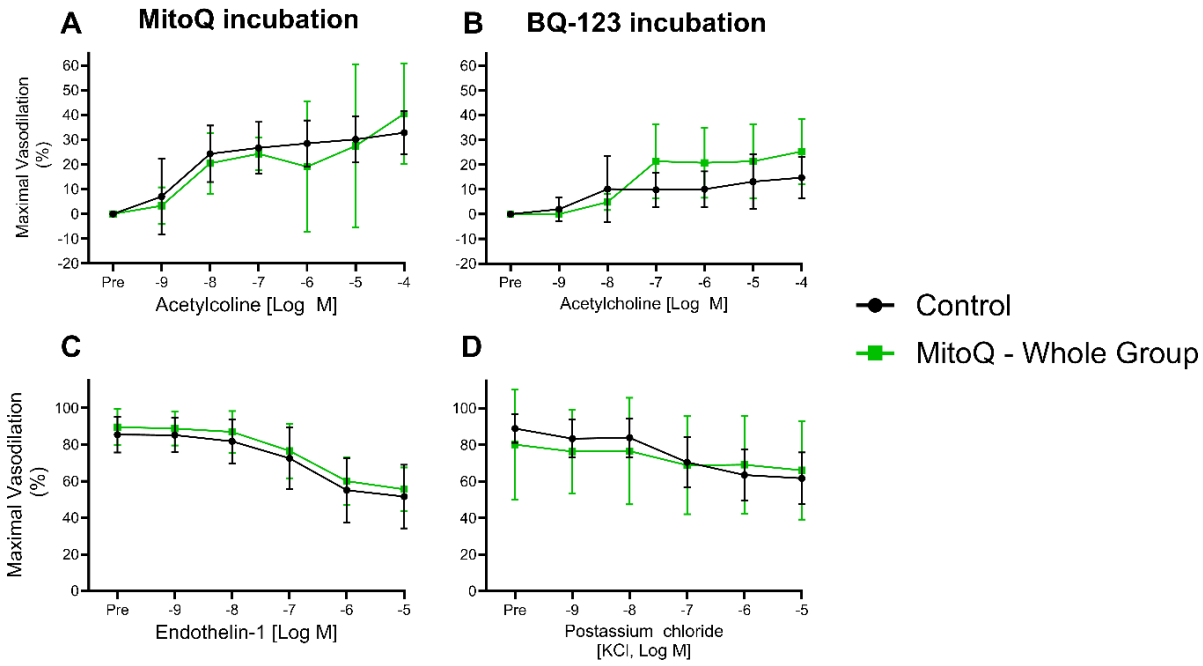

Figure 4.7 Effects of MitoQ and endothelin-1 on vasodilation, and vasoconstrictor responses are not different among control and MitoQ treated mice. Dose response curves for **A)** ACh with MitoQ incubation, **B)** ACh with BQ-123 incubation, **C)** Endothelin-1 (ET-1), and **D)** potassium chloride (KCl), in control and MitoQ treated mice. Arteries were incubated with MitoQ [0.5µM] for 60 minutes, and BQ-123 [10µM] for 30 minutes. Data are mean±SD. Statistics include a RM-ANOVA for whole group. N = 2 - 8 / group.

Cerebral Artery Stiffness

PCA β-stiffness was greater in mice treated with MitoQ compared to control mice in both the whole group (p=0.12) and in the females (p=0.013, Fig. 8A-C). The same trend existed in males but did not reach statistical significance. At both low and high pressures, EM was higher in MitoQ treated mice compared to control mice in the whole group (low: p=0.026, high: p=0.020, Fig. 9A). The same trends were observed for both male and female groups, but the only statistical significance was with greater EM at high pressures in MitoQ treated male mice compared to controls (p=0.022, Fig. 9B-C).

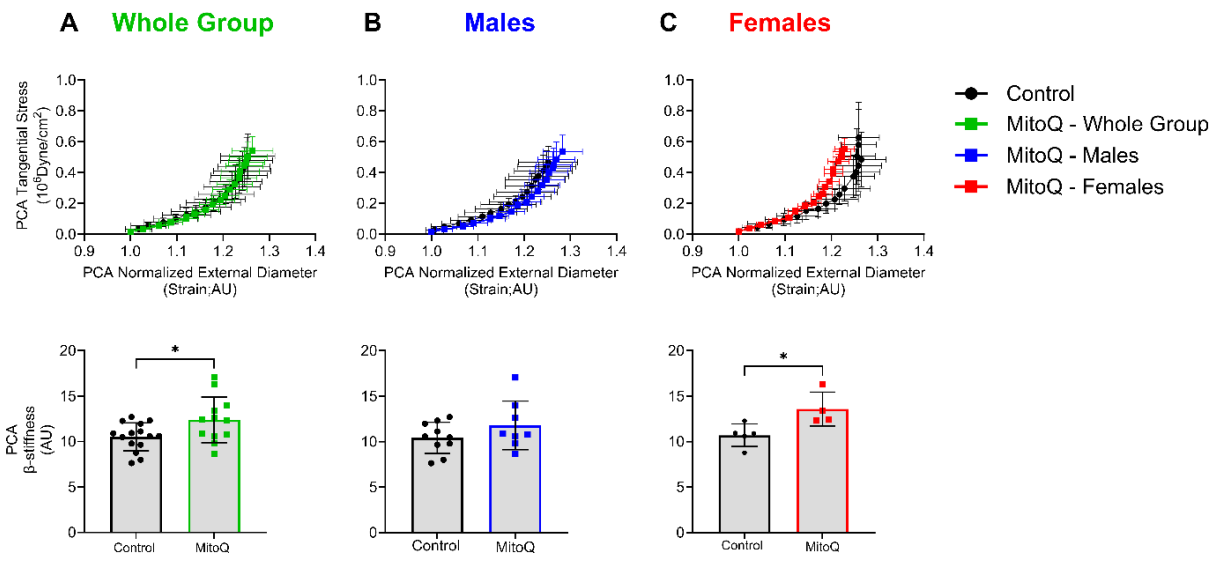

Figure 4.8 PCA β-stiffness is greater in MitoQ treated mice. Control and MitoQ treated PCA stress/strain curves (top), and β-stiffness (bottom) for **A)** Whole Group, **B)** Males, and **C)** Females. Data are mean±SD. Statistics include a Student's t-test for all groups. *p<0.05.

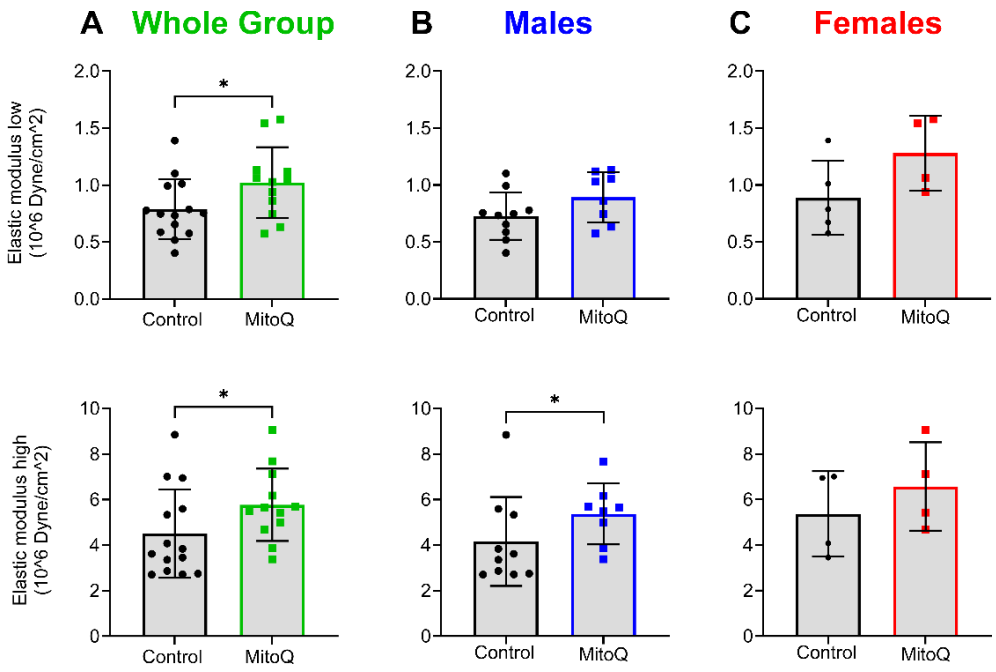

Figure 4.9 PCA elastic modulus was higher in MitoQ treated mice compared to control mice. Control and MitoQ treated PCA elastic modulus at low pressures (top), and elastic modulus at high pressures (bottom) for **A)** Whole Group, **B)** Males, and **C)** Females. Data are mean±SD. Statistics include a Student's t-test for all groups. *p<0.05.

Behavior Outcomes

For the whole group comparison, MitoQ mice spent more time on the rotarod during an accelerating protocol (p=0.01, Fig. 10A) When grouped by sex however, there were no treatment differences in rotarod time in neither males (p=0.216), nor females (p=0.271, Fig.10B-C). For nest building, pre-to-post intervention scores as well as Δ change from baseline were not significantly different in any group (p>0.05 for all, Fig. 11A-C).

There was no difference in the latency to platform among treatment groups over the course of the training period (Fig. 12A). During the probe trial, there were no main effects but an interaction

effect between treatment and quadrant type (p=0.001). MitoQ treated mice spent more time in the target quadrant searching for the platform compared to control mice (p=0.001, Fig. 12B). MitoQ treated mice also spent more time in the target quadrant compared to the average time spent in other quadrants (p=0.006). Additionally, Control mice spent significantly more time in other quadrants on average compared to target quadrant (p=0.026). There are no differences in the number of platform crosses or average speed in either group (Fig. 12C-D).

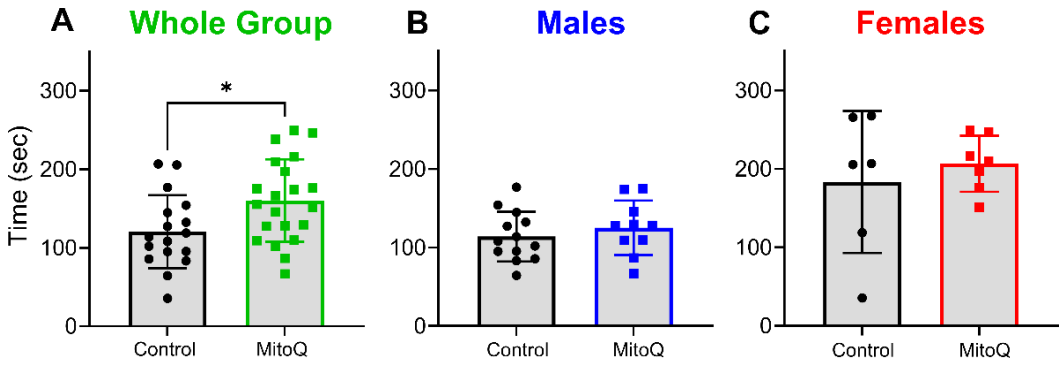

Figure 4.10 Rotarod time was greater in mice treated with MitoQ in the whole group. Average time spent on rotarod during an accelerating protocol in the **A)** Whole Group, **B)** Males, and **C)** Females. Data are mean±SD. Statistics include a Student's t-test for all groups. *p<0.05.

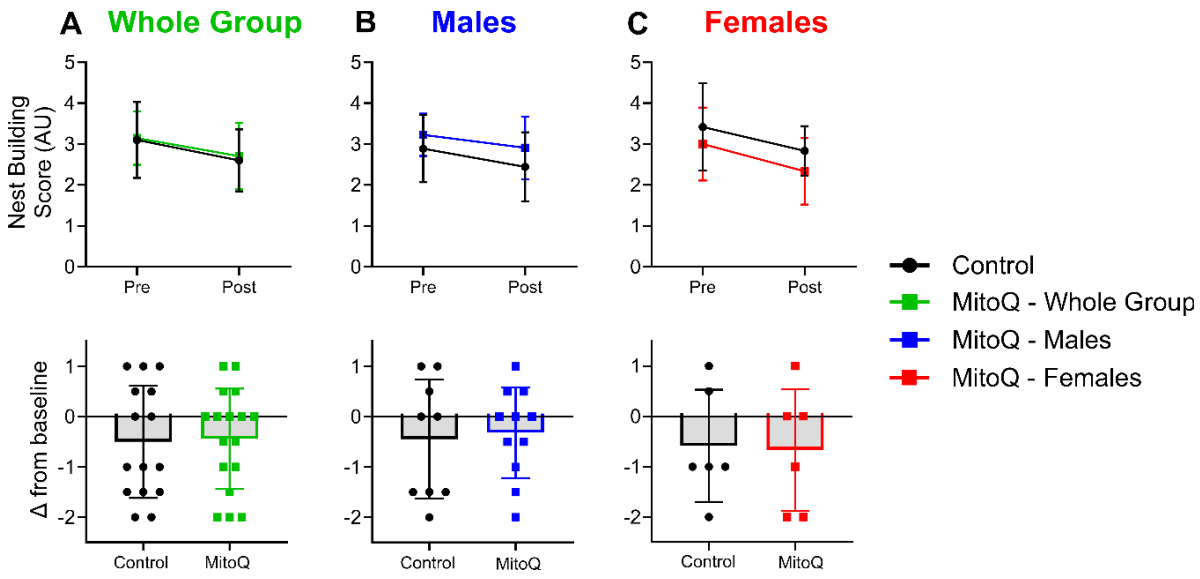

Figure 4.11 Nest building scores were not changed or different in control and MitoQ treated animals. Pre-to-post nest building assessment scores (top), and average change from baseline (bottom) in control and MitoQ treated mice. Average time spent on rotarod during an accelerating protocol in the **A)** Whole Group, **B)** Males, and **C)** Females. Data are mean±SD. Statistics include a Student's t-test for all groups.

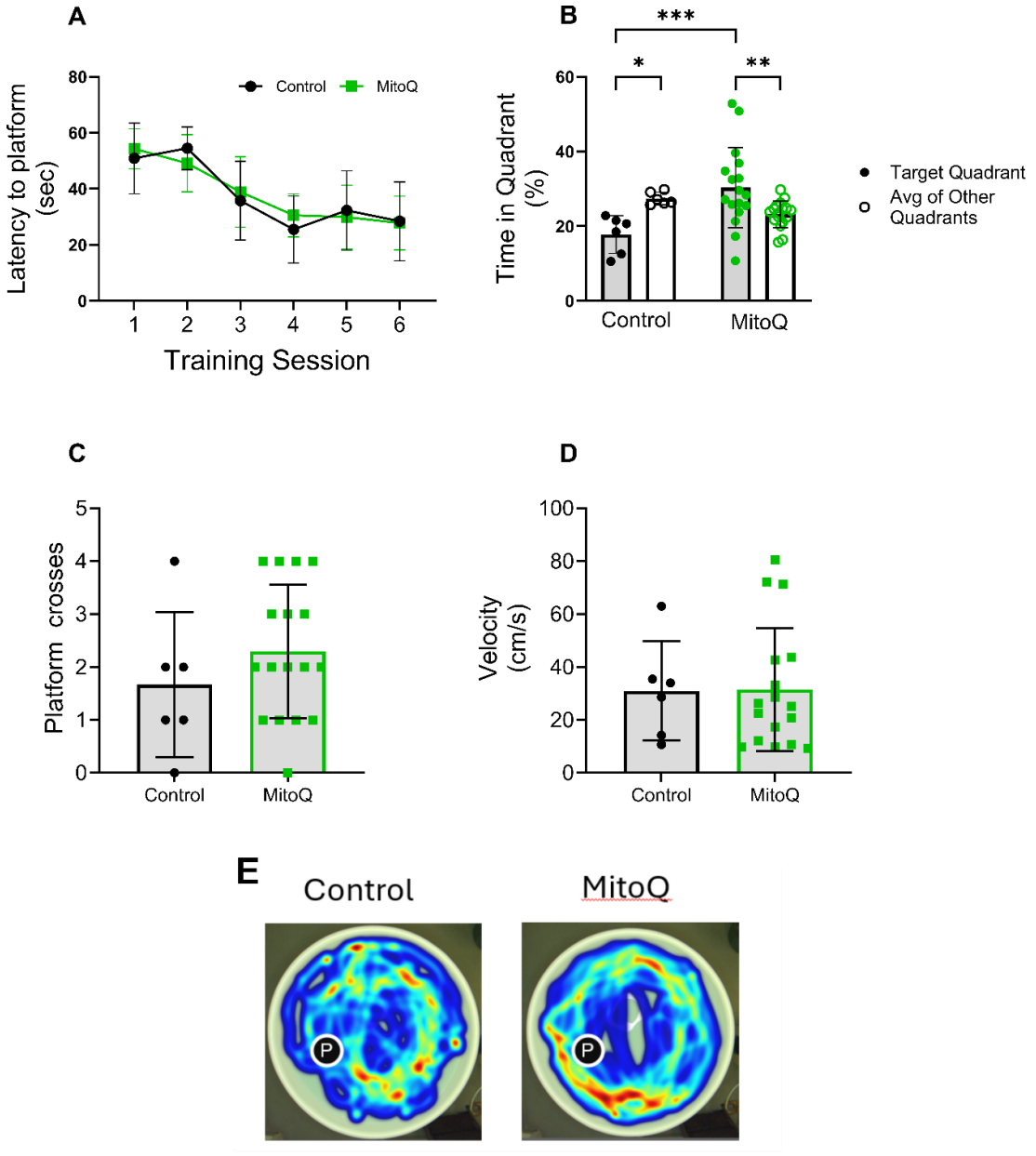

Figure 4.12 Spatial memory is preserved in MitoQ treated animals. Whole group data of Morris water maze outcomes including **A)** latency to platform during training sessions, **B)** Time spent in target quadrant during a probe trial **C)** Number of platform crosses during a probe trial, **D)** average speed during a beacon trial, and **E)** representative combined heat maps of swim path during a probe trial. Data are mean±SD. Statistics include a 2-way ANOVA and Student's t-test for all groups. *p<0.05, ***p<0.001, ****p<0.0001.

Neuroinflammation and pathology

To assess neuroinflammation and pathology, we measured activated astrocytes (GFAP) and Amyloid-β (4G8) in the entorhinal cortex, hippocampus, and thalamus regions of the brain in all mice. We found no differences in cell count, cell size, or cell percent area in GFAP staining in the entorhinal cortex (Fig. 13A-C). In the hippocampus, male MitoQ mice had significantly greater cell percent area than control mice ($p=0.034$, Fig. 14B). In the thalamus, there was an opposite trend, where male MitoQ mice trended towards lower levels of activated astrocytes, but this failed to reach significance ($p=0.058$, Fig. 15B). In the 4G8 staining, there was a strong trend towards higher Amyloid-β in the control mice vs 17-month mice ($p=0.058$, Fig. 16A). There were no other differences in Amyloid-β content in the brain among groups ($p>0.05$ for all, Fig.16B-C).

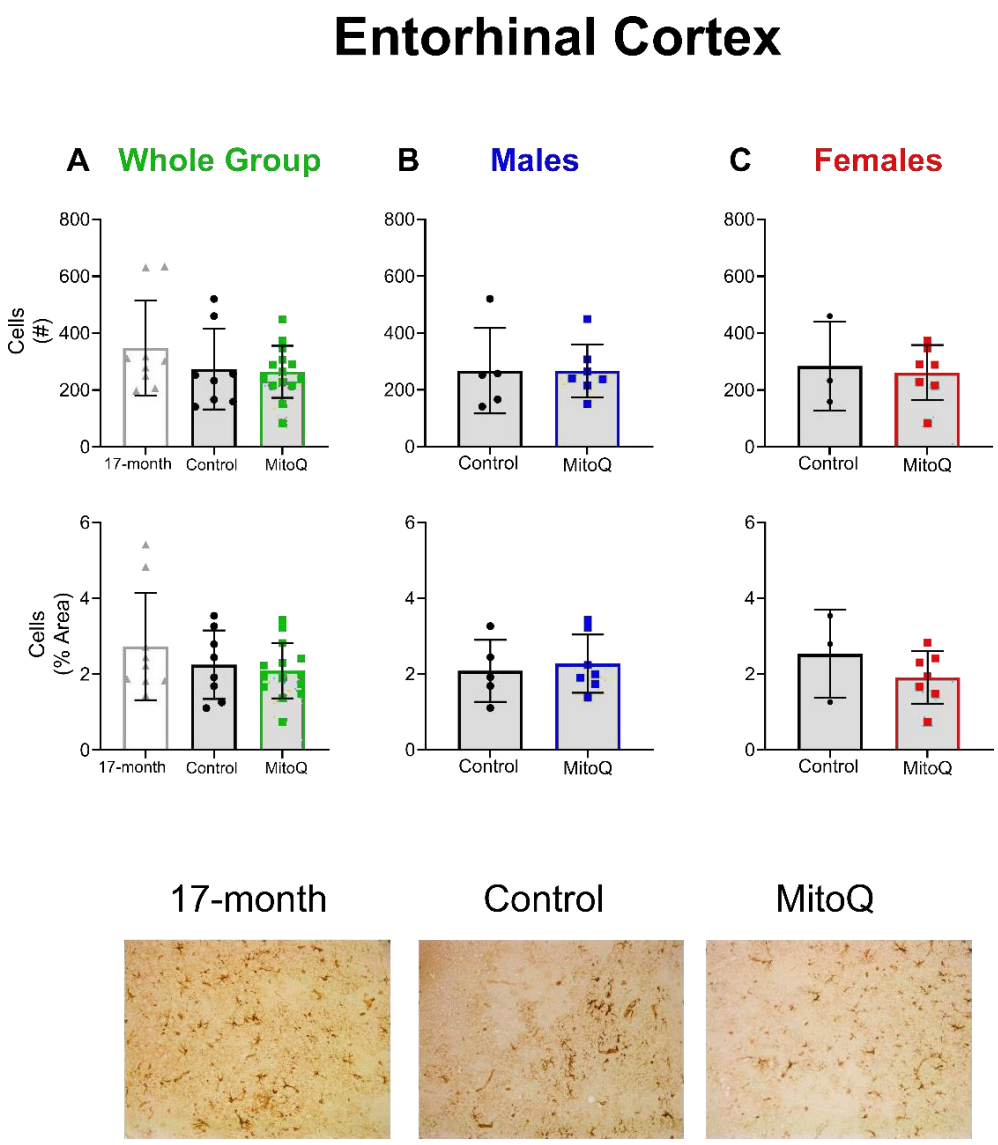

Figure 4.13 No differences in activated astrocyte levels in 17-month, control, and MitoQ treated mice in the entorhinal cortex. Glial fibrillary acidic protein (GFAP) staining in the entorhinal cortex displaying cell count (top), and cells in percent area (bottom), of 17-month, control and mitoQ treated mice. Data is displayed for **A)** Whole Group, **B)** Males, and **C)** Females. Data are mean±SD. Statistics include a Kruskal-Wallis and Mann-Whitney test.

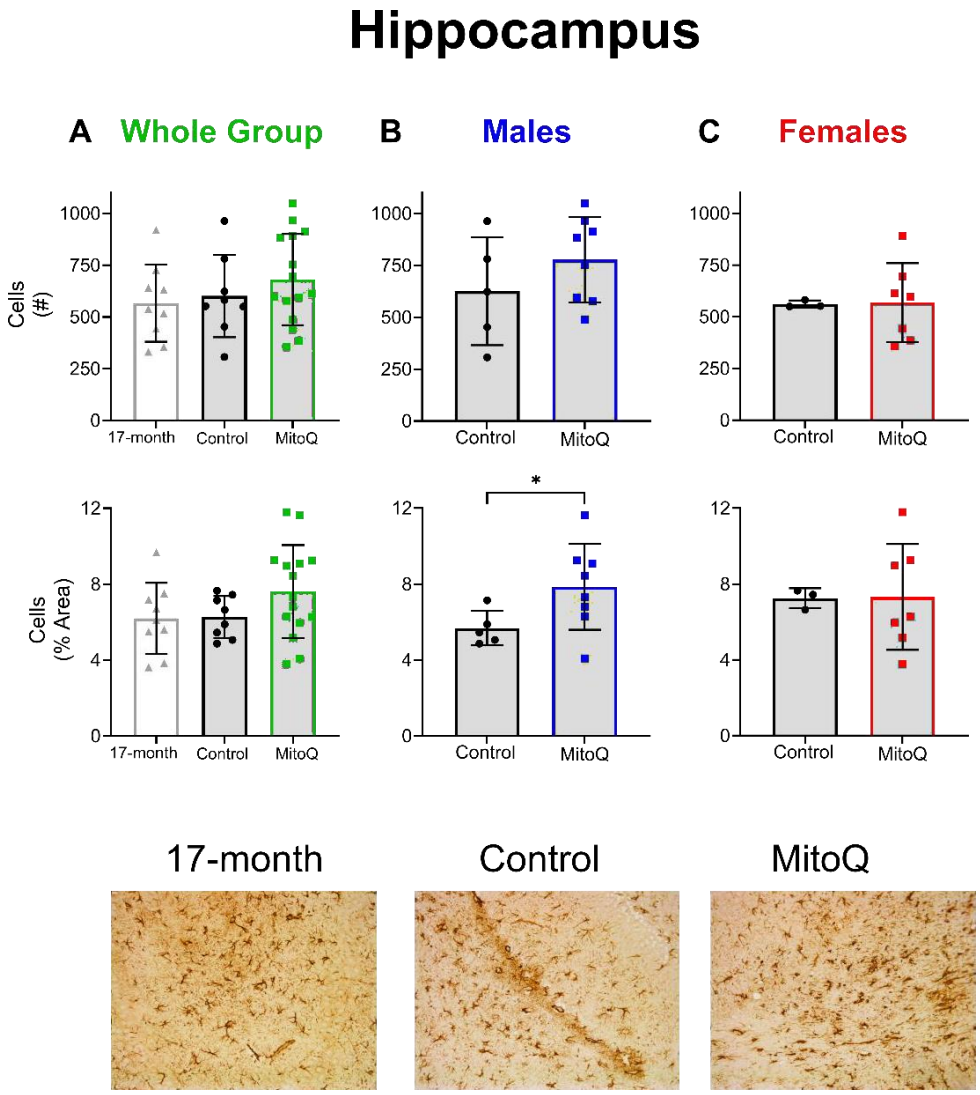

Figure 4.14 MitoQ treated male mice trend towards greater activated astrocytes than controls in the hippocampus. Glial fibrillary acidic protein (GFAP) staining in the hippocampus displaying cell count (top), cell size (middle), and cells in percent area (bottom), of 17-month, control and MitoQ treated mice. Data is displayed for **A)** Whole Group, **B)** Males, and **C)** Females. Data are mean±SD. Statistics include a one-way ANOVA and Student's t-test. *p<0.05.

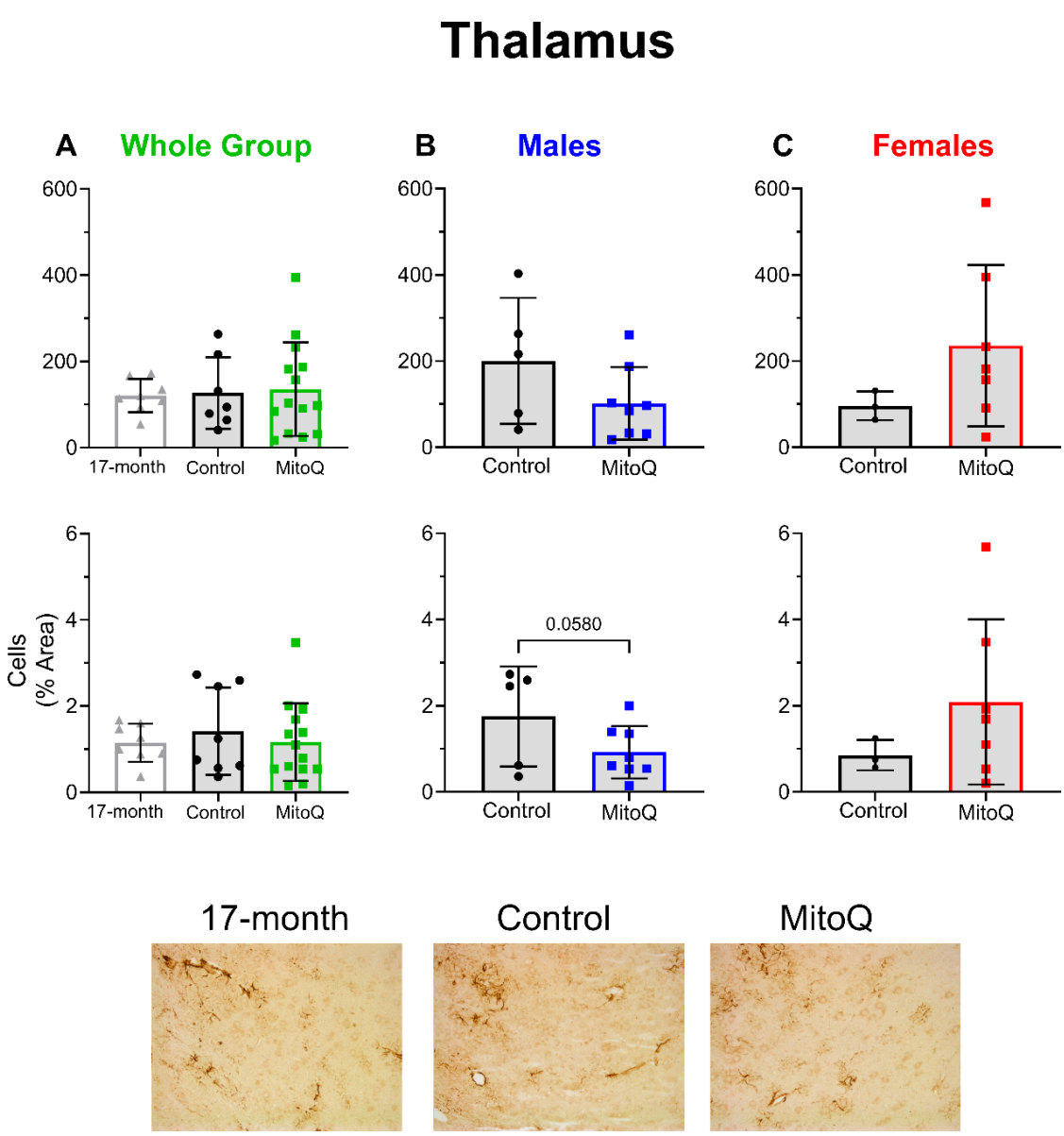

Figure 4.15 No differences in activated astrocyte levels in 17-month, control, and MitoQ treated mice in the thalamus. Glial fibrillary acidic protein (GFAP) staining in the thalamus displaying cell count (top), cell size (middle), and cells in percent area (bottom), of 17-month, control and MitoQ treated mice. Data is displayed for **A)** Whole Group, **B)** Males, and **C)** Females. Data are mean±SD. Statistics include a one-way ANOVA and Student's t-test.

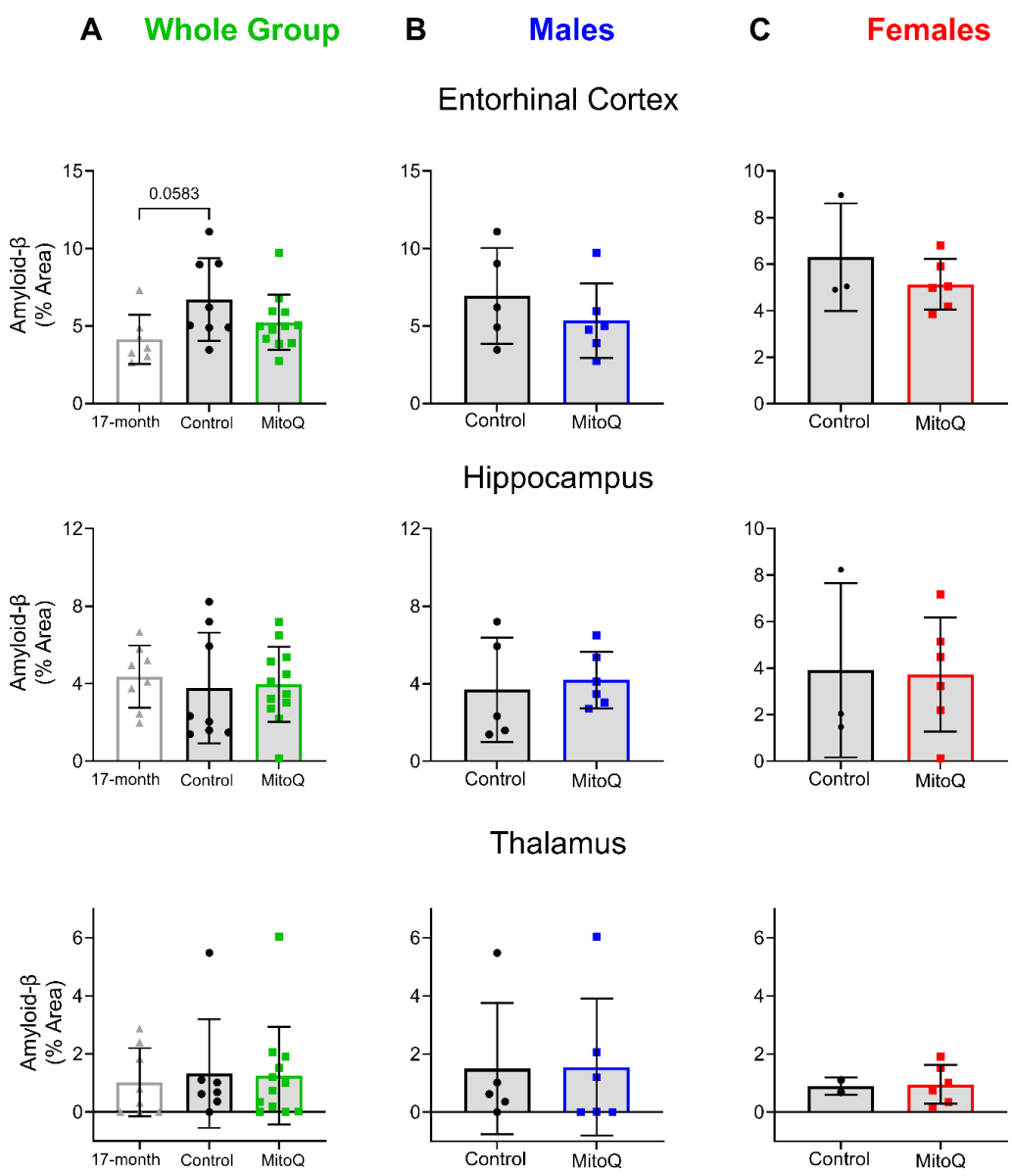

Figure 4.16 No differences in activated Amyloid-β levels in 17-month, control, and MitoQ treated mice in the brain. 4G8 staining for Amyloid-β in the entorhinal cortex (top), hippocampus (middle), and thalamus (bottom). Data is displayed for **A)** Whole Group, **B)** Males, and **C)** Females. Data are mean±SD. Statistics include a one-way ANOVA and Student's t-test.

4.4 **Discussion**

The purpose of this study was to investigate the potential therapeutic effects of MitoQ in mitigating large artery stiffness, cerebrovascular dysfunction, and AD-like pathology in older mice with heightened Aβ production. First, we found no significant difference in large artery stiffness outcomes between control mice and MitoQ treated mice. In the cerebral arteries, there were no group differences in maximal vasodilation, but MitoQ treated mice were resistant to constrictor properties of ACh compared to control mice. Cerebral artery stiffness was greater in MitoQ mice compared to control mice. Cognitive function showed modest improvements with MitoQ treatment. Lastly, AD-pathology was not different between MitoQ and control treatment. Overall, these findings suggest that in APP^{NL-F} mice, MitoQ treatment did not influence large arteries or neuroinflammation but showed modest beneficial effects in cerebral artery function and cognitive function.

Large Artery Stiffness

Mitochondrial oxidative stress is a contributor to age-related large artery stiffening. (43). In old C57Bl/6 mice, markers of mitochondrial redox signaling and repair, marked by increases in p66shc and superoxide production, and were associated with increased PWV in the aorta (143). Therefore, targeting mitochondrial health is a promising strategy to ameliorate adverse vascular aging and the downsteam effects (144). Additionally, previous research has demonstrated that MitoQ treatment reduces age-related arterial stiffness in old mice (64). In humans, treatment with MitoQ reduced large artery stiffness and oxidative stress levels in the plasma (65). We expected large artery stiffness to decrease in mice treated with MitoQ, aligning with previous findings. However, we found that MitoQ treatment did not affect active or passive measurements of large artery stiffness, which does not corroborate previous studies. This suggests that reducing

mitochondrial oxidative stress does not rescue age-related increases in large artery stiffness in the APP^{NL-F} mouse. A potential reason we did not observe this finding could be if baseline levels of large artery stiffness were already high. It is possible arterial function was already impaired and therefore unable to be rescued by mitigating mitochondrial oxidative stress.

Wall thickness

Increased wall thickness and remodeling is a maladaptation to age that impacts large artery stiffness (145). The impact of antioxidant treatment on large artery wall thickness has shown conflicting findings in the literature. Antioxidant effects from aerobic exercise did not modify wall thickness in older humans, but dietary intake of antioxidants was positively correlated with lower wall thickness (145, 146). A previous study using a MitoQ intervention in humans did not report differences in carotid intima media thickness (66). The literature on MitoQ effects on wall thickness extremely limited, making our findings novel. Additionally, media wall thickness in male MitoQ mice was less than control mice, while there was no difference in female mice. This suggests that mitochondrial antioxidant supplementation may preserve aortic structure in males more than females. This also suggests that smooth muscle cells in the media layer may be more impacted by the MitoQ treatment than the adventitial layer. Quantifying wall thickness is important for understanding the effects of mitochondrial function on large arteries because increases in wall thickness can indicate proliferation vascular smooth muscle cells or deposition of collagen, which influence the arterial diameter and pulse pressure dynamics. So far no published studies have quantified artery wall thickness with MitoQ treatment. However, many human studies conclude that greater antioxidant intake is related to lower artery wall thickness ((146, 147)

We found that wall thickness was greater in aortas 21-month old mice compared to the 17-month mice, in both the media and media + adventitia. These results suggest that aging in the APP^{NL-F} mice increased aortic wall thickness. Since these mice did not show increases in Amyloid-β, this effect is likely due to the effects of aging in this study. No other studie has reported vascular outcomes like we do in this APP^{NL-F} model, thus there is no precedent for the expected phenotype in these animals when related to vascular function. While no previous studies have shown wall thickness with MitoQ outcomes, there are a few studies that point towards generalized antioxidants being beneficial for maintaining proper wall thickness with age (146, 147).

Cerebral Artery Function

Cerebral arteries regulate blood flow to the working tissues of the brain, and when impaired, can cause reduced cerebral blood flow in AD patients (148). Cerebral blood flow is reduced due to impairments in EDD with aging and AD (149). Increased oxidative stress and reduce NO-bioavailability contribute to endothelial damage and decreased dilatory function. Previous studies have demonstrated that antioxidant treatment, notably MitoQ supplement, improves endothelial function in both animals and humans (64–66, 150). In this study, there was no impact of MitoQ treatment on maximal dilation response to the ACh on APP^{NL-F} mice. However, we observed that MitoQ mice resisted ACh mediated constriction when NO synthases are inhibited compared to control mice. The notable difference is that the cerebral arteries constricted to ACh in the presence of L-NAME for the control mice, but not in the MitoQ mice. When analyzed by sex, this finding held true only in female mice. This suggests that mitochondrial antioxidant treatment may alter non-NO-dependent mechanisms that regulate vascular tone. It is possible

that other dilatory pathways, such as prostacyclins, may be compromised with age in this AD mouse model, and potentially rescued by MitoQ treatment. Future studies should examine vasodilation responses to non NO-mediated dilators with MitoQ treatment.

Neuroinflammation

Neuroinflammation is implicated in AD and neurodegeneration. In the presence of ROS and cytokines, astrocytes become reactive and further perpetuate a neuroinflammatory response (151). Astrocytes are a part of the blood brain barrier. While inactivated astrocytes are protective, activated astrocytes stimulate inflammation and damage surrounding neural and cerebrovascular tissue. In the hippocampus, male mice treated with MitoQ mice had a greater percentage of area covered by activated astrocytes than control mice. In the thalamus, however, there were strong trends for less activated astrocytes in MitoQ treated mice compared to control mice. We did not observe this trend in females, suggesting there may be sex differences in the effect of mitochondrial antioxidants on neuroinflammation in these mice. The entorhinal cortex and hippocampus regions are the first to be impacted in AD and other dementias, spreading to the thalamus in later stages of disease. Before MtioQ treatment began, Amyloid-β deposition and astrocyte activation may have begun in the hippocampus and entorhinal cortex but not in the thalamus region. This could be one potential explanation as to why we saw beneficial trends in the thalamus and none in the other regions. Another study using the 3xTg-AD mouse model found that long-term MitoQ treatment reduced GFAP levels in the brain (138, 139). These studies were performed in young mice, while our model uses old mice. Thus, the confounding effects of age may explain why we saw little to no changes in neuroinflammation markers with MitoQ treatment.

4.5 Limitations

One limitation to the study is that mice received MitoQ in their communal drinking water. Because of this, the amount of MitoQ received by each mouse in the treatment group may have varied. We chose an intervention start time based on the natural AD progression in this model. However, it is possible that starting the intervention earlier may be beneficial and irreversible pathology may have already occurred by the start of the intervention. Beginning the internvention at 17-month mark might have been too late, and and intervention soon may yield different results. Lastly, we did not include a wildtype mouse group, and thus, we cannot compare these results to non-AD mice.

4.6 Conclusion

The main findings from this study are that treatment with a mitochondrial antioxidant in an AD mouse model showed therapeutic potential for mitigating memory impairments and motor coordination. MitoQ treated mice also showed modest beneficial effects on vascular function and wall thickness. The results of this study suggest that mitochondria and oxidative stress are promising therapeutic targets for mitigating disease. Furthermore, mitochondrial specific antioxidants continue to show beneficial effects on vascular and cognitive function. Future research should explore the effects of MitoQ treatment on other mouse models related to Alzheimer's disease and aging.

V. DISCUSSION

Chapter I provides background of the current literature and provides proper rationale for the aims and studies conducted in this dissertation. A brief summary of findings from Aims 1, 2, and 3 are discussed below.

5.1 Summary and Conclusions of Chapter I

This literature review covers concepts of aging, neurodegeneration, mechanisms for both large artery and cerebral artery dysfunction, and therapeutic targets of interest to combat these pathologies. The primary conclusion from this chapter is that aging leads to increases in large artery stiffness and cerebrovascular dysfunction which play a causal role in neurodegenerative diseases like AD. Preventing large artery stiffness and targeting mitochondrial have emerged as promising therapeutic targets to combat age-related diseases.

5.2 Summary and Conclusions of Chapter II

Chapter II explores the effects of both short-term and long-term elastin haploinsufficiency on large artery function, cerebrovascular function, and cognitive function. Overall, the results of this study suggest that long-term exposure to elastin haploinsufficiency causes aortic wall remodeling, impairs spatial memory, and may contribute to higher levels of neuroinflammation. Also, there are differences in how this long-term exposure to elastin haploinsufficiency affects males and females, where females tend to be more susceptible to these effects compared to males. In summary, long-term exposure to elastin haploinsufficiency can cause detrimental effects on cerebrovascular function and cognitive function.

5.3 Summary and Conclusions of Chapter III

Chapter III investigates the effects of the collagen crosslink breaker, ALT-711, on preventing age-related large artery stiffness, cerebrovascular dysfunction, and cognitive impairment. Overall, we found that long-term treatment with ALT-711 in old mice did not reduce large artery stiffness, preserve endothelial function, or lower collagen crosslinking. Among old mice, we found that cerebral artery stiffness is related to endothelial function and cognitive function.

5.4 Summary and Conclusions of Chapter IV

Chapter IV pivots to investigate the effects of MitoQ, a mitochondrial targeted antioxidant, on large artery stiffness, cerebrovascular function, and neurodegenerative diseases. The main findings from this study are that treatment with a mitochondrial antioxidant in an AD mouse model showed therapeutic potential for mitigating memory impairments and motor coordination. MitoQ treated mice also showed modest beneficial effects on vascular function and wall thickness. The results of this study suggest that mitochondria and oxidative stress are promising therapeutic targets for mitigating disease. Furthermore, mitochondrial specific antioxidants continue to show beneficial effects on vascular and cognitive function. Future research should explore the effects of MitoQ treatment on other mouse models related to Alzheimer's disease and aging.

5.5 Future Directions

One future direction for this aim is investigate more direct relationships between elastin haploinsufficiency and cognitive function. The mechanisms by which elastin haploinsufficiency leads to worse cognitive function and decreased antioxidant gene expression in the brain is still unknown. To address this, future researchers could focus on making a mouse model with inducible haploinsufficiency. This would present a more translatable approach to understanding elastin's role in the context of human disease. Since elastin haploinsufficiency from birth is rare and may develop adaptations to combat this deficiency, and inducible haploinsufficiency knockout would help determine whether elastin's role is crucial to proper cognitive function. Future studies should focus more preventing elastin degradation and fragmentation. Since elastin production ceases early in life, treatment to increase elastin production had proven ineffective (152). However elastin degradation contributes to vascular complications such as aortic aneurysm (153).

Another important future direction for aim #1 is to investigate how this cohort of elastin haploinsufficient mice was resistant to the typical phenotypes of large artery stiffness and cerebral artery endothelial dysfunction previously reported from this transgenic model. Other properties of the extracellular matrix, like collagen, proteoglycans, etc., function with elastin to regulate stiffness of the tissue (154, 155). For example, fibulin-4 and fibulin-5 are proteins that are essential for assembling and anchoring elastin to other extracellular matrix structures. A future direction with this project could be to quantify these proteins to determine if any differences in their expression have occurred in elastin haploinsufficiency animals. It is also helpful to quantify these proteins to determine if any upregulation of these proteins occurred to account for genotypic deficiency in elastin. Understanding how these mice maintained adequate elastin and large artery structure will give insight into how these mice may have resisted the expected pathological phenotype. These mechanisms will give insight to the scientific community on how vascular pathology may be subverted or mitigated.

A future direction highlighted from Aim #2 could be investigating compounds that target cerebral artery stiffness. This study highlighted the difficulties in targeting large arteries as a therapeutic strategy. Since cerebral artery stiffness is so strongly correlated with cognitive function in my results, targeting this stiffness may have beneficial effects on cerebrovascular and cognitive function. Future studies should explore therapies that focus on mitigating cerebral artery stiffness. One well-known therapy to try would be aerobic exercise since there is evidence demonstrating beneficial effects of exercise on cerebrovascular function (156–158). Additionally, pharmacological interventions to absolve hypertension have beneficial effects on arterial stiffness in patients with increased blood pressure (159). While there have been no direct

studies of the effects of these interventions on cerebral artery stiffness, I hypothesize these therapeutics could also mitigate increases in cerebral artery stiffness with age. Additionally, in the future, it is worth investigating whether ALT-711 breaks cross-links in vivo using the high-performance liquid chromatography (HPLC) technique. Since this technique is regarded as the gold standard, this measurement may yield more accurate results than the hydroxyproline assay method used in Aim #2. Additionally, this technique would allow researchers to determine if other non-AGEs induced cross-links are affected by ALT-711. So far, no research has investigated if ALT-711 can break non-AGEs crosslinks. The thiazolium structure of ALT-711 breaks α-diketones (57). Thus, I hypothesize that non-AGEs mediated crosslinks that contain α-diketones are also susceptible to being broken by ALT-711. More research is still needed to characterize non-AGEs mediated crosslinks with crosslink-breaker treatment. Ultimately, the long-term future direction from this aim would be to develop new compounds that more effectively break AGEs-mediated collagen crosslinking in vivo.

Furthermore, from Aim #3, mitochondrial-specific antioxidants continue to show beneficial effects on vascular and cognitive function. Future research should explore the effects of MitoQ treatment on other mouse models related to Alzheimer's disease and aging. The actions of MitoQ are not exclusive to the vasculature. Most cells contain mitochondria, thus MitoQ treatment may be beneficial in mitigating other pathologies. AD is characterized by high levels of neuroinflammation, but we did not fully investigate the extent of neuroinflammation in this study. Therefore, an immediate future direction for this study is to expand upon this outcome. Comparing protein expression and gene expression of pro-inflammatory and anti-oxidant related proteins in the cerebral arteries and cortex will contribute to a better understanding of role

mitochondrial derived ROS play in neuroinflammation. This study also highlights the importance of mitochondrial function. While we did not measure mitochondrial function directly in this study, previous studies have demonstrated reduced mitochondrial ROS content in the vasculature with MitoQ treatment.Few studies have addressed off-target effects of MitoQ on mitochondria, but it appears MitoQ treatment does not negatively impact mitochondrial oxidative phosphorylation (160, 161). Thus, future studies should consider investigating compounds that aim to preserve mitochondrial health and proper function, including MitoQ. Immediate future directions for this aim should be to quantify mitochondrial oxidative stress in both the cerebral arteries and brain. These studies would provide further proof of concept that MitoQ treatment acts to reduce oxidative stress in vivo and further suggest that oxidative stress plays a critical role in dysfunction. While NO-mediated dilation was not affected in the cerebral arteries in this study, it is possible non-NO-mediated dilatory pathways were preserved in cerebral arteries with MitoQ treatment. Future studies should investigate the role that prostaglandins and endothelium-derived hyperpolarizing factors play in cerebral artery EDD in this mouse model. I hypothesize that APP^{NL-F} mice treated with MitoQ have higher sensitivity to non-NO mediated dilatory pathways. Ultimately, this basic research hopes to influence future translational and clinical research on strategies or treatments to combat vascular dysfunction and neurodegenerative diseases. combat vascular dysfunction and neurodegenerative diseases.

5.6 This Dissertation in a Paragraph

This body of work highlights that 1) Age-related large artery and cerebral artery dysfunction contribute to neurodegenerative disease, and 2) cerebral artery function and mitochondrial function are promising therapeutic targets for mitigating age-related pathologies. Finally, the

overall importance of this dissertation is that it contributes to the wealth of knowledge on aging and disease that will ultimately influence future treatments or therapies to improve the quality of life.

VI. REFERENCES

1. **Cai Y**, **Song W**, **Li J**, **Jing Y**, **Liang C**, **Zhang L**, **Zhang X**, **Zhang W**, **Liu B**, **An Y**, **Li J**, **Tang B**, **Pei S**, **Wu X**, **Liu Y**, **Zhuang C-L**, **Ying Y**, **Dou X**, **Chen Y**, **Xiao F-H**, **Li D**, **Yang R**, **Zhao Y**, **Wang Y**, **Wang L**, **Li Y**, **Ma S**, **Wang S**, **Song X**, **Ren J**, **Zhang L**, **Wang J**, **Zhang W**, **Xie Z**, **Qu J**, **Wang J**, **Xiao Y**, **Tian Y**, **Wang G**, **Hu P**, **Ye J**, **Sun Y**, **Mao Z**, **Kong Q-P**, **Liu Q**, **Zou W**, **Tian X-L**, **Xiao Z-X**, **Liu Y**, **Liu J-P**, **Song M**, **Han J-DJ**, **Liu G-H**. The landscape of aging. *Sci China Life Sci* 65: 2354–2454, 2022. doi: 10.1007/s11427-022-2161-3.

2. **Aunan JR**, **Watson MM**, **Hagland HR**, **Søreide K**. Molecular and biological hallmarks of ageing. *Br J Surg* 103: e29-46, 2016. doi: 10.1002/bjs.10053.

3. **Li Y**, **Berliocchi L**, **Li Z**, **Rasmussen LJ**. Interactions between mitochondrial dysfunction and other hallmarks of aging: Paving a path toward interventions that promote healthy old age. *Aging Cell* 23: e13942, 2024. doi: 10.1111/acel.13942.

4. **Jin K**. Modern Biological Theories of Aging. *Aging Dis* 1: 72–74, 2010.

5. **Liguori I**, **Russo G**, **Curcio F**, **Bulli G**, **Aran L**, **Della-Morte D**, **Gargiulo G**, **Testa G**, **Cacciatore F**, **Bonaduce D**, **Abete P**. Oxidative stress, aging, and diseases. *Clin Interv Aging* 13: 757–772, 2018. doi: 10.2147/CIA.S158513.

6. **Furman D**, **Campisi J**, **Verdin E**, **Carrera-Bastos P**, **Targ S**, **Franceschi C**, **Ferrucci L**, **Gilroy DW**, **Fasano A**, **Miller GW**, **Miller AH**, **Mantovani A**, **Weyand CM**, **Barzilai N**, **Goronzy JJ**, **Rando TA**, **Effros RB**, **Lucia A**, **Kleinstreuer N**, **Slavich GM**. Chronic inflammation in the etiology of disease across the life span. *Nat Med* 25: 1822–1832, 2019. doi: 10.1038/s41591-019-0675-0.

7. **Moldogazieva NT**, **Mokhosoev IM**, **Mel'nikova TI**, **Porozov YB**, **Terentiev AA**. Oxidative Stress and Advanced Lipoxidation and Glycation End Products (ALEs and AGEs) in Aging and Age-Related Diseases. *Oxid Med Cell Longev* 2019: 3085756, 2019. doi: 10.1155/2019/3085756.

8. **De Winter G**. Aging as disease. *Med Health Care Philos* 18: 237–243, 2015. doi: 10.1007/s11019-014-9600-y.

9. **Donato AJ**, **Machin DR**, **Lesniewski LA**. Mechanisms of Dysfunction in the Aging Vasculature and Role in Age-Related Disease. *Circ Res* 123: 825–848, 2018. doi: 10.1161/CIRCRESAHA.118.312563.

10. **Quinn U**, **Tomlinson LA**, **Cockcroft JR**. Arterial stiffness. *JRSM Cardiovasc Dis* 1: cvd.2012.012024, 2012. doi: 10.1258/cvd.2012.012024.

11. **Wagenseil JE**, **Mecham RP**. Elastin in large artery stiffness and hypertension. *Journal of Cardiovascular Translational Research* 5: 264, 2012. doi: 10.1007/s12265-012-9349-8.

12. **Bonnans C**, **Chou J**, **Werb Z**. Remodelling the extracellular matrix in development and disease. *Nat Rev Mol Cell Biol* 15: 786–801, 2014. doi: 10.1038/nrm3904.

13. **Izzo JL**, **Shykoff BE**. Arterial stiffness: clinical relevance, measurement, and treatment. *Rev Cardiovasc Med* 2: 29–34, 37–40, 2001.

14. **Chirinos JA**, **Segers P**, **Hughes T**, **Townsend R**. Large-Artery Stiffness in Health and Disease: JACC State-of-the-Art Review. *J Am Coll Cardiol* 74: 1237–1263, 2019. doi: 10.1016/j.jacc.2019.07.012.

15. **Harraz OF**, **Jensen LJ**. Vascular calcium signalling and ageing. *J Physiol* 599: 5361–5377, 2021. doi: 10.1113/JP280950.

16. **Stauffer BL**, **Westby CM**, **DeSouza CA**. Endothelin-1, aging and hypertension. *Curr Opin Cardiol* 23: 350–355, 2008. doi: 10.1097/HCO.0b013e328302f3c6.

17. **Van Guilder GP**, **Westby CM**, **Greiner JJ**, **Stauffer BL**, **DeSouza CA**. Endothelin-1 vasoconstrictor tone increases with age in healthy men but can be reduced by regular aerobic exercise. *Hypertension* 50: 403–409, 2007. doi: 10.1161/HYPERTENSIONAHA.107.088294.

18. **Yasmin null**, **McEniery CM**, **Wallace S**, **Dakham Z**, **Pulsalkar P**, **Maki-Petaja K**, **Ashby MJ**, **Cockcroft JR**, **Wilkinson IB**. Matrix metalloproteinase-9 (MMP-9), MMP-2, and serum elastase activity are associated with systolic hypertension and arterial stiffness. *Arterioscler Thromb Vasc Biol* 25: 372, 2005. doi: 10.1161/01.ATV.0000151373.33830.41.

19. **Singh R**, **Barden A**, **Mori T**, **Beilin L**. Advanced glycation end-products: a review. *Diabetologia* 44: 129–146, 2001. doi: 10.1007/s001250051591.

20. **Perrone A**, **Giovino A**, **Benny J**, **Martinelli F**. Advanced Glycation End Products (AGEs): Biochemistry, Signaling, Analytical Methods, and Epigenetic Effects. *Oxid Med Cell Longev* 2020: 3818196, 2020. doi: 10.1155/2020/3818196.

21. **Sajithlal GB**, **Chithra P**, **Chandrakasan G**. Advanced glycation end products induce crosslinking of collagen in vitro. *Biochim Biophys Acta* 1407: 215–224, 1998. doi: 10.1016/s0925-4439(98)00043-x.

22. **Lee H-Y**, **Oh B-H**. Aging and arterial stiffness. *Circ J* 74: 2257–2262, 2010. doi: 10.1253/circj.cj-10-0910.

23. **Ungvari Z**, **Tarantini S**, **Donato AJ**, **Galvan V**, **Csiszar A**. Mechanisms of Vascular Aging. *Circ Res* 123: 849–867, 2018. doi: 10.1161/CIRCRESAHA.118.311378.

24. **Hsu H-J**, **Lee C-F**, **Locke A**, **Vanderzyl SQ**, **Kaunas R**. Stretch-induced stress fiber remodeling and the activations of JNK and ERK depend on mechanical strain rate, but not FAK. *PLoS One* 5: e12470, 2010. doi: 10.1371/journal.pone.0012470.

25. **Jacob MP**. Extracellular matrix remodeling and matrix metalloproteinases in the vascular wall during aging and in pathological conditions. *Biomed Pharmacother* 57: 195–202, 2003. doi: 10.1016/s0753-3322(03)00065-9.

26. **Zhou X**, **Bohlen HG**, **Unthank JL**, **Miller SJ**. Abnormal nitric oxide production in aged rat mesenteric arteries is mediated by NAD(P)H oxidase-derived peroxide. *Am J Physiol Heart Circ Physiol* 297: H2227-2233, 2009. doi: 10.1152/ajpheart.00325.2009.

27. **Abbott NJ**, **Patabendige AAK**, **Dolman DEM**, **Yusof SR**, **Begley DJ**. Structure and function of the blood–brain barrier. *Neurobiology of Disease* 37: 13–25, 2010. doi: 10.1016/j.nbd.2009.07.030.

28. **Baierle M**, **Nascimento SN**, **Moro AM**, **Brucker N**, **Freitas F**, **Gauer B**, **Durgante J**, **Bordignon S**, **Zibetti M**, **Trentini CM**, **Duarte MMMF**, **Grune T**, **Breusing N**, **Garcia SC**. Relationship between inflammation and oxidative stress and cognitive decline in the institutionalized elderly. *Oxid Med Cell Longev* 2015: 804198, 2015. doi: 10.1155/2015/804198.

29. **Thorin-Trescases N**, **de Montgolfier O**, **Pinçon A**, **Raignault A**, **Caland L**, **Labbé P**, **Thorin E**. Impact of pulse pressure on cerebrovascular events leading to age-related cognitive decline. *Am J Physiol Heart Circ Physiol* 314: H1214–H1224, 2018. doi: 10.1152/ajpheart.00637.2017.

30. **Krüger-Genge A**, **Blocki A**, **Franke R-P**, **Jung F**. Vascular Endothelial Cell Biology: An Update. *Int J Mol Sci* 20: E4411, 2019. doi: 10.3390/ijms20184411.

31. **Michiels C**. Endothelial cell functions. *J Cell Physiol* 196: 430–443, 2003. doi: 10.1002/jcp.10333.

32. **Yanagisawa M**, **Kurihara H**, **Kimura S**, **Tomobe Y**, **Kobayashi M**, **Mitsui Y**, **Yazaki Y**, **Goto K**, **Masaki T**. A novel potent vasoconstrictor peptide produced by vascular endothelial cells. *Nature* 332: 411–415, 1988. doi: 10.1038/332411a0.

33. **Raignault A**, **Bolduc V**, **Lesage F**, **Thorin E**. Pulse pressure-dependent cerebrovascular eNOS regulation in mice. *J Cereb Blood Flow Metab* 37: 413–424, 2017. doi: 10.1177/0271678X16629155.

34. **Cyr AR**, **Huckaby LV**, **Shiva SS**, **Zuckerbraun BS**. Nitric Oxide and Endothelial Dysfunction. *Crit Care Clin* 36: 307–321, 2020. doi: 10.1016/j.ccc.2019.12.009.

35. **Sun D**, **Huang A**, **Yan EH**, **Wu Z**, **Yan C**, **Kaminski PM**, **Oury TD**, **Wolin MS**, **Kaley G**. Reduced release of nitric oxide to shear stress in mesenteric arteries of aged rats. *Am J Physiol Heart Circ Physiol* 286: H2249-2256, 2004. doi: 10.1152/ajpheart.00854.2003.

36. **Bourque SL**, **Davidge ST**, **Adams MA**. The interaction between endothelin-1 and nitric oxide in the vasculature: new perspectives. *Am J Physiol Regul Integr Comp Physiol* 300: R1288-1295, 2011. doi: 10.1152/ajpregu.00397.2010.

37. **Trott DW**, **Seawright JW**, **Luttrell MJ**, **Woodman CR**. NAD(P)H oxidase-derived reactive oxygen species contribute to age-related impairments of endothelium-dependent dilation in rat soleus feed arteries. *J Appl Physiol (1985)* 110: 1171–1180, 2011. doi: 10.1152/japplphysiol.01037.2010.

38. **Dikalov SI**, **Nazarewicz RR**, **Bikineyeva A**, **Hilenski L**, **Lassègue B**, **Griendling KK**, **Harrison DG**, **Dikalova AE**. Nox2-induced production of mitochondrial superoxide in angiotensin II-mediated endothelial oxidative stress and hypertension. *Antioxid Redox Signal* 20: 281–294, 2014. doi: 10.1089/ars.2012.4918.

39. **Förstermann U**. Oxidative stress in vascular disease: causes, defense mechanisms and potential therapies. *Nat Clin Pract Cardiovasc Med* 5: 338–349, 2008. doi: 10.1038/ncpcardio1211.

40. **Loffredo L**, **Martino F**, **Carnevale R**, **Pignatelli P**, **Catasca E**, **Perri L**, **Calabrese CM**, **Palumbo MM**, **Baratta F**, **Del Ben M**, **Angelico F**, **Violi F**. Obesity and hypercholesterolemia are associated with NOX2 generated oxidative stress and arterial dysfunction. *J Pediatr* 161: 1004–1009, 2012. doi: 10.1016/j.jpeds.2012.05.042.

41. **Lenda DM**, **Sauls BA**, **Boegehold MA**. Reactive oxygen species may contribute to reduced endothelium-dependent dilation in rats fed high salt. *Am J Physiol Heart Circ Physiol* 279: H7–H14, 2000. doi: 10.1152/ajpheart.2000.279.1.H7.

42. **Tschudi MR**, **Mesaros S**, **Lüscher TF**, **Malinski T**. Direct in situ measurement of nitric oxide in mesenteric resistance arteries. Increased decomposition by superoxide in hypertension. *Hypertension* 27: 32–35, 1996. doi: 10.1161/01.hyp.27.1.32.

43. **Kirkman DL**, **Robinson AT**, **Rossman MJ**, **Seals DR**, **Edwards DG**. Mitochondrial contributions to vascular endothelial dysfunction, arterial stiffness, and cardiovascular diseases. *Am J Physiol Heart Circ Physiol* 320: H2080–H2100, 2021. doi: 10.1152/ajpheart.00917.2020.

44. **Widlansky ME**, **Gutterman DD**. Regulation of Endothelial Function by Mitochondrial Reactive Oxygen Species. *Antioxid Redox Signal* 15: 1517–1530, 2011. doi: 10.1089/ars.2010.3642.

45. **Uribarri J**, **del Castillo MD**, **de la Maza MP**, **Filip R**, **Gugliucci A**, **Luevano-Contreras C**, **Macías-Cervantes MH**, **Markowicz Bastos DH**, **Medrano A**, **Menini T**, **Portero-Otin M**, **Rojas A**, **Sampaio GR**, **Wrobel K**, **Wrobel K**, **Garay-Sevilla ME**. Dietary advanced glycation end products and their role in health and disease. *Adv Nutr* 6: 461–473, 2015. doi: 10.3945/an.115.008433.

46. **Raghavan CT**. Advanced Glycation End Products in Neurodegenerative Diseases. *J Mol Neurosci* 74: 114, 2024. doi: 10.1007/s12031-024-02297-1.

47. **Hayashi K**, **Hirayama E**. Age-related changes of wall composition and collagen cross-linking in the rat carotid artery - In relation with arterial mechanics. *J Mech Behav Biomed Mater* 65: 881–889, 2017. doi: 10.1016/j.jmbbm.2016.10.007.

48. **Wang D**, **Wang J**, **Liu X**, **Du K**, **Liu H**, **Yang X**, **Liu T**, **Liu Q**, **Wang M**, **Guo J**. Quantifying carboxymethyl lysine and carboxyethyl lysine in human plasma: clinical insights into aging research using liquid chromatography-tandem mass spectrometry. *BMC Biotechnol* 24: 12, 2024. doi: 10.1186/s12896-024-00838-5.

49. Sodium nitrite de-stiffening of large elastic arteries with aging: role of normalization of advanced glycation end-products - PubMed [Online]. [date unknown]. https://pubmed.ncbi.nlm.nih.gov/22588062/ [6 Jun. 2025].

50. **Hallam KM**, **Li Q**, **Ananthakrishnan R**, **Kalea A**, **Zou YS**, **Vedantham S**, **Schmidt AM**, **Yan SF**, **Ramasamy R**. Aldose reductase and AGE-RAGE pathways: central roles in the pathogenesis of vascular dysfunction in aging rats. *Aging Cell* 9: 776–784, 2010. doi: 10.1111/j.1474-9726.2010.00606.x.

51. **Ren X**, **Ren L**, **Wei Q**, **Shao H**, **Chen L**, **Liu N**. Advanced glycation end-products decreases expression of endothelial nitric oxide synthase through oxidative stress in human coronary artery endothelial cells. *Cardiovascular Diabetology* 16: 52, 2017. doi: 10.1186/s12933-017-0531-9.

52. **Reeve EH**, **Kronquist EK**, **Wolf JR**, **Lee B**, **Khurana A**, **Pham H**, **Cullen AE**, **Peterson JA**, **Meza A**, **Colton Bramwell R**, **Villasana L**, **Machin DR**, **Henson GD**, **Walker AE**. Pyridoxamine treatment ameliorates large artery stiffening and cerebral artery endothelial dysfunction in old mice. *J Cereb Blood Flow Metab* 43: 281–295, 2023. doi: 10.1177/0271678X221130124.

53. **McEniery CM**. Novel therapeutic strategies for reducing arterial stiffness. *Br J Pharmacol* 148: 881–883, 2006. doi: 10.1038/sj.bjp.0706805.

54. **Vasan S**, **Foiles P**, **Founds H**. Therapeutic potential of breakers of advanced glycation end product-protein crosslinks. *Arch Biochem Biophys* 419: 89–96, 2003. doi: 10.1016/j.abb.2003.08.016.

55. **Ramis R**, **Ortega-Castro J**, **Caballero C**, **Casasnovas R**, **Cerrillo A**, **Vilanova B**, **Adrover M**, **Frau J**. How Does Pyridoxamine Inhibit the Formation of Advanced Glycation End Products? The Role of Its Primary Antioxidant Activity. *Antioxidants (Basel)* 8: E344, 2019. doi: 10.3390/antiox8090344.

56. **García-Díez G**, **Monreal-Corona R**, **Mora-Diez N**. Complexes of Copper and Iron with Pyridoxamine, Ascorbic Acid, and a Model Amadori Compound: Exploring Pyridoxamine's Secondary Antioxidant Activity. *Antioxidants (Basel)* 10: 208, 2021. doi: 10.3390/antiox10020208.

57. **Vasan S**, **Zhang X**, **Zhang X**, **Kapurniotu A**, **Bernhagen J**, **Teichberg S**, **Basgen J**, **Wagle D**, **Shih D**, **Terlecky I**, **Bucala R**, **Cerami A**, **Egan J**, **Ulrich P**. An agent cleaving glucose-derived protein crosslinks in vitro and in vivo. *Nature* 382: 275–278, 1996. doi: 10.1038/382275a0.

58. **Asif M**, **Egan J**, **Vasan S**, **Jyothirmayi GN**, **Masurekar MR**, **Lopez S**, **Williams C**, **Torres RL**, **Wagle D**, **Ulrich P**, **Cerami A**, **Brines M**, **Regan TJ**. An advanced glycation endproduct cross-link breaker can reverse age-related increases in myocardial stiffness. *Proc Natl Acad Sci U S A* 97: 2809–2813, 2000. doi: 10.1073/pnas.040558497.

59. **Kass DA**, **Shapiro EP**, **Kawaguchi M**, **Capriotti AR**, **Scuteri A**, **deGroof RC**, **Lakatta EG**. Improved arterial compliance by a novel advanced glycation end-product crosslink breaker. *Circulation* 104: 1464–1470, 2001. doi: 10.1161/hc3801.097806.

60. **Liu J**, **Masurekar MR**, **Vatner DE**, **Jyothirmayi GN**, **Regan TJ**, **Vatner SF**, **Meggs LG**, **Malhotra A**. Glycation end-product cross-link breaker reduces collagen and improves cardiac function in aging diabetic heart. *Am J Physiol Heart Circ Physiol* 285: H2587-2591, 2003. doi: 10.1152/ajpheart.00516.2003.

61. **Toprak C**, **Sirmagul B**, **Yigitaslan S**. Functional Effects of Alagebrium (ALT-711)–Isolated Rat Carotid Artery. *Eurasian J Med* 49: 188–192, 2017. doi: 10.5152/eurasianjmed.2017.17046.

62. **Smith RAJ**, **Murphy MP**. Animal and human studies with the mitochondria-targeted antioxidant MitoQ. *Ann N Y Acad Sci* 1201: 96–103, 2010. doi: 10.1111/j.1749-6632.2010.05627.x.

63. **Clayton ZS**, **Brunt VE**, **Hutton DA**, **VanDongen NS**, **D'Alessandro A**, **Reisz JA**, **Ziemba BP**, **Seals DR**. Doxorubicin-Induced Oxidative Stress and Endothelial Dysfunction in Conduit Arteries Is Prevented by Mitochondrial-Specific Antioxidant Treatment. *JACC CardioOncol* 2: 475–488, 2020. doi: 10.1016/j.jaccao.2020.06.010.

64. **Gioscia-Ryan RA**, **Battson ML**, **Cuevas LM**, **Eng JS**, **Murphy MP**, **Seals DR**. Mitochondria-targeted antioxidant therapy with MitoQ ameliorates aortic stiffening in old

mice. *J Appl Physiol (1985)* 124: 1194–1202, 2018. doi: 10.1152/japplphysiol.00670.2017.

65. **Rossman MJ**, **Santos-Parker JR**, **Steward CAC**, **Bispham NZ**, **Cuevas LM**, **Rosenberg HL**, **Woodward KA**, **Chonchol M**, **Gioscia-Ryan RA**, **Murphy MP**, **Seals DR**. Chronic Supplementation With a Mitochondrial Antioxidant (MitoQ) Improves Vascular Function in Healthy Older Adults. *Hypertension* 71: 1056–1063, 2018. doi: 10.1161/HYPERTENSIONAHA.117.10787.

66. **Murray KO**, **Ludwig KR**, **Darvish S**, **Coppock ME**, **Seals DR**, **Rossman MJ**. Chronic mitochondria antioxidant treatment in older adults alters the circulating milieu to improve endothelial cell function and mitochondrial oxidative stress. *Am J Physiol Heart Circ Physiol* 325: H187–H194, 2023. doi: 10.1152/ajpheart.00270.2023.

67. **Iskandar Z**, **Dodd M**, **Huang J**, **Chin CWL**, **Stuart G**, **Caputo M**, **Clayton T**, **Child A**, **Jin XY**, **Aragon-Martin JA**, **Gibb J**, **Flather M**, **Choy A-M**. Exaggerated elastin turnover in young individuals with Marfan syndrome: new insights from the AIMS trial. *Eur Heart J Open* 3: oead095, 2023. doi: 10.1093/ehjopen/oead095.

68. **Winder NR**, **Reeve EH**, **Walker AE**. Large artery stiffness and brain health: insights from animal models. *Am J Physiol Heart Circ Physiol* 320: H424–H431, 2021. doi: 10.1152/ajpheart.00696.2020.

69. **Faury G**, **Pezet M**, **Knutsen RH**, **Boyle WA**, **Heximer SP**, **McLean SE**, **Minkes RK**, **Blumer KJ**, **Kovacs A**, **Kelly DP**, **Li DY**, **Starcher B**, **Mecham RP**. Developmental adaptation of the mouse cardiovascular system to elastin haploinsufficiency. American Society for Clinical Investigation: 2003.

70. **Li DY**, **Brooke B**, **Davis EC**, **Mecham RP**, **Sorensen LK**, **Boak BB**, **Eichwald E**, **Keating MT**. Elastin is an essential determinant of arterial morphogenesis. *Nature* 393: 276–280, 1998. doi: 10.1038/30522.

71. **Brengle BM**, **Lin M**, **Roth RA**, **Jones KD**, **Wagenseil JE**, **Mecham RP**, **Halabi CM**. A new mouse model of elastin haploinsufficiency highlights the importance of elastin to vascular development and blood pressure regulation. *Matrix Biology* 117: 1–14, 2023. doi: 10.1016/j.matbio.2023.02.003.

72. **Walker AE**, **Henson GD**, **Reihl KD**, **Morgan RG**, **Dobson PS**, **Nielson EI**, **Ling J**, **Mecham RP**, **Li DY**, **Lesniewski LA**, **Donato AJ**. Greater impairments in cerebral artery compared with skeletal muscle feed artery endothelial function in a mouse model of increased large artery stiffness. *J Physiol* 593: 1931–1943, 2015. doi: 10.1113/jphysiol.2014.285338.

73. **Lin KA**, **Choudhury KR**, **Rathakrishnan BG**, **Marks DM**, **Petrella JR**, **Doraiswamy PM**, **Alzheimer's Disease Neuroimaging Initiative**. Marked gender differences in

progression of mild cognitive impairment over 8 years. *Alzheimers Dement (N Y)* 1: 103–110, 2015. doi: 10.1016/j.trci.2015.07.001.

74. **Kehmeier MN**, **Walker AE**. Sex Differences in Large Artery Stiffness: Implications for Cerebrovascular Dysfunction and Alzheimer's Disease. *Front Aging* 2: 791208, 2021. doi: 10.3389/fragi.2021.791208.

75. **Wagenseil JE**, **Nerurkar NL**, **Knutsen RH**, **Okamoto RJ**, **Li DY**, **Mecham RP**. Effects of elastin haploinsufficiency on the mechanical behavior of mouse arteries. *American Journal of Physiology-Heart and Circulatory Physiology* 289: H1209–H1217, 2005. doi: 10.1152/ajpheart.00046.2005.

76. **Henson GD**, **Walker AE**, **Reihl KD**, **Donato AJ**, **Lesniewski LA**. Dichotomous mechanisms of aortic stiffening in high-fat diet fed young and old B6D2F1 mice. *Physiol Rep* 2: e00268, 2014. doi: 10.1002/phy2.268.

77. **Donato AJ**, **Walker AE**, **Magerko KA**, **Bramwell RC**, **Black AD**, **Henson GD**, **Lawson BR**, **Lesniewski LA**, **Seals DR**. Life-long caloric restriction reduces oxidative stress and preserves nitric oxide bioavailability and function in arteries of old mice. *Aging Cell* 12: 772–783, 2013. doi: 10.1111/acel.12103.

78. **Lesniewski LA**, **Connell ML**, **Durrant JR**, **Folian BJ**, **Anderson MC**, **Donato AJ**, **Seals DR**. B6D2F1 Mice are a suitable model of oxidative stress-mediated impaired endothelium-dependent dilation with aging. *J Gerontol A Biol Sci Med Sci* 64: 9–20, 2009. doi: 10.1093/gerona/gln049.

79. **Baumbach GL**, **Hajdu MA**. Mechanics and composition of cerebral arterioles in renal and spontaneously hypertensive rats. *Hypertension* 21: 816–826, 1993. doi: 10.1161/01.hyp.21.6.816.

80. **Dunn WR**, **Gardiner SM**. Differential alteration in vascular structure of resistance arteries isolated from the cerebral and mesenteric vascular beds of transgenic [(mRen-2)27], hypertensive rats. *Hypertension* 29: 1140–1147, 1997. doi: 10.1161/01.hyp.29.5.1140.

81. **Izzard AS**, **Horton S**, **Heerkens EH**, **Shaw L**, **Heagerty AM**. Middle cerebral artery structure and distensibility during developing and established phases of hypertension in the spontaneously hypertensive rat. *J Hypertens* 24: 875–880, 2006. doi: 10.1097/01.hjh.0000222757.54111.06.

82. **Deacon R**. Assessing Burrowing, Nest Construction, and Hoarding in Mice. *J Vis Exp* : 2607, 2012. doi: 10.3791/2607.

83. **Duvoisin RM**, **Villasana L**, **Pfankuch T**, **Raber J**. Sex-Dependent Cognitive Phenotype of Mice Lacking mGluR8. *Behav Brain Res* 209: 21–26, 2010. doi: 10.1016/j.bbr.2010.01.006.

84. **Reeve EH**, **Barnes JN**, **Moir ME**, **Walker AE**. Impact of arterial stiffness on cerebrovascular function: a review of evidence from humans and preclincal models. *Am J Physiol Heart Circ Physiol* 326: H689–H704, 2024. doi: 10.1152/ajpheart.00592.2023.

85. **Pase MP**, **Herbert A**, **Grima NA**, **Pipingas A**, **O'Rourke MF**. Arterial stiffness as a cause of cognitive decline and dementia: a systematic review and meta-analysis. *Intern Med J* 42: 808–815, 2012. doi: 10.1111/j.1445-5994.2011.02645.x.

86. **Pase MP**, **Beiser A**, **Himali JJ**, **Tsao C**, **Satizabal CL**, **Vasan RS**, **Seshadri S**, **Mitchell GF**. Aortic Stiffness and the Risk of Incident Mild Cognitive Impairment and Dementia. *Stroke* 47: 2256–2261, 2016. doi: 10.1161/STROKEAHA.116.013508.

87. **Cooper LL**, **Mitchell GF**. Aortic Stiffness, Cerebrovascular Dysfunction, and Memory. *Pulse (Basel)* 4: 69–77, 2016. doi: 10.1159/000448176.

88. **Kozel BA**, **Knutsen RH**, **Ye L**, **Ciliberto CH**, **Broekelmann TJ**, **Mecham RP**. Genetic modifiers of cardiovascular phenotype caused by elastin haploinsufficiency act by extrinsic noncomplementation. *J Biol Chem* 286: 44926–44936, 2011. doi: 10.1074/jbc.M111.274779.

89. **Pezet M**, **Jacob M-P**, **Escoubet B**, **Gheduzzi D**, **Tillet E**, **Perret P**, **Huber P**, **Quaglino D**, **Vranckx R**, **Li DY**, **Starcher B**, **Boyle WA**, **Mecham RP**, **Faury G**. Elastin haploinsufficiency induces alternative aging processes in the aorta. *Rejuvenation Res* 11: 97–112, 2008. doi: 10.1089/rej.2007.0587.

90. **Knutsen RH**, **Beeman SC**, **Broekelmann TJ**, **Liu D**, **Tsang KM**, **Kovacs A**, **Ye L**, **Danback JR**, **Watson A**, **Wardlaw A**, **Wagenseil JE**, **Garbow JR**, **Shoykhet M**, **Kozel BA**. Minoxidil improves vascular compliance, restores cerebral blood flow, and alters extracellular matrix gene expression in a model of chronic vascular stiffness. *Am J Physiol Heart Circ Physiol* 315: H18–H32, 2018. doi: 10.1152/ajpheart.00683.2017.

91. **Kehmeier MN**, **Khurana A**, **Bedell BR**, **Cullen AE**, **Cannon AT**, **Henson GD**, **Walker AE**. Effects of dietary soy content on cerebral artery function and behavior in ovariectomized female mice. *American Journal of Physiology-Heart and Circulatory Physiology* 326: H636–H647, 2024. doi: 10.1152/ajpheart.00618.2023.

92. **Walker AE**, **Kronquist EK**, **Chinen KT**, **Reihl KD**, **Li DY**, **Lesniewski LA**, **Donato AJ**. Cerebral and skeletal muscle feed artery vasoconstrictor responses in a mouse model with greater large elastic artery stiffness. *Exp Physiol* 104: 434–442, 2019. doi: 10.1113/EP087453.

93. **Muhire G**, **Iulita MF**, **Vallerand D**, **Youwakim J**, **Gratuze M**, **Petry FR**, **Planel E**, **Ferland G**, **Girouard H**. Arterial Stiffness Due to Carotid Calcification Disrupts Cerebral Blood Flow Regulation and Leads to Cognitive Deficits. *J Am Heart Assoc* 8: e011630, 2019. doi: 10.1161/JAHA.118.011630.

94. **Sadekova N, Iulita MF, Vallerand D, Muhire G, Bourmoum M, Claing A, Girouard H**. Arterial stiffness induced by carotid calcification leads to cerebral gliosis mediated by oxidative stress. *J Hypertens* 36: 286–298, 2018. doi: 10.1097/HJH.0000000000001557.

95. **Winder NR**, **Reeve EH**, **Kronquist EK**, **Khurana A**, **Lee B**, **Nguyen T**, **Henson GD**, **Walker AE**. High pulse pressure impairs cerebral artery endothelial function in young, but not old, mice. *Exp Gerontol* 173: 112101, 2023. doi: 10.1016/j.exger.2023.112101.

96. **Juan SMA**, **Adlard PA**. Ageing and Cognition. *Subcell Biochem* 91: 107–122, 2019. doi: 10.1007/978-981-13-3681-2_5.

97. **Harada CN**, **Natelson Love MC**, **Triebel KL**. Normal cognitive aging. *Clin Geriatr Med* 29: 737–752, 2013. doi: 10.1016/j.cger.2013.07.002.

98. **Jaroudi W**, **Garami J**, **Garrido S**, **Hornberger M**, **Keri S**, **Moustafa AA**. Factors underlying cognitive decline in old age and Alzheimer's disease: the role of the hippocampus. *Rev Neurosci* 28: 705–714, 2017. doi: 10.1515/revneuro-2016-0086.

99. **Tian Z**, **Ji X**, **Liu J**. Neuroinflammation in Vascular Cognitive Impairment and Dementia: Current Evidence, Advances, and Prospects. *Int J Mol Sci* 23: 6224, 2022. doi: 10.3390/ijms23116224.

100. **Giergiel M**, **Lopucki M**, **Stachowicz N**, **Kankofer M**. The influence of age and gender on antioxidant enzyme activities in humans and laboratory animals. *Aging Clin Exp Res* 24: 561–569, 2012. doi: 10.3275/8587.

101. **van Sloten TT**, **Protogerou AD**, **Henry RMA**, **Schram MT**, **Launer LJ**, **Stehouwer CDA**. Association between arterial stiffness, cerebral small vessel disease and cognitive impairment: A systematic review and meta-analysis. *Neurosci Biobehav Rev* 53: 121–130, 2015. doi: 10.1016/j.neubiorev.2015.03.011.

102. **Rabkin SW**. Arterial stiffness: detection and consequences in cognitive impairment and dementia of the elderly. *J Alzheimers Dis* 32: 541–549, 2012. doi: 10.3233/JAD-2012-120757.

103. **Graff-Radford J**. Vascular Cognitive Impairment. *Continuum (Minneap Minn)* 25: 147–164, 2019. doi: 10.1212/CON.0000000000000684.

104. **Levit A**, **Hachinski V**, **Whitehead SN**. Neurovascular unit dysregulation, white matter disease, and executive dysfunction: the shared triad of vascular cognitive impairment and

Alzheimer disease. *Geroscience* 42: 445–465, 2020. doi: 10.1007/s11357-020-00164-6.

105. **Waldstein SR**, **Rice SC**, **Thayer JF**, **Najjar SS**, **Scuteri A**, **Zonderman AB**. Pulse pressure and pulse wave velocity are related to cognitive decline in the Baltimore Longitudinal Study of Aging. *Hypertension* 51: 99–104, 2008. doi: 10.1161/HYPERTENSIONAHA.107.093674.

106. **Ruitenberg A**, **den Heijer T**, **Bakker SLM**, **van Swieten JC**, **Koudstaal PJ**, **Hofman A**, **Breteler MMB**. Cerebral hypoperfusion and clinical onset of dementia: the Rotterdam Study. *Ann Neurol* 57: 789–794, 2005. doi: 10.1002/ana.20493.

107. **Stone J**, **Johnstone DM**, **Mitrofanis J**, **O'Rourke M**. The mechanical cause of age-related dementia (Alzheimer's disease): the brain is destroyed by the pulse. *J Alzheimers Dis* 44: 355–373, 2015. doi: 10.3233/JAD-141884.

108. **Mitchell GF**, **Parise H**, **Benjamin EJ**, **Larson MG**, **Keyes MJ**, **Vita JA**, **Vasan RS**, **Levy D**. Changes in arterial stiffness and wave reflection with advancing age in healthy men and women: the Framingham Heart Study. *Hypertension* 43: 1239–1245, 2004. doi: 10.1161/01.HYP.0000128420.01881.aa.

109. **Wolffenbuttel BH**, **Boulanger CM**, **Crijns FR**, **Huijberts MS**, **Poitevin P**, **Swennen GN**, **Vasan S**, **Egan JJ**, **Ulrich P**, **Cerami A**, **Lévy BI**. Breakers of advanced glycation end products restore large artery properties in experimental diabetes. *Proc Natl Acad Sci U S A* 95: 4630–4634, 1998. doi: 10.1073/pnas.95.8.4630.

110. **Susic D**, **Varagic J**, **Ahn J**, **Frohlich ED**. Cardiovascular and renal effects of a collagen cross-link breaker (ALT 711) in adult and aged spontaneously hypertensive rats. *Am J Hypertens* 17: 328–333, 2004. doi: 10.1016/j.amjhyper.2003.12.015.

111. **Vaitkevicius PV**, **Lane M**, **Spurgeon H**, **Ingram DK**, **Roth GS**, **Egan JJ**, **Vasan S**, **Wagle DR**, **Ulrich P**, **Brines M**, **Wuerth JP**, **Cerami A**, **Lakatta EG**. A cross-link breaker has sustained effects on arterial and ventricular properties in older rhesus monkeys. *Proc Natl Acad Sci U S A* 98: 1171–1175, 2001. doi: 10.1073/pnas.98.3.1171.

112. **Abbott CB**, **Lawrence MM**, **Kobak KA**, **Lopes EBP**, **Peelor FF III**, **Donald EJ**, **Van Remmen H**, **Griffin TM**, **Miller BF**. A Novel Stable Isotope Approach Demonstrates Surprising Degree of Age-Related Decline in Skeletal Muscle Collagen Proteostasis. *Function* 2: zqab028, 2021. doi: 10.1093/function/zqab028.

113. **Faakye A**, **Harold KM**, **Matsuzaki S**, **Pranay A**, **Mendez Garcia MF**, **Loveland BL**, **Rigsby SN**, **Peelor FF**, **Eyster C**, **Miller BF**, **Griffin TM**, **Kinter M**, **Chiao YA**, **Humphries KM**. The effect of enhanced glycolysis on cardiac aging. .

114. **Smith LR**, **Hammers DW**, **Sweeney HL**, **Barton ER**. Increased collagen cross-linking is a signature of dystrophin-deficient muscle. *Muscle Nerve* 54: 71–78, 2016. doi: 10.1002/mus.24998.

115. **Sell DR**, **Monnier VM**. Molecular basis of arterial stiffening: role of glycation - a mini-review. *Gerontology* 58: 227–237, 2012. doi: 10.1159/000334668.

116. **Zieman SJ**, **Melenovsky V**, **Clattenburg L**, **Corretti MC**, **Capriotti A**, **Gerstenblith G**, **Kass DA**. Advanced glycation endproduct crosslink breaker (alagebrium) improves endothelial function in patients with isolated systolic hypertension. *J Hypertens* 25: 577–583, 2007. doi: 10.1097/HJH.0b013e328013e7dd.

117. **Freidja ML**, **Tarhouni K**, **Toutain B**, **Fassot C**, **Loufrani L**, **Henrion D**. The AGE-Breaker ALT-711 Restores High Blood Flow–Dependent Remodeling in Mesenteric Resistance Arteries in a Rat Model of Type 2 Diabetes. *Diabetes* 61: 1562–1572, 2012. doi: 10.2337/db11-0750.

118. **Longtine AG**, **Venkatasubramanian R**, **Zigler MC**, **Lindquist AJ**, **Mahoney SA**, **Greenberg NT**, **VanDongen NS**, **Ludwig KR**, **Moreau KL**, **Seals DR**, **Clayton ZS**. Female C57BL/6N mice are a viable model of aortic aging in women. *Am J Physiol Heart Circ Physiol* 324: H893–H904, 2023. doi: 10.1152/ajpheart.00120.2023.

119. **Wang R**, **Mattson JM**, **Zhang Y**. Effect of aging on the biaxial mechanical behavior of human descending thoracic aorta: Experiments and constitutive modeling considering collagen crosslinking. *J Mech Behav Biomed Mater* 140: 105705, 2023. doi: 10.1016/j.jmbbm.2023.105705.

120. **Tarumi T**, **Shah F**, **Tanaka H**, **Haley AP**. Association between central elastic artery stiffness and cerebral perfusion in deep subcortical gray and white matter. *Am J Hypertens* 24: 1108–1113, 2011. doi: 10.1038/ajh.2011.101.

121. **Hartog JWL**, **Willemsen S**, **van Veldhuisen DJ**, **Posma JL**, **van Wijk LM**, **Hummel YM**, **Hillege HL**, **Voors AA**, **BENEFICIAL investigators**. Effects of alagebrium, an advanced glycation endproduct breaker, on exercise tolerance and cardiac function in patients with chronic heart failure. *Eur J Heart Fail* 13: 899–908, 2011. doi: 10.1093/eurjhf/hfr067.

122. **Reddy GK**. AGE-related cross-linking of collagen is associated with aortic wall matrix stiffness in the pathogenesis of drug-induced diabetes in rats. *Microvasc Res* 68: 132–142, 2004. doi: 10.1016/j.mvr.2004.04.002.

123. **Aronson D**. Cross-linking of glycated collagen in the pathogenesis of arterial and myocardial stiffening of aging and diabetes. *J Hypertens* 21: 3–12, 2003. doi: 10.1097/00004872-200301000-00002.

124. **Steinback CD**, **Poulin MJ**. Influence of Hypoxia on Cerebral Blood Flow Regulation in Humans. *Adv Exp Med Biol* 903: 131–144, 2016. doi: 10.1007/978-1-4899-7678-9_9.

125. **Liu C**, **Lee SH**, **Loewenstein DA**, **Galvin JE**, **Levin BE**, **McKinney A**, **Alperin N**. Early Amnestic Mild Cognitive Impairment Is Associated with Reduced Total Cerebral Blood Flow with no Brain Tissue Loss. *J Alzheimers Dis* 91: 1313–1322, 2023. doi: 10.3233/JAD-220734.

126. 2025 Alzheimer's disease facts and figures - PMC [Online]. [date unknown]. https://pmc.ncbi.nlm.nih.gov/articles/PMC12040760/ [6 Jun. 2025].

127. **Atlante A**, **Amadoro G**, **Latina V**, **Valenti D**. Therapeutic Potential of Targeting Mitochondria for Alzheimer's Disease Treatment. *J Clin Med* 11: 6742, 2022. doi: 10.3390/jcm11226742.

128. **Atlante A**, **Valenti D**, **Latina V**, **Amadoro G**. Dysfunction of Mitochondria in Alzheimer's Disease: ANT and VDAC Interact with Toxic Proteins and Aid to Determine the Fate of Brain Cells. *Int J Mol Sci* 23: 7722, 2022. doi: 10.3390/ijms23147722.

129. **Zorov DB**, **Juhaszova M**, **Sollott SJ**. Mitochondrial ROS-induced ROS release: an update and review. *Biochim Biophys Acta* 1757: 509–517, 2006. doi: 10.1016/j.bbabio.2006.04.029.

130. **Srinivas US**, **Tan BWQ**, **Vellayappan BA**, **Jeyasekharan AD**. ROS and the DNA damage response in cancer. *Redox Biol* 25: 101084, 2019. doi: 10.1016/j.redox.2018.101084.

131. **Beal MF**. Mitochondria take center stage in aging and neurodegeneration. *Ann Neurol* 58: 495–505, 2005. doi: 10.1002/ana.20624.

132. **Islam MT**. Oxidative stress and mitochondrial dysfunction-linked neurodegenerative disorders. *Neurol Res* 39: 73–82, 2017. doi: 10.1080/01616412.2016.1251711.

133. **Trifunovic A**, **Wredenberg A**, **Falkenberg M**, **Spelbrink JN**, **Rovio AT**, **Bruder CE**, **Bohlooly-Y M**, **Gidlöf S**, **Oldfors A**, **Wibom R**, **Törnell J**, **Jacobs HT**, **Larsson N-G**. Premature ageing in mice expressing defective mitochondrial DNA polymerase. *Nature* 429: 417–423, 2004. doi: 10.1038/nature02517.

134. **Janaszak-Jasiecka A**, **Płoska A**, **Wierońska JM**, **Dobrucki LW**, **Kalinowski L**. Endothelial dysfunction due to eNOS uncoupling: molecular mechanisms as potential therapeutic targets. *Cell Mol Biol Lett* 28: 21, 2023. doi: 10.1186/s11658-023-00423-2.

135. **Alonso D**, **Radomski MW**. The nitric oxide-endothelin-1 connection. *Heart Fail Rev* 8: 107–115, 2003. doi: 10.1023/a:1022155206928.

136. **Taddei S**, **Virdis A**, **Ghiadoni L**, **Salvetti A**. Vascular effects of endothelin-1 in essential hypertension: relationship with cyclooxygenase-derived endothelium-dependent contracting factors and nitric oxide. *J Cardiovasc Pharmacol* 35: S37-40, 2000. doi: 10.1097/00005344-200000002-00009.

137. **Clayton ZS**, **Hutton DA**, **Brunt VE**, **VanDongen NS**, **Ziemba BP**, **Casso AG**, **Greenberg NT**, **Mercer AN**, **Rossman MJ**, **Campisi J**, **Melov S**, **Seals DR**. Apigenin restores endothelial function by ameliorating oxidative stress, reverses aortic stiffening, and mitigates vascular inflammation with aging. *Am J Physiol Heart Circ Physiol* 321: H185–H196, 2021. doi: 10.1152/ajpheart.00118.2021.

138. **McManus MJ**, **Murphy MP**, **Franklin JL**. The mitochondria-targeted antioxidant MitoQ prevents loss of spatial memory retention and early neuropathology in a transgenic mouse model of Alzheimer's disease. *J Neurosci* 31: 15703–15715, 2011. doi: 10.1523/JNEUROSCI.0552-11.2011.

139. **Young ML**, **Franklin JL**. The Mitochondria-Targeted Antioxidant MitoQ Inhibits Memory Loss, Neuropathology, and Extends Lifespan in Aged 3xTg-AD Mice. *Mol Cell Neurosci* 101: 103409, 2019. doi: 10.1016/j.mcn.2019.103409.

140. **Saito T**, **Matsuba Y**, **Mihira N**, **Takano J**, **Nilsson P**, **Itohara S**, **Iwata N**, **Saido TC**. Single App knock-in mouse models of Alzheimer's disease. *Nat Neurosci* 17: 661–663, 2014. doi: 10.1038/nn.3697.

141. **Masuda A**, **Kobayashi Y**, **Kogo N**, **Saito T**, **Saido TC**, **Itohara S**. Cognitive deficits in single App knock-in mouse models. *Neurobiol Learn Mem* 135: 73–82, 2016. doi: 10.1016/j.nlm.2016.07.001.

142. **Schultz MB**, **Kane AE**, **Mitchell SJ**, **MacArthur MR**, **Warner E**, **Vogel DS**, **Mitchell JR**, **Howlett SE**, **Bonkowski MS**, **Sinclair DA**. Age and life expectancy clocks based on machine learning analysis of mouse frailty. *Nat Commun* 11: 4618, 2020. doi: 10.1038/s41467-020-18446-0.

143. **LaRocca TJ**, **Hearon CM**, **Henson GD**, **Seals DR**. Mitochondrial Quality Control and Age-Associated Arterial Stiffening. *Exp Gerontol* 0: 78–82, 2014. doi: 10.1016/j.exger.2014.07.008.

144. **Rossman MJ**, **Gioscia-Ryan RA**, **Clayton ZS**, **Murphy MP**, **Seals DR**. Targeting mitochondrial fitness as a strategy for healthy vascular aging. *Clin Sci (Lond)* 134: 1491–1519, 2020. doi: 10.1042/CS20190559.

145. **Tanaka H**, **Seals DR**, **Monahan KD**, **Clevenger CM**, **DeSouza CA**, **Dinenno FA**. Regular aerobic exercise and the age-related increase in carotid artery intima-media thickness in healthy men. *J Appl Physiol (1985)* 92: 1458–1464, 2002. doi: 10.1152/japplphysiol.00824.2001.

146. **Kritchevsky SB**, **Shimakawa T**, **Tell GS**, **Dennis B**, **Carpenter M**, **Eckfeldt JH**, **Peacher-Ryan H**, **Heiss G**. Dietary Antioxidants and Carotid Artery Wall Thickness. *Circulation* 92: 2142–2150, 1995. doi: 10.1161/01.CIR.92.8.2142.

147. **Iannuzzi A**, **Celentano E**, **Panico S**, **Galasso R**, **Covetti G**, **Sacchetti L**, **Zarrilli F**, **Michele MD**, **Rubba P**. Dietary and circulating antioxidant vitamins in relation to carotid plaques in middle-aged women123. *The American Journal of Clinical Nutrition* 76: 582–587, 2002. doi: 10.1093/ajcn/76.3.582.

148. **Kelleher RJ**, **Soiza RL**. Evidence of endothelial dysfunction in the development of Alzheimer's disease: Is Alzheimer's a vascular disorder? *Am J Cardiovasc Dis* 3: 197–226, 2013.

149. **SEALS DR**, **JABLONSKI KL**, **DONATO AJ**. Aging and vascular endothelial function in humans. *Clin Sci (Lond)* 120: 357–375, 2011. doi: 10.1042/CS20100476.

150. **Park S-Y**, **Pekas EJ**, **Headid RJ**, **Son W-M**, **Wooden TK**, **Song J**, **Layec G**, **Yadav SK**, **Mishra PK**, **Pipinos II**. Acute mitochondrial antioxidant intake improves endothelial function, antioxidant enzyme activity, and exercise tolerance in patients with peripheral artery disease. *Am J Physiol Heart Circ Physiol* 319: H456–H467, 2020. doi: 10.1152/ajpheart.00235.2020.

151. **Patani R**, **Hardingham GE**, **Liddelow SA**. Functional roles of reactive astrocytes in neuroinflammation and neurodegeneration. *Nat Rev Neurol* 19: 395–409, 2023. doi: 10.1038/s41582-023-00822-1.

152. **Boëté Q**, **Lo M**, **Liu K-L**, **Vial G**, **Lemarié E**, **Rougelot M**, **Steuckardt I**, **Harki O**, **Couturier A**, **Gaucher J**, **Bouyon S**, **Demory A**, **Boutin-Paradis A**, **El Kholti N**, **Berthier A**, **Pépin J-L**, **Briançon-Marjollet A**, **Lambert E**, **Debret R**, **Faury G**. Physiological Impact of a Synthetic Elastic Protein in Arterial Diseases Related to Alterations of Elastic Fibers: Effect on the Aorta of Elastin-Haploinsufficient Male and Female Mice. *Int J Mol Sci* 23: 13464, 2022. doi: 10.3390/ijms232113464.

153. **Halsey G**, **Sinha D**, **Dhital S**, **Wang X**, **Vyavahare N**. Role of elastic fiber degradation in disease pathogenesis. *Biochim Biophys Acta Mol Basis Dis* 1869: 166706, 2023. doi: 10.1016/j.bbadis.2023.166706.

154. **Yue B**. Biology of the Extracellular Matrix: An Overview. .

155. **Mecham R**. *The Extracellular Matrix: an Overview*. Springer Science & Business Media, 2011.

156. **Reed KS**, **Frescoln AM**, **Keleher Q**, **Brellenthin AG**, **Kohut ML**, **Lefferts WK**. Effects of aerobic exercise training on cerebral pulsatile hemodynamics in middle-aged adults with elevated blood pressure/stage 1 hypertension. *J Appl Physiol (1985)* 136: 1376–1387, 2024. doi: 10.1152/japplphysiol.00689.2023.

157. **Barnes JN**, **Pearson AG**, **Corkery AT**, **Eisenmann NA**, **Miller KB**. Exercise, arterial stiffness, and cerebral vascular function: potential impact on brain health. *J Int Neuropsychol Soc* 27: 761–775, 2021. doi: 10.1017/S1355617721000394.

158. **Tomoto T**, **Zhang R**. Arterial Aging and Cerebrovascular Function: Impact of Aerobic Exercise Training in Older Adults. *Aging Dis* 15: 1672–1687, 2024. doi: 10.14336/AD.2023.1109-1.

159. **Wu C-F**, **Liu P-Y**, **Wu T-J**, **Hung Y**, **Yang S-P**, **Lin G-M**. Therapeutic modification of arterial stiffness: An update and comprehensive review. *World J Cardiol* 7: 742–753, 2015. doi: 10.4330/wjc.v7.i11.742.

160. **Pham T**, **MacRae CL**, **Broome SC**, **D'souza RF**, **Narang R**, **Wang HW**, **Mori TA**, **Hickey AJR**, **Mitchell CJ**, **Merry TL**. MitoQ and CoQ10 supplementation mildly suppresses skeletal muscle mitochondrial hydrogen peroxide levels without impacting mitochondrial function in middle-aged men. *Eur J Appl Physiol* 120: 1657–1669, 2020. doi: 10.1007/s00421-020-04396-4.

161. **Gottwald EM**, **Duss M**, **Bugarski M**, **Haenni D**, **Schuh CD**, **Landau EM**, **Hall AM**. The targeted anti-oxidant MitoQ causes mitochondrial swelling and depolarization in kidney tissue. *Physiol Rep* 6: e13667, 2018. doi: 10.14814/phy2.13667.